THE APPLICATION OF SYSTEM MODELLING TO DIGITAL ELECTRONIC SYSTEMS FOR ACTIVE CONTROL OF ACOUSTIC NOISE

by

Thomas M. Gurrie

A thesis submitted to the University of London for the degree of Doctor of Philosophy.

Physics Department
Royal Holloway and Bedford New College
University of London

August 1988

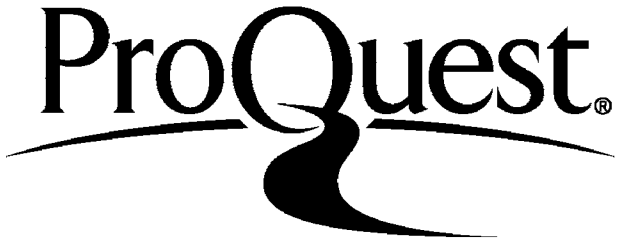

ABSTRACT

Active noise control (ANC) is concerned with achieving some degree of cancellation between unwanted acoustic noise and the output from one or more actively controlled secondary sources. The minimum configuration for an A.N.C. system is a detecting microphone to detect the unwanted acoustic noise and a single loudspeaker to act as a secondary source. The basic problem is to specify the electronic system needed between the detecting microphone and the loudspeaker to achieve cancellation. The system has an inherent feedback path between the loudspeaker and the detecting microphone that may cause instability. The system described in this thesis uses the principle of parallel feedback to ensure system stability. The basic idea of this is to use a second electronic system in a feedback path parallel to the electroacoustic feedback path to, in effect, remove this feedback. Incorporating both this feedback modelling and the appropriate forward transfer function between the detecting microphone and the loudspeaker should produce a practical stable working system.

This thesis considers implementation of these two electronic systems as sampled data systems employing finite impulse response (FIR) filters. Measurements on an experimental duct are used as input data for the study of system performance, this data being analysed using a

least squares approach to find best fit FIR filters. The system is assessed in terms of the lengths of FIR filters required in the feedforward and feedback paths to achieve satisfactory operation, i.e. that the system produce a significant level of attenuation and be stable.

The predicted level of performance of the ANC system indicates that the use of two independent FIR filters to model the feedforward and feedback paths produces a stable working system, capable of producing a significant level of attenuation over a broad frequency range. However, the length of FIR filter needed in each path has to be long in order to achieve a satisfactory level of performance.

To my dear Mother and my five Brothers

and especially to the memory of my late Father.

ACKNOWLEDGEMENT

Initially my thanks must go to my supervisor, Dr. S.J. Flockton, and to Dr. A.E. Brown, who taught me as an undergraduate in the subject areas of Signal Processing and Electroacoustics. Their courses got me interested in doing research work that led to my decision to register for a PhD in ANC.

I would like sincerely to thank my supervisor for his guidance, patience and encouragement shown to me throughout the entire project and especially in the writing of this thesis. I will always be indebted for the kindness and support he has shown to me.

My gratitude and thanks also to my colleague, Colin Bean, for useful discussions and also for help in programming the TMS32010 digital processor, especially the writing of the data capture program. Also I would like to thank Mike North whose technical assistance and help has been greatly appreciated, and special thanks to Michèle Webb for typing this thesis.

My thanks also go to GEC the company who sponsored my SERC CASE award. My industrial supervisor at GEC, John Edwards, and his colleague Niko Dekker I thank for their interest and encouragement.

Finally my thanks to SERC for financial support throughout the duration of the project.

CONTENTS

REVIEW CHAPTER

CHAPTER 2

PRINCIPLES OF THE DESIGN OF AN ANC SYSTEM

CHAPTER 3

SYSTEM MODELLING AND PARAMETER ESTIMATION

CHAPTER 4

MODELLING AND PARAMETER ESTIMATION OF THE FEEDBACK PATH

CHAPTER 5

MODELLING AND PARAMETER ESTIMATION FOR THE FEEDFORWARD PATH

CHAPTER 6

EVALUATION OF THE OVERALL SYSTEM PERFORMANCE

CHAPTER 7

CONCLUDING CHAPTER

LIST OF SYMBOLS

AA — Analog anti-aliasing filter

A/D — Analog to digital converter

ATTN — Attenuation

a_m — Coefficient for a finite impulse response filter

b_n — Coefficient for an infinite impulse response filter

C — Capacitor shown in figure D.1

$C_1(w)$-$C_5(w)$ — Duct acoustic transfer functions shown in figure 2.5

c — Velocity of sound in the duct

D(z) — General digital filter transfer function

$\hat{D}(z)$ — Approximation to the transfer function D(z)

D/A — Digital to analog converter

$D_{FF}(z)$ and $D_{FB}(z)$ — Transfer functions needed in the feedforward and feedback paths of a digital based ANC system

$\hat{D}_{FF}(z)$ and $\hat{D}_{FB}(z)$ — Approximation to the transfer functions $D_{FF}(z)$ and $D_{FB}(z)$

$D_{LP}(z)$ — Transfer function for digital filter defined by equation D.4

d(n) — Digital filter impulse response as shown in figure 3.3

$d_{FB}(n)$ — Feedback digital filter impulse response

d1, d2 and d3 — Poles of loudspeaker transfer function

E(w), E(z) or e(t) — Error signal in the frequency, or time domain

F(z) — Transfer function defined by equation C.4

$\hat{F}(z)$ — Approximation to F(z)

f — Frequency

f_1 — Start frequency for the swept sinusoid signal

f_2 — Final frequency for the swept sinusoid signal

G(w) — Transfer function for a general continuous system, as shown in figure 3.4

$G_o(z)$ Overall transfer function for the system shown inside the dotted box in figure 6.1

$G_{CL}(z)$ Closed loop transfer function for the ANC system

$G_{OP}(z)$ Open loop transfer function for the ANC system

$G_t(z)$ Transfer function for the discrete time delay system shown in figure C.1

$H_{o1}(w)$, $H_{o3}(w)$, $H_{23}(w)$ and $H_{21}(w)$
Electroacoustic transfer functions between the terminals 0, 1, 2 and 3 shown in figure 2.1 and defined by equations 2.1-2.4.

$H_{BB}(w)$ Black box transfer function shown in figure 2.1 and defined by equation 2.6.

$H_{FF}(w)$ and $H_{FB}(w)$
Transfer functions for the feedforward and feedback paths for the black box recursive realisation shown in figure 2.2(b)

$H_{FW}(w)$ and $H_{RP}(w)$
Transfer function for feedforward and feedback paths for the recursive black box realisation shown in figure 2.2(c)

$H_{mic1}(w)$ and $H_{mic2}(w)$
Detector and monitor microphone transfer function respectively

$H_{LS1}(w)$ and $H_{LS2}(w)$
Primary and secondary source loudspeaker transfer functions respectively

$H_{LS}(s)$ Lapace transfer function of loudspeaker (equation A.1)

$H_{T1}(w)-H_{t4}(w)$
Electroacoustic transfer function to represent the product of the duct transducers transfer functions, defined in equations 2.16-2.19.

$H_{com}(w)$
Transfer function of the filter compensating for the transducers in the ANC system feedforward path

$H_E(w)$ Product of all the duct transducers transfer functions as defined in equation 2.22

$H_{LP}(s)$ Second order low pass analog filter Laplace transfer function as defined by equation D.1

$H_{AA}(w)$ Electrical transfer function for the input anti-aliasing filter in a sampled data system

$H_{RC}(w)$ Electrical transfer function for the output re-construction filter in a sampled data system.

$H_{AI}(w)$ Transfer function for the analog input stage of a sampled data system

$H_{AO}(w)$ Transfer function for the analog output stage of a sampled data system

$H_{A/D}$ Transfer function associated with analog to digital converter

$h_{LS}(t)$ Loudspeaker impulse response (equation A.9)

j $\sqrt{-1}$

k Stiffness of a loudspeaker cone

L_1-L_5 Various duct lengths, as shown in figure 2.1

L Overall length of duct in figure 2.1

L_E Electrical inductance

m Integer subscript, also used to denote the order for a FIR filter

m_r Added mass corresponding to the radiation reactance of loudspeaker

n Integer subscript, also used to denote the order for a IIR filter

P/A Power amplifier

p_1 and p_2 Poles of a second order lowpass digital filter

R Resistors shown in figure D.1

R_E Electrical resistance

R_r Radiation resistance

R_m Mechanical resistance

RC Analog re-construction filter

r Reflection coefficient

s Laplace variable

S/H Sample and hold

$S_{HFF}(w)$ Feedforward sensitivity function

$S_T(w)$ Residual feedback sensitivity function

$S_{H21}(w)$ Acoustic feedback sensitivity function

T Sampling period

$T(w)$ Transfer function for the residual feedback in the ANC system

t_p Phase delay

t_g Group delay

$V_0(w)$ - $V_3(w)$
Complex spectra of voltages at the duct terminals 0, 1, 2 and 3 respectively (shown in figure 2.1)

$V_{IN}(s)$ and $V_{out}(s)$
Laplace transform of the input/output voltages for the second order low pass analog filter shown in figure D.1

w Angular frequency

w_c Analog filter cut-off frequency

w_c Digital filter cut-off frequency

$w(t)$ Time series due to the convolution of a sampled bandlimited verion of the input signal $x(t)$, and the digital filter coefficients $d(t)$ as shown in figure 3.3

$x(n)$ Digital input excitation signal

$X(w)$ or $x(t)$
Input excitation signal in either the frequency or time domain for a sampled data system to model a continuous system as shown in figure 3.3

$Y_{ss}(z)$ Input tapered swept sinusoid excitation signal

$Y_1(z)$, $Y_2(z)$ and $Y_3(z)$
z-transform of $y_1(n)$-$y_3(n)$

$y_1(n)$, $y_2(n)$ and $y_3(n)$
Time series for the signals used in figure 3.4

$Y_{01}(z)$ (or $y_{01}(n)$ etc.
z-transform (or time series) of the captured signals. The subscripts 0 and 1 etc, denote the point of capture of the signal (say terminal 1) and the point of injection of the excitation signal (say terminal 0).

$Y_{AR}(z)$ Frequency response of the captured signal from passing the swept sinusoid signal through the cascaded combination of the analog filtering of the feedforward and feedback sampled data systems.

$Y_{BL}(w)$	Band limited reconstructed swept sine wave signal (figure 4.18)
$Y_0(z)$	Zero delay version of the signal $Y_{BL}(z)$.
z	z-transform variable
Z_e	Electrical impedance
Z_m	Mechanical impedance.

LIST OF FIGURES

Appendixes

CHAPTER 1

REVIEW CHAPTER

1.1 INTRODUCTION

Active noise control (ANC) is concerned with achieving some degree of cancellation between the primary field from a sound source and the output from one or more actively controlled secondary sources. Though an ANC system can be used to control 3-dimensional sound fields [1] [2] [3], most work has been carried out on the simpler problem of controlling a 1-dimensional sound field. One particular practical application of ANC (that has received considerable attention over the past 10-15 years, on a laboratory scale) is that of the control of the sound field inside a ventilation duct. The problem of achieving attenuation of unwanted low frequency acoustic noise in ventilation ducts is a desirable practical goal. Active control has been used for the attenuation of noise below the cut-off frequency of the ducts, where there is no transverse mode propagation (i.e. 1-dimensional sound field). Below the cut-off frequency the necessary complexity and arrangement of secondary sources is simplified, leading to the possibility of a practical solution to the problem. Attenuation of wideband low frequency noise by passive means can be expensive and not very effective because of the long wavelengths involved. At high frequencies passive means of attenuation are very effective so therefore a combination of active and passive control could be the solution to the removal of unwanted wideband noise [4].

Active attenuation in a duct can occur by absorption of the primary sound energy or by reflection of the sound energy back upstream in the direction of the source. The two processes involved are absorption and reflection of sound energy. With the reflective type of attenuator a standing wave is set up on the upstream side of the secondary source(s). With an absorptive attenuator the secondary source(s) are used to absorb energy from the incident primary field. The main requirement for this type of attenuator is that the secondary source(s) should give a unidirectional output in the downstream direction.

One advantage of an ANC system is that the presence of the secondary source(s) in the duct need not impede the flow of air through it, unlike some conventional silencers which do cause a pressure drop to be developed.

1.2 REVIEW OF ANC SYSTEMS

1.2.1 Introduction

A number of ANC systems have been designed and experimentally tested over the past 10-15 years. A summary of the various types of system which use either one, two or three loudspeakers as secondary sources, and

employ one or more microphones as sensing transducers is shown in table 1.

Table 1

ANC Systems	
Reflective Attenuator	Absorptive Attenuator
Conventional Monopole	Jessel System
Tandem Monopole	Swinbanks System
Chelsea Monopole	
Chelsea Dipole	

What follows is a brief account of the ANC systems given in the table with emphasis on the monopole type of attenuator.

The experimental results for the above systems are given for systems installed using off-the-shelf analog hardware to control these systems.

1.2.2 Conventional monopole system [6] [26]

This is the simplest type of ANC system basically consisting of a sensing transducer (microphone) to detect the incident primary field and a secondary transducer (loudspeaker) to produce the inverse field (see figure 1 (a)). By employing a simple electrical delay between the microphone and the loudspeaker this

system will give maximum attenuation at a frequency where the microphone loudspeaker spacing is a quarter of a wavelength. However, the frequency range over which attenuation is effective is very narrow and for this and other reasons the conventional monopole system will not lead to a practical solution to attenuation of wideband low frequency noise.

1.2.3 Compensated monopole system

With the conventional monopole system the incident sound is reflected upstream toward the source end. This reflection is due to an impedance change caused by operating the secondary source in antiphase to the primary sound field. This impedance change leads to the formation of a standing wave on the upstream side of the secondary source. This means that an omnidirectional microphone will sense both the incident and reflected sound pressure. For the monopole to be effective then, it is desirable that the microphone should respond to the incident pressure only. This requirement necessitates the use of a unidirectional microphone. But this microphone needs to satisfy the requirement of good unidirectionality over the entire frequency range of interest. Also the use of a unidirectional microphone will introduce additional amplitude and phase shift into the system. Since a high level of accuracy is needed in both amplitude and phase to obtain good attenuation, this

will mean that any additional amplitude and phase shift introduced into the system will have to be compensated for. In practice it may be difficult to get the required degree of unidirectionality over the frequency range of interest, and to be able to compensate for the frequency dependent amplitude and phase shift caused by the use of the microphone.

Instead of trying to eliminate the effect of the reflection, it may be better to incorporate it into the attenuator design. The attenuator would have to be able to compensate for the fact that the microphone will detect both the incident and reflected waves. The reflected waves will act as a feedback signal between the loudspeaker and the microphone positions. Because of this feedback, then, the concepts used in control theory can be applied to the design of the attenuator.

One of the consequences of the feedback signal is the likelihood of the system going unstable, rendering the system practically useless. This is a major problem with the conventional monopole system where the feedback signal is not compensated for. The idea of designing and implementing an electronic system or black box that when placed between the detecting microphone and the secondary source loudspeaker would cancel electrically the effect of feedback and also have the desired transfer function to achieve cancellation of the unwanted acoustic noise was experimentally investigated by Leventhall & Eghtesadi

[6]. They showed that for the very simple model they looked at that the requirement for the black box was that the transfer functions needed to model the system feedforward and feedback path were pure time delays, namely the acoustic propagation time between the detecting microphone and the secondary source loudspeaker. The implication therefore was that the black box could be synthesised by having two electrical time delays connected in a feedback configuration. Experimental investigation into such a system, implemented by analog means, gave the following results. The system was capable of producing an average 12dB attenuation across a frequency range of 40-320Hz when the primary source excitation was pure tones. However when the input excitation was broadband random noise, the level of attenuation was only 5dB across the frequency range 40-240Hz. The main conclusion drawn from this experiment was that there was a need to take into account and compensate for the effect of the secondary source transducers. It is of interest to note that the investigators did not specify how stable the system was, which is important for any practical implementation of an ANC system. The stability problem and the need to compensate for the secondary source transducers discouraged investigators from trying to synthesise the black box using analog means.

1.2.4 Tight-coupled monopole system

In order to simplify the requirements for the black box Leventhall and Eghtesadi [10] proposed that the detecting microphone should be placed close to the secondary loudspeaker in order to minimise the amount of acoustic delay in the system. This resulted in a system that they called the "Tight Coupled Monopole". The amount of attenuation reported from experimental investigation was an average of 12dB for pure tones over the frequency range 40-300Hz. The attenuation of random noise having a bandwidth of 316Hz was variable, and of the order 1-20dB. The performance of the system was found to be limited by stability which constrained the amount of gain that could be incorporated into the system and the effect of cross modes in the duct. The effect of the duct cross modes below the duct cut-off frequency means that the sensing microphone should be in a position upstream of the secondary source loudspeaker (far field) so that these evanescent waves (loudspeaker near field) have decayed to an insignificant level [7].

Trinder and Nelson [8] attempted to predict analytically the optimum position for the sensing microphone, taking into account the effect of the loudspeaker near field. Their prediction initially resulted in a system that was unstable at frequencies in excess of 500Hz. In order to stabilise the system they employed an active filter with a cut-off frequency of

400Hz to sufficiently attenuate these frequencies so that the resultant system would be stable. It was then found that the system produced a maximum amount of attenuation (up to 20dB) at the duct longitudinal modes frequencies. However at certain frequencies in between the longitudinal modes very little or no attenuation was achieved, which they claimed was due to the system's open loop response having a low value of gain at these frequencies and the influence of longitudinal modes between the loudspeaker and the downstream end of the duct.

It should be emphasised that the performance of the 'Tight Coupled Monopole' depends critically on the amount of gain in the system feedforward path, and that in principle in order to achieve maximum attenuation means increasing the gain to the level where the system is on the verge of instability. Practically this means that if the system is left unattended then it may go unstable due to parameter changes such as temperature, analog drift etc.. Also the system performance in terms of stability and attenuation is sensitive to the selection of the transducers and the positioning of the sensing microphone with respect to the secondary source. This was graphically illustrated to the author when he did some experimental investigation of the Tight Coupled Monopole system himself, and found drastic differences in system performance when small changes were made to these things.

1.2.5 Tight-Coupled Tandem Monopole [5]

This system consists of two single monopole systems working in tandem (see figure 1 b)). It is supposed to work on the principle that the residual sound field remaining after cancellation by the upstream monopole, will act as the primary noise input to the downstream monopole. Hence operating both systems together should enhance the level of attenuation compared to what would be achieved with a single monopole system.

It is difficult to assess the advantage of using such a system over single monopole system in practice, on account of the complex interaction that occurs between the two systems i.e. the system will have more complicated feedforward and feedback path transfer functions. The system also has the inherent problem associated with the single monopole system of employing high open loop gain that can cause instability. For this reason the results obtained from experimental investigation have not been quoted here.

1.2.6 Jessel System

In an attempt to produce a unidirectional secondary source both the Jessel [11] and the Swinbanks [14] systems were proposed. The Jessel system was

operated as a tripole system i.e. monopole/dipole combination (see figure 1(c)). The monopole source loudspeaker is placed between the two loudspeakers forming the dipole pair and is operated in such a way as to prevent the dipole pair from radiating upstream towards the primary source. This system with its added complexity is seen to have the advantage that it prevents the formation of the standing wave, and the consequent increase in sound pressure level between the primary and secondary sources. This implies that the system will prevent any feedback from the secondary source to the sensing microphone so that the system should be stable.

This system was experimentally investigated by Jessel, Mangiante and Canevet [11] [12] [13]. Though these investigators were able to attenuate pure tones, the system failed to produce any encouragement when it came to using broadband random noise, giving nil attenuation.

1.2.7 Swinbanks System

The Swinbanks system [14] consists of two secondary source loudspeakers driven as a dipole pair, such that the system produces the desired effect of cancelling the primary sound field downstream of the secondary source (see figure 1 d). The system is intended to prevent any radiation from the downstream loudspeaker travelling back up the duct toward the sensing

microphone, by operating the upstream loudspeaker so that it will absorb the secondary source radiation travelling in that direction. The system offers the same advantages as the Jessel system without the added complexity of having three loudspeakers.

Experimentally the Swinbanks system was investigated by Poole and Leventhall [15] who obtained encouraging result from manually adjusting amplifiers and phase shifters in the system to obtain maximum attenuation at spot frequencies in the range 140-320Hz. The average level of attenuation over this range was 20dB. For 100Hz broadband noise with centre frequency 243Hz, the average attenuation recorded was 16dB.

1.2.8 Chelsea Dipole System

In the Chelsea Dipole [9] the sensing microphone was located at the geometric centre between two secondary source loudspeakers (see figure 1 e). The idea here is to drive the two loudspeakers in such a way that the net secondary sound field at the sensing microphone is zero. This implies that microphone will respond only to the incident primary field, and there will be no feedback present in the system and hence the system would be stable. However the dipole source will radiate secondary sound pressure in the upstream direction towards the primary source forming a standing

wave. Experimentally the system was found to give results similar to those of the monopole system .

1.2.4 Summary

It must be emphasised that the experimental results obtained for the various system described in this section were all implemented using analog hardware. Much of the experimental data was obtained by manually adjusting the controlling hardware (i.e. amplifiers, phase shifters, time delays etc) to obtain maximum attenuation at spot frequencies. There was no attempt to try and compensate for the non-ideal transducers such as the loudspeaker, which introduce significant amplitude and phase distortion. However the need for such compensation was advocated by a number of authors [4] [6] [14] [15]. The geometry of the secondary source transducers gave a frequency dependent response which limited the performance of the systems. In discussion of the problem of system stability and the elimination of feedback by either electrical filtering or by suitable geometrical separation of secondary source transducers [6] [9] [11] [14] there is no experimental data to quantify the relative improvement in stability. In the light Coupled Monopole System it was advocated that the system gain should be increased until the system was on the verge of going unstable.

It is difficult to determine the relative merits of the systems discussed in this section, on account of the fact that the experimental data were recorded under widely different conditions, e.g. type and size of duct, secondary source loudspeaker etc., so the results reported are for particular situations only. However the indications are that, in terms of performance and simplicity, the compensated monopole system is worthy of further investigation. However the advantage of having a unidirectional secondary source, for minimum added complexity favours the use of the Swinbanks System and also the experimental evidence favours the Swinbanks System rather than the Jessel type attenuator that employs three loudspeakers. It may well be that a combination of the ideas behind the compensated monopole together with a Swinbanks type of detector and source arrangement may prove the best.

1.3 DIGITAL FILTERING

1.3.1 Fixed filters

The objectives of any ANC system should be the following:

a) to achieve as much attenuation as possible across a broad frequency band,

b) to be a stable system,

c) to produce no enhancement at any frequency.

these objectives ideally should be met without the need for manual adjustment or re-calibration of the system. There are limitations on the physical realisability and complexity of the electronic system if it is to be implemented as an analog filter. However these limitations are not so severe if digital filtering is used. The advent of low cost, high speed microprocessors since the late 1970's has meant the application of digital filtering to the problem of ANC has now become economical. The superiority of digital filtering over that of analog indicates that a digital based system should give better performance. For this reason the results obtained from applying digital filtering to the problem of ANC are considered next.

It is hoped that the use of digital filtering will mean that it will be possible to design and implement an ANC system capable of working under widely diverse conditions, so that such a system will one day be available off the shelf. A system for widespread applications must be capable of giving a guaranteed level of performance in terms of attenuation and stability, and also it must be robust and reliable enough to work in adverse conditions. The system robustness will depend in part on the selection of suitable secondary source transducers to meet the particular environmental conditions.

One of the major advantages of digital filtering over analog is the relative ease with which it is possible to implement an arbitrary impulse response. The significance of this is that the transfer function(s) needed in the ANC system can be determined experimentally from the real system and then implemented directly using digital filter(s). This was recognised by Ross [16] [17] who developed an algorithm that could be used to determine the characteristic of the 'black box'. In his paper Ross advocated the use of system identification to find the properties required of the black box and its implementation as a fixed digital filter. The experimental results from applying his method to an air conditioning duct was attenuation of the order 15-20dB across the frequency range 25-350Hz. The input excitation signal was random noise, and the detector consisted of three microphones connected in a Swinbanks type arrangement. Ross was also successful in controlling the low frequency 1-dimensional sound field inside a large enclosure, using a single microphone and loudspeaker with a digital filter of order 20. The results showed that it was possible to obtain attenuation of the order of 10dB of the low frequency sound field in an anechoic test chamber [18].

The system used by Ross offered a significant increase in the level of attenuation obtained from an ANC system compared with that ever achieved from the use of analog filtering for the cancellation of broadband random noise.

La Fontaine and Shepherd [19] were also successful in applying digital filtering to the design of a 'black box' for broadband cancellation in a duct, using the Swinbanks arrangement to produce a unidirectional detector and secondary source. The black box was implemented as a transversal filter designed using complex Fourier analysis and a weighted least squares algorithm. With a random input excitation signal the system was found to give on average 20dB attenuation over the frequency range 20-750Hz.

In addition to producing a system that will be stable and capable of producing broadband attenuation there is the important question of how sensitive will the system performance be to parameter changes e.g. temperature, analog drift etc.. The applications of digital filtering discussed so far were all concerned with fixed filter implementations, with the implicit assumption that the system to be controlled is time invariant. However a real system may well be time varying. For such situations the black box needs to have self-learning capability enabling it to track parameter changes, so that the performance of the system may be maintained near its optimum level. The implication is that the black box needs to be adaptive.

1.3.2 Adaptive filters

Adaptive filtering leads to the possibility of a practical solution to the ANC problem, that will be capable of working in widely diverse situations, independently of whether the system is time varying or not. This is why adaptive filtering for ANC purposes has received considerable interest by recent researchers such as Ross, Warnaka, Roure, Burgess, Roebuck [20] [21] [22] [23] [24]. What follows is a brief review of the experimental results obtained from the application of adaptive filtering.

Ross [20] extended his algorithm so that the system could be self adaptive. The system did not adapt in a continuous fashion, but the digital filter coefficients were periodically updated to take account of parameter changes. When Ross experimentally applied his self adapted algorithm to the cancellation of a 1-dimensional sound field inside a wind tunnel with air flow, the system was capable of producing attenuation that was within 2dB of the theoretical optimum level. The system employed digital filters having a transfer function containing 20 poles and zeros, plus an extra filter to give delay, and the off-line system identification calculations to update the digital filter were done every 16 seconds.

A paper by Poole and Warnaka [21] discusses the realisation of a self adaptive system employing three adaptive transversal digital filters, using a modified Widrow-Hoff least mean square algorithm. A feedback filter is employed to preserve the system stability, a second filter is used to produce cancellation of the unwanted acoustic noise, and the third filter is needed to compensate or equalise the error signal, so as to turn this signal into a purely delayed version of the desired error signal. This extra delay is allowed for in the update algorithm. However the authors did not disclose any information regarding the order of digital transversal filters used, nor did they comment on the extent of the improvement of the system stability from using a parallel feedback filter. The system was reported as being capable of producing 20dB attenuation for broadband random noise.

Work carried out by Roure [22], produced a self adaptive system similar to that used by Ross. The experimental results show that the system produced attenuation of the order 20-25dB in a duct with air flow of 10 m/s at frequencies up to the duct first cross mode. The digital filter used was transversal and the update was done by a host computer. The author did not state what order of filter was used nor comment on the stability of the system.

The results quoted in this section mean that we can confidently look forward to the migration of ANC systems from the laboratory to the solution of real practical problems e.g. industrial air conditioning ducts etc. However the widespread application of ANC systems outside the laboratory may well depend on the development of continuously adaptive systems as only this type of system will be capable of tracking highly time varying systems. However it should be appreciated that there are problems associated with producing a continuously adaptive system, as opposed to having the system self-adaptive in an off-line manner. It is hoped that these problems can be overcome so that the use of ANC will one day gain widespread acceptance.

1.4 SCOPE OF THE THESIS

The superiority of digital filtering over analog has now been well established in the area of ANC. It is for this reason that it is the application of digital filtering to an ANC system that is considered in this thesis. In the review given in this chapter, the systems experimentally tested were assessed only in terms of attenuation, however it must be appreciated that the system stability is of paramount importance for a practical system (an unstable system is useless).

information concerning the relative stability of the various systems tested has not been published and it is therefore difficult to evaluate their performance for real practical situations, where system stability needs to be guaranteed. What has also been lacking is some quantitive information concerning the sensitivity of system performance to the amount of uncertainty present (e.g. parameter changes, disturbances). The problem of uncertainty can to a certain extent be overcome by using adaptive filtering but this introduces some problems of its own. For fixed filter implementation the sensitivity of the system to small parameters changes is an important question. There are also causal and stability constraints on the 'black box' in an ANC system, and in the published work reviewed here these have not been discussed in any detail.

It is with the assessment of performance of an ANC system in terms of attenuation, stability and sensitivity to the degree of uncertainty that the work in this thesis is concerned. The performance of an ANC system consisting of a single microphone and loudspeaker in an experimental wooden duct is evaluated and assessed in some detail. The design and implementation of the 'black box' needed to make the system is discussed. The black box is designed, using control theory to derive a design. The constraints of causality and system stability are addressed separately, by recognising that the black box needs a closed loop characteristic. The concept of

causality is important in connection with the feedforward path whereas the system stability depends primarily on the feedback path. Hence the two constraints of causality and stability can be dealt with separately. In this thesis the modelling is carried out using FIR system identification, to define the digital filter needed in each path.

Because of the complexity and the unknown nature of the transfer functions needed in the black box, there is a need to determine them experimentally by carrying out measurements on the system. To achieve this, a measuring system employing a TMS32010 digital processor was used to obtain appropriate signals and a least squares algorithm to determine the FIR filter coefficients. The advantage of this approach is that the performance of the system can be predicted easily before any installation costs have been incurred.

The physical system to be modelled is a continuous system, and the FIR filters are used in sampled data systems. With the two independent FIR filters needed in the black box realisation it is shown that there are two different possible ways of modelling the electroacoustic feedback path. In one, a hybrid configuration, a sampled data system is used to model the electroacoustic path independently of the sampled data system used for the feedforward path. In the other

configuration the feedback filter is all-digital and incorporates the analog filtering associated with the sampled data system in the feedforward path.

Results obtained from an experimental duct are presented. The system is assessed in terms of attenuation, stability and sensitivity to uncertainty for different orders of FIR filters. The results are presented for the two different ways of modelling the feedback path, and with three different termination conditions for the duct. The main conclusion drawn from these results is that the longer the FIR filters in each path the better the performance of the system. It has also been found that, for given lengths of FIR filters in the system feedforward and feedback paths, the performance is better using the hybrid configuration rather than the all-digital one.

CHAPTER 2

PRINCIPLES OF THE DESIGN OF AN ANC SYSTEM

2.1 - INTRODUCTION

In this chapter consideration will be given to both the design and the implementation of the black box needed in an ANC system. Using control theory a design formula is derived from various system frequency responses. The application of this design formula to some simple cases is considered and related to the approaches adopted by such authors as Olson [27, 28], Eghtesadi [6], Hong [5], Wheeler [43] and Trinder [8]. The black box is seen to have a transfer function characteristic of a closed loop system, suggesting the idea of implementing it using independent feedforward and feedback paths, and the implications of this type of realisation are discussed. For real systems, the difficulty of predicting the transfer functions needed in order to design the black box necessitates the carrying out of electrical measurements on the system to determine the transfer functions experimentally. A computer simulation of a way in which this can be achieved is described.

2.2 - DERIVATION OF SYSTEM RESPONSE

Figure 2.1 shows a basic ANC system in a duct. There is a loudspeaker (PS) acting as a primary source of unwanted sound. Note that the details of the primary source are not of prime importance as the ANC system is

independent of it. Next there is a detecting microphone, (D), to sense the primary sound field; the detected primary sound pressure signal is to be processed so that after injecting it back into the duct, using the secondary source loudspeaker (SS), the sound pressure at the monitor microphone (M), downstream of the loudspeaker, will by superposition be made identically zero. The processing of the signal is to be done by connecting a "black box" of transfer function $H_{BB}(w)$ between the detecting microphone and the loudspeaker (terminals 1 and 2). The purpose of this section is to derive an expression for the response required of this black box.

If $V_0(w)$, $V_1(w)$, $V_2(w)$ and $V_3(w)$ are the Fourier transforms of the voltages at points 0, 1, 2 and 3 respectively, the following transfer functions may be defined:

$$H_{01}(w) = \frac{V_1(w)}{V_0(w)} \quad \text{for } V_2(w) = 0 \qquad (2.1)$$

$$H_{03}(w) = \frac{V_3(w)}{V_0(w)} \quad \text{for } V_2(w) = 0 \qquad (2.2)$$

$$H_{21}(w) = \frac{V_1(w)}{V_2(w)} \quad \text{for } V_0(w) = 0 \qquad (2.3)$$

$$H_{23}(w) = \frac{V_3(w)}{V_2(w)} \quad \text{for } V_0(w) = 0 \qquad (2.4)$$

For the ANC system to make the sound pressure at the monitor identically equal to zero independent of the input to the primary source the transfer function of the path from primary source input to monitor output via the duct alone must be equal but opposite to the transfer function of the path between the same points via the ANC system. The transfer function of the first of these is, by definition, $H_{o3}(w)$. The second is more complex, involving as it does both the transfer function of the black box, $H_{BB}(w)$, and the effect of feedback between secondary source and detector. It can be expressed in terms of the previously defined transfer functions as:

$$H_{o1}(w)\left[\frac{H_{BB}(w)}{1-H_{21}(w)H_{BB}(w)}\right]H_{23}(w) \qquad (2.5)$$

Hence in order to achieve perfect cancellation the condition to be met is that:

$$H_{BB}(w) = \frac{-H_{o3}(w)}{H_{o1}(w)H_{23}(w) - H_{o3}(w)H_{21}(w)} \qquad (2.6)$$

This then, is the fundamental design formula for the transfer function of the "black box" for an ANC system.

Note that this expression implies two possible approaches, either:

i) detailed knowledge of the transfer functions of and between the transducers, or

ii) measurements on the system to obtain the various H's directly.

Note that the result is independent of the source producing the unwanted acoustic sound in the duct.

2.3 - APPLICATION TO SIMPLIFIED MODELS

2.3.1 - Unity feedback system

If the detecting and monitoring microphones and secondary source loudspeaker are placed in close proximity so that $H_{o1}(w) \sim H_{o3}(w)$, and $H_{e3}(w) \sim H_{e1}(w)$, then the required transfer function for the black box obtained by substituting into equation (2.6) will lead to the result that the system requires infinite gain.

This is the approach used originally by Olson, and more recently by authors such as Wheeler, Eghtesadi, Hong and Trender, who use terms of description such as "tight-coupled monopole" or "acoustic virtual earth".

The major drawback of any practical system based on this rationale is that in order for it to work anything like well the open loop gain must be high (to approach the theoretically required ∞), but this necessarily results in a system prone to instability. Indeed to achieve the best performance possible in any given situation demands that it be operated at the highest open loop gain

attainable, i.e. right on the edge of instability. Even when so operated, it may in fact produce no attenuation, depending on the transfer functions of its component parts.

There are some circumstances where the advantages of simplicity of such a system can be sufficiently attractive to outweigh its problems, such as in the active ear defender. Here the volume in which the field is to be controlled is small, so phase shifts are also small and may by careful choice of system components be contained within less than 180° over the passband of the system (e.g. Wheeler [43]), but even for this particular problem it is not viewed as an entirely satisfactory system.

2.3.2. - Infinite length duct

Consider the duct shown in fig. 2.1 to be lossless and infinitely long. The duct acoustic transfer functions can be modelled (below the cut-off frequency of the first cross-mode) as pure delays, so the various H's can be represented as follows:

$$H_{os}(w) = H_{ls1}(w)\exp(-jw(l_2+l_3+l_4)/c)H_{mic2}(w) \quad (2.7)$$

$$H_{o1}(w) = H_{ls1}(w)\exp(-jw(l_2/c))H_{mic1}(w) \quad (2.8)$$

$$H_{p1}(w) = H_{ls2}(w)\exp(-jw(l_3/c))H_{mic1}(w) \quad (2.9)$$

$$H_{FB}(w) = H_{LS2}(w)\exp(-jw(l_A/c))H_{MIC2}(w) \qquad (2.10)$$

where c= speed of sound in the duct.

Substituting (2.7) to(2.10) into (2.6) gives

$$H_{BB}(w) = \frac{1}{H_{MIC1}(w)H_{LS2}(w)} \left[\frac{-\exp(-jwl_B/c)}{1-\exp(-2jwl_B/c)} \right] \qquad (2.11)$$

From this expression it can be seen that the black box required is the cascade of two transfer functions, the first of which compensates for the transducers in the feedforward path, while the second (in the square brackets) is equal to

$\frac{-1}{2j \sin(wl_B/c)}$, the expression previously derived by, e.g. Leventhall and Eghtesadi (6).

2.4 - TOPOLOGY OF BLACK BOX IMPLEMENTATION

2.4.1 - Feedforward filter

There are a number of different possible configurations for implementing the black box transfer function. The simplest approach is to implement it as a single feedforward filter as shown in figure 2.2(a). Because the resulting filter will have to duplicate the impulse response of a system having feedback (see equation 2.6), then the required filter will in general have to have a very long duration in order for it to be a good match to the required response.

Another problem with this type of implementation is that the closed loop formed by the feedback path between secondary source and detector in cascade with this feedforward-only approximation to the characteristic required for the perfect black box may well prove to be unstable.

2.4.2 - Recursive filter

The problem of instability may be overcome by adoption of one of the configurations shown in figure 2.2b and 2.2c. These are alternative implementations of a general recursive filter and provided the feedback section is made to have a transfer function equal but opposite to that of the electroacoustic system with which it is in parallel, the resulting system will be unconditionally stable.

For the configuration in Figure 2.2b this implies that:

H_{FB} must equal $-H_{e1}$ (2.12)

Since the overall transfer function of the filter is equal to $H_{FF}/(1-H_{FF}H_{FB})$, substitution in (2.6) yields the result that:

$$H_{FF} \text{ must equal } \frac{-H_{o3}}{H_{o1}H_{e3}} \quad (2.13)$$

For the configuration shown in Figure 2.2c, in order for the recursive part of the filter to cancel the acoustic feedback:

H_{RF} must equal $-H_{21}H_{FW}$ (2.14)

The overall transfer function of this filter is equal to $H_{FW}/(1-H_{RF})$, and substituting this into (2.6) and (2.14) yields the same result for H_{FW} as was obtained for H_{FF} in (2.13). Hence the requirement on H_{RF} is that:

$$H_{RF} = \frac{H_{21} H_{03}}{H_{01} H_{23}} \qquad (2.15)$$

2.4.3 - Comparison of implementations

It has been seen in section 2.4.1 that a feedforward-only implementation leads to a system whose stability is not necessarily well assured. This leads to the conclusion that one or other of the recursive schemes, which can be arranged to give assured stability, is a better candidate for a practical system. As it was the intention of the present work to calculate the characteristics required for the black box implementation from measurements on the system the scheme of Figure 2.2b is preferable, as comparison of (2.12) and (2.15) shows that it is simpler to obtain an estimate of H_{FB} than of H_{RF}, while the requirements for H_{FF} and H_{FW} are exactly the same. Hence it was the filter configuration of Figure 2.2b that was used for the rest of the work described here.

Note that the assignment of transfer functions H_{FF} and H_{FB} as in (2.12) and (2.13) is not unique; it is a consequence of the decision to stabilise the system by

the use of parallel feedback.

2.5 - DIGITAL IMPLEMENTATION OF THE "BLACK BOX" FOR REAL SYSTEMS

2.5.1 - Introduction

Having decided to implement the black box as a combination of feedforward and feedback filter as shown in figure 2.2b, consideration will next be given to the use of digital filtering as a means of synthesising the required feedforward and feedback filters. To avoid aliasing effects a digital filter must have a analog anti-aliasing and re-construction filters on the input and output respectively. Both of these analog filters must have good low pass cut-off characteristics, so that for frequencies greater than half the sampling frequency, the filters will attenuate sufficiently to ensure that there will be negligible aliasing errors. The composite of the digital filter together with the two analog filters is called a sampled data system (see appendix B). Because of the necessity of employing these analog filters, there is the need to compensate for their effect if tight control of both amplitude and phase is required, as it is in order to achieve a satisfactory level of performance from an ANC system.

the way in which a sampled data system can be used to achieve the required black box feedforward and feedback paths is considered in the following section, for two alternative ways of synthesising the feedback filter.

2.5.2 - Alternative configurations for the digital filters

2.5.2.1 - Introduction

What will be considered in this section is the realisation of both the black box feedforward and feedback filters as sampled data systems. The principle behind two alternative ways of implementing the feedback filter is considered, one of which will be referred to as an "all digital system", and the other as a "hybrid system".

2.5.2.2 - All-digital system feedback cancellation

Figure (2.3) shows the layout for an ANC system in a duct with the black box realised as a single sampled data system. Following equation (2.12) the digital filter $D_{FB}(z)$ is required to cancel out all components due to feedback, by duplicating the inverted impulse response between the points 2 to 1 shown in figure 2.3. This feedback path is seen to incorporate the responses of all of the analog filtering associated with the feedforward sampled data system. This implies that the digital filter

$D_{FB}(z)$ is required to duplicate the response of this analog filtering together with the electroacoustic feedback path, between the secondary source loudspeaker and the detecting microphone. Note that the presence of the analog filtering in the feedforward sampled data system means that the closed loop via the feedback path will be bandlimited and therefore the digital feedback cancellation filter only need to work over a limited bandwidth.

2.5.2.3 - Sampled data system feedback cancellation ("Hybrid System")

As an alternative to using the all-digital arrangement to model the black box feedback path, it is possible to implement the feedback filter as an independent sampled data system (independent of the sampled data system providing the feedforward path) as shown in figure 2.4. The implication of this is that the effect of feedback between the secondary source and the detecting microphone is to be cancelled out by using an analog summer to add the outputs from the electroacoustic path and from the parallel feedback sampled data system. Perfect cancellation would require that the feedback sampled data system should duplicate exactly the inverted impulse response between the points 2 to 1 shown in figure 2.4, which is completely independent of the feedforward sampled data system.

Note that in this case the feedback filter $D_{FB}(z)$ will need to incorporate equalisation or compensation for all of the analog filtering of the feedback sampled data system. Also this hybrid system needs extra hardware to realise the two independent sampled data systems.

2.6 - PREDICTIONS FOR A SIMPLE FINITE DUCT

2.6.1 - Introduction

As can be seen from the previous section the component parts of the black box are required to model a combination of the electroacoustic transfer functions of the detector and secondary source and the acoustic transfer functions in the duct. Since these will in general be very complex and will vary widely with situation, the only realistic approach is to measure in some way the required responses and attempt to model these using digital filters.

However it is possible to obtain analytical results for the transfer functions required in the black box for a simplified model of the duct. The use of such a model is considered here, in order to gain an insight into the nature of the responses for the various filters required and to obtain a better understanding of how the system works.

To achieve this the four electroacoustic transfer functions $H_{O1}(w)$, $H_{O2}(w)$, $H_{E1}(w)$ and $H_{E2}(w)$ were calculated for a finite duct. These transfer functions were then used to specify the requirements of the black box feedforward and feedback paths. Also these transfer functions were used to specify the overall transfer function of the black box for feedforward-only filter implementation. Finally computer simulations of the impulse responses required for the black box feedforward and feedback paths are presented.

2.6.2.1 - Frequency response predictions for $H_{FF}(w)$ and $H_{FB}(w)$

The following expressions for the transfer functions necessary to design the black box for the set up shown in Figure 2.5 can be obtained by applying the principle of superposition and summing to infinity the geometric progressions obtained [44].

$$H_{O2}(w) = H_{T1}(w) \frac{C_2(w)C_3(w)C_4(w)\,[1+C_1(w)][1+C_5(w)]}{1-C_1(w)C_2^2(w)C_3^2(w)C_4^2(w)C_5(w)} \qquad (2.16)$$

where $H_{T1}(w) = H_{1S1}(w)\, H_{MIC2}(w)$

$$H_{O1}(w) = H_{T2}(w) \frac{C_2(w)\,[1+C_1(w)][1+C_3^2(w)C_4^2(w)C_5(w)]}{1-C_1(w)C_2^2(w)C_3^2(w)C_4^2(w)C_5(w)} \qquad (2.17)$$

where $H_{T2}(w) = H_{1S1}(w)\, H_{MIC1}(w)$

$$H_{PD}(w) = H_{T3}(w)\ \frac{C_4(w)\,[1+C_5(w)]\,[1+C_1(w)C_2^2(w)C_3^2(w)]}{1-C_1(w)C_2^2(w)C_3^2(w)C_4^2(w)C_5(w)} \qquad (2.18)$$

where $H_{T3}(w) = H_{LSP}(w)\ H_{MIC2}(w)$

$$H_{PM}(w) = H_{T4}(w)\ \frac{C_3(w)\,[1+C_1(w)C_2^2(w)]\,[1+C_4^2(w)C_5(w)]}{1-C_1(w)C_2^2(w)C_3^2(w)C_4^2(w)C_5(w)} \qquad (2.19)$$

where $H_{T4}(w) = H_{LSP}(w)\ H_{MIC1}(w)$

In the above expressions, the various C's are the in-duct transfer functions corresponding to propagation. Moving from left to right in figure 2.5 $C_1(w)$ represents the transfer function between the primary source (PS) via the left hand end of the duct back to the primary source position and includes the reflection coefficient of the left hand end of the duct. The transfer function $C_2(w)$ is directly between the primary source position (PS) and the detecting microphone (D) (which is the same as that from detecting microphone position to primary source position). Likewise $C_3(w)$ is defined as the transfer function directly between the detecting microphone position (D) and the secondary source position (SS), (the same as that from secondary source position to detecting microphone position). Similarly $C_4(w)$ is the transfer function from the secondary source position directly to monitoring microphone (M) or vice versa. Finally the transfer function $C_5(w)$ is the transfer function from monitoring microphone position back to itself via the right hand end of the duct, including the reflection coefficient of the right-hand end of the duct.

Substituting in terms of these four electroacoustic transfer functions into equations 2.13 and 2.12 respectively, gives the following expressions for the black box feedforward and feedback filter frequency responses:

$$H_{FF}(w) = H_{COM}(w)\frac{C_3(w)\,[1-C_1(w)C_2^2(w)C_3^2(w)C_4^2(w)C_5(w)]}{[1+C_3^2(w)C_4^2(w)C_5(w)][1+C_1(w)C_2^2(w)C_3^2(w)]} \quad (2.20)$$

where $H_{COM}(w) = 1/H_{MIC1}(w)\ H_{LS2}(w)$

$$H_{FB}(w) = H_{LS2}(w)H_{MIC1}(w)\frac{C_3(w)\,[1+C_1(w)C_2^2(w)][1+C_4^2(w)C_5(w)]}{1-C_1(w)C_2^2(w)C_3^2(w)C_4^2(w)C_5(w)} \quad (2.21)$$

In order to interpret these expressions, one needs to consider the individual acoustic transfer functions within in the brackets. Taking for example the response required for the parallel feedback filter, then it can be seen that this filter is required to do the following:

(a) Duplicate the frequency response for the transducers in the feedforward path,

(b) Cancel out the effect of various acoustic paths inside the duct.

The first term in square brackets in the numerator is due to the detecting microphone sensing the first reflection from the left hand end of the duct (corresponding to a delay of $2(l_1+l_2)/c$). Also this microphone will respond to the first reflection from the right hand end of the duct as shown by the term $[1+C_4^2(w)C_5(w)]$

(corresponding to a delay of $2(l_A+l_B)/c$). The denominator can be expanded using the binominal theorem, to illustrate the presence of multiple reflections via both ends of the duct (involving a propagation delay of l/c, where l is the overall length of the duct). This term describes the reverberation present in the duct due to reflection from both ends, and thus has a significant effect on the overall time duration of the impulse response corresponding to $H_{FB}(w)$ and hence the length of the impulse response of the feedback filter used to cancel the feedback path.

2.6.2.2 - Overall transfer function, $H_{BB}(w)$

What follows is a derivation for the requirement of the overall transfer function for the black box needed in a finite length duct. In section 2.2 the following expression was obtained for the black box transfer function:

$$H_{BB} = \frac{-H_{OB}}{H_{O1}H_{BB}-H_{OB}H_{B1}} \qquad (2.6)$$

From this expression, it can be seen that a knowledge of four electroacoustic transfer functions is all that is needed to specify the overall black box transfer function. Hence using equation (2.16)-(2.19), an expression for the black box transfer function can be obtained as follows.

The two terms in the denominator of equation 2.6 can be written down as:

$$H_{01}H_{23}=H_E\frac{C_2C_4(1+C_1)(1+C_5)[1+C_1C_2^2C_3^2+C_3^2C_4^2C_5+C_1C_2^2C_3^4C_4^2C_5]}{(1-C_1C_2^2C_3^2C_4^2C_5)^2} \quad (2.22)$$

$$H_{03}H_{21}=H_E\frac{C_2C_4(1+C_1)(1+C_5)[C_3^2+C_1C_2^2C_3^2+C_3^2C_4^2C_5+C_1C_2^2C_3^2C_4^2C_5]}{(1-C_1C_2^2C_3^2C_4^2C_5)^2} \quad (2.23)$$

Hence the difference between equations 2.22 and 2.23 is equal to:

$$H_E\frac{C_2C_4(1+C_1)(1+C_5)[(1-C_3^2)(1-C_1C_2^2C_3^2C_4^2C_5)]}{(1-C_1C_2^2C_3^2C_4^2C_5)^2} \quad (2.24)$$

where $H_E = H_{MIC1}\,H_{LS1}\,H_{MIC2}\,H_{LS2}$

Substituting back into equation 2.6, using equations 2.16 and 2.24 gives the following:

$$H_{BB} = \frac{1}{H_{MIC1}H_{LS2}}\left[\frac{-C_3}{1-C_3^2}\right] \quad (2.25)$$

Note that this expression is the same as equation 2.11, and shows that for a finite length duct the transfer function of the black box is dependent only in the transducers in the system feedforward path and the acoustic transfer function between the detecting microphone and secondary source. Hence it is independent of reflections from either end of duct and the overall length of the duct.

Thus it is seen that if the duct is finite in length then the requirements for the black box are, perhaps

surprisingly identical with those for the infinite length duct. It can, however, be explained because:

(a) no sound reaches the right hand termination when the system is working, hence its properties cannot affect the required properties for the ANC system and,

(b) reflections from the left hand end simply alter the primary source field to be cancelled and, as has been previously noted, the black box properties are independent of the primary source.

2.6.3 - Computer simulation of the impulse response needed for a digital system implementation

A computer program in Fortran was written to evaluate the electroacoustic transfer functions making the idealistic assumption that the complex reflection coefficient of each end of the duct was a constant independent of frequency and that propagation along the duct was non-dispersive and lossless. These assumptions make the problem simpler so that the ANC system can be simulated more quickly and easily whilst still retaining the major characteristics of the system.

2.6.3.1 - Analog filtering of sampled data system

The low pass analog filters needed in the sampled data system were modelled as three second order, low pass

filters cascaded with a first order high pass filter to form a bandpass filter. The analog filters therefore have an upper cut-off characteristic of 36dB per octave, and the cut off frequency was set to 350Hz. The first order high pass filter had a cut off frequency of 50Hz, because there is very little output from the ANC system below this frequency, due to the loudspeaker operating below its resonance. Note that for the sake of simplicity the transfer functions of the A/D converter and D/A converter needed in the realisation of a sampled data system were assumed to be unity. A Fortran computer program was used to compute the frequency response and the impulse response for the analog filters, and these are shown in Figure 2.6. Figure 2.7 shows the effect of cascading the anti-aliasing and re-construction filters with the loudspeaker response, and illustrates the bandlimiting effect associated with the ANC system feedforward path.

2.6.3.2 - Feedback filter impulse response

Using the analog filters described in the previous section, together with equation 2.21, it is possible to evaluate the impulse response required for the "all-digital" system configuration shown in Figure 2.3. Computer predictions were obtained for a duct of length 10m, with relative duct transducers spacings and reflection coefficients as given in table 2.1.

Table 2.1

Primary Source Near End Reflection Coefficient r=0.2 arg r=0.0 Primary Source Far End Reflection Coefficient r=0.8 arg r=0.0	
Relative Duct Spacings (m)	
L_1	0.0
L_2	3.0
L_3	1.0
L_4	4.0
L_5	2.0
L	10.0

The reason for choosing the duct to have a length of 10m was to make the duct length comparable to the length of the duct to be used in later laboratory experiments.

The program was used to find the impulse response required for the digital filter used for cancellation of the electroacoustic feedback. Initially the program was used to compute the feedback filter impulse response under the assumption that the duct was infinitely long, by setting the end reflection coefficients to zero.

The results obtained for the feedback filter impulse response is displayed in figure 2.8. As the duct is non reflective it means that the feedback filter needs only to model the impulse response due to all the transducers and analog elements in the feedforward path plus the acoustic propagation delay from the output from the secondary source loudspeaker to the input to the

detecting microphone. From the impulse response shown it can be seen that the system impulse response has a duration of the order of 50 samples at a sampling frequency of 1275Hz.

The computer program was then used to compute the feedback filter impulse response and frequency response when the duct had non-zero reflection coefficient for each end. The results are shown in Figure 2.9. The graphical display of the impulse response shows how this compensating filter reproduces in antiphase all the reflections in the electroacoustic feedback path.

Table 2.2 shows the transit times (in terms of the number of samples) for each reflection from either duct end that contributes to the electroacoustic feedback filter impulse response.

Table 2.2

Duct Reflections Transit Times Sampling Frequency fs = 1275Hz Reflection Coefficient from source near end r_1=0.2 arg r_1=0.0 Reflection Coefficient from source far end r_2=0.8 arg r_2=0.0		
Order of Reflection	Reflection Coefficient |r| arg r = 0.0	Duct Transit Time (No. of samples)
0	0.0	6
1	0.2	28
2	0.8	50
3	0.2	73
4	0.8	80
5	0.2	102
6	0.8	125
7	0.2	147

The impulse response lasts for a duration of approximation 180 samples before the reflections from either end decay to a insignificant level. The superposition of the filter response and that of the feedback path will ideally be zero for all time, and hence will isolate the feedforward filter from any information concerning sound that is radiated from the secondary loudspeaker toward the detecting microphone, preventing the system from going unstable due to continuous amplification of secondary sound radiation around the feedforward-feedback loop. Provided near-perfect cancellation of the electroacoustic feedback path can be achieved, then the feedforward filter can be designed under the assumption that there is zero feedback in the system.

However perfect working of the parallel feedback filter puts an added constraint on the realisation of the feedforward filter as was highlighted by Flockton [25]. In his paper he discusses the increase in complexity required in the realisation of the feedforward filter due to the prevention of any secondary loudspeaker radiation reaching the input to the feedforward filter. Provided the parallel feedback filter is working perfectly the input to the feedforward filter contains no information concerning the working of the secondary source, and hence the only way that the feedforward filter can cause cancellation of sound from this secondary loudspeaker is to have prior knowledge about the secondary sound field.

This added complexity will be shown in the next section when consideration will be given to the realisation of the feedforward filter impulse response.

2.6.4 - Feedforward filter impulse response

Figure 2.10 shows the impulse and frequency response of the feedforward filter for the same duct conditions as those used to obtain figure 2.9. It was obtained from 2.13 by substituting values obtained from 2.16 to 2.18.

Notice the similarity between the working of this filter and that of the feedback filter, in that the effect of reflections are clearly evident. The length of the required filter is seen to be significiantly increased in length compared to the order of feedback filter needed for the modelling of the electroacoustic feedback path.

Note that the responses shown here for the black box feedforward and feedback paths depend on the duct length, the positioning and responses of the transducers, and the reflection coefficients of the ends of the duct.

2.7 - SUMMARY

This chapter considered the design of a black box to make an ANC system in a duct. It considered different possible implementations of this black box. One particular implementation was decided upon, because of ease of implementation and the relatively assured stability of system that can be obtained. A consequence of the implementation chosen is that two filters are required, one to remove the effect of feedback, the other to produce cancellation at the monitoring microphone.

Computer simulation was used to assess the working of an ANC system. This was done mainly to gain information concerning the carrying out of electrical measurements on a real practical duct.

The added complexity of the feedforward filter due to the prevention of information about the secondary source behaviour entering the feedforward filter has been pointed out.

It must be realised that major simplifying assumptions have been used here to obtain estimates of the two independent feedforward and feedback filter responses. In real situations the transfer functions involved are much complicated but then it is possible to determine them experimentally by carrying out measurements on the system.

The use of system identification to obtain coefficients for FIR filters with which to make an ANC system will be discussed in the next chapter.

CHAPTER 3

SYSTEM MODELLING AND PARAMETER ESTIMATION

3.1 - INTRODUCTION

This chapter contains a summary of the ideas of linear system modelling and parameter estimation using a model reference approach. The application of these ideas to an ANC system is considered from both a theoretical and experimental viewpoint.

3.2 - SYSTEM MODELLING AND PARAMETER ESTIMATION

The term modelling is used here in the context that one can represent the parameters describing the dynamics of a system by a mathematical model, this model being obtained by suitable processing of data obtained by experiment. The problem then becomes that of using system identification for the purpose of estimating the parameters of this mathematical model, so as to achieve a certain level of performance (which can be measured by using some kind of error criterion). The way in which the parameter estimation can be done consists of three distinct choices [37]: (a) type of model to be used, (b) selection of a suitable criterion function, and (c) implementation of an algorithm. What follows is a brief discussion of the implications of these choices when developing and implementing a parameter estimation procedure for an ANC system.

3.2.1 - Types of model available

The model chosen to represent a real system can be either deterministic or probabilistic, linear or non-linear. Also there is the question whether the model should be time-varying or not, depending on how significantly the properties of the real system change with time. What is helpful when making the choice of a suitable model is to have some prior knowledge about the real system dynamics. It is true that all real systems are to some degree non-linear, probabilistic, and time-varying in nature. However if the system properties do not change significantly with time, then the system can in most cases be approximated to a sufficient degree of accuracy using a linear deterministic time-invariant model and this is the approach adopted here.

Given that the real system can be modelled by a linear time-invariant system, there are three distinct types of model that can be used for the purpose of parameter estimation. A brief description of each of these is given below.

The three models are called (from the nature of their Laplace (or z) Transform representation):
(i) all-zero, also called moving average (MA) or finite impulse response (FIR), having a transfer function of the form:

$a_0+a_1z^{-1}+a_2z^{-2}+.....a_mz^{-m}$ (3.1)

(ii) all-pole, also called autoqressive (AR), having a transfer function of the form:

$G/(1+b_1z^{-1}+b_2z^{-2}+b_3z^{-3}+...b_mz^{-m})$ (3.2)

(iii) pole-zero, or autoreqressive moving average (ARMA), having a transfer function of the form of the product of the MA and the AR model.

Both types (ii) and (iii) correspond to a model having an infinite impulse response (IIR).

For any linear time invariant system there is a minimum number of parameters needed to describe that system's dynamic behaviour adequately [33]. This is given by the number of poles and zeros in the system transfer function. It is obviously very desirable for computational purposes to be able to estimate accurately this minimum number. In practice, however, this is very difficult, especially when using a pole-zero model. One has to guess the order to be used in the estimation, and then use some error criterion to assess when to stop the estimation process.

However though a real system will almost always be a pole-zero system, nevertheless an all-zeros model can be used. Some of the estimated zeros will in fact be approximating the response due to the poles of the real system [46]. Obviously if the real system does contain a lot of poles, which cause the system to be very frequency selective, then the all-zero model will need to contain a

large number of zeros, especially as many zeros are required to approximate even a single pole to a reasonable degree of accuracy. This can be a real practical limitation on the use of an all-zero model in real time applications. Incidentally, a similar argument can be applied to the use of an all-pole model when the real system contains a large number of zeros (e.g. a system with a flattish frequency response).

3.2.2 - Choice of model for this work

From the three models discussed in the previous section, the all-zero (or moving average) has been chosen for the following reasons. This model can be realised as a finite impulse response (FIR) or non-recursive filter. Because there is no feedback involved this filter will be unconditionally stable. This is a practical advantage when compared to the recursive realisation for which the stability of the filter needs to be carefully considered. Also a FIR type filter is less susceptible to rounding errors due to truncation of the coefficients in comparison to a recursive (IIR) filter. Note, however, that one disadvantage of a FIR realisation compared to a recursive one is that the number of coefficients needed to achieve an adequate level of performance may be excessively high; this question of the necessary number of coefficients was one of the things to be studied here [41].

The way in which these coefficients can be estimated by performing some sort of fit to measured data, using an all-zero transfer function, will be discussed in the following section.

3.3 - PARAMETER ESTIMATION

3.3.1 - Time domain/frequency domain

Using system identification for the purposes of estimating the parameters of the FIR model, there is the choice of whether the estimation should be done in the time or frequency domain. This needs to be carefully considered in the light of any physical insights one has about the real system to be modelled.

For an ANC system in a duct, the problem is to specify the transfer functions or impulse responses in the feedforward and feedback filters in the black box.

The choice between frequency domain and time domain for the analysis is not clear cut, since the overall perceived effectiveness of an ANC system is dependent on the human subjective response. This would tend to imply that a weighted frequency domain approach would be the best, but that is relatively difficult to implement.

Much easier to implement, in that it gives values for the FIR filter coefficients directly, is a scheme involving identification in the time domain. This is the approach adopted here. The bandwidth of the system is controlled using the analog filters associated with the sampled data system implementation.

3.3.2 - Error criteria

Consideration must be given to the type of error criterion function used to assess the goodness of fit of the model. The criterion chosen should both lead to a unique solution and be mathematically tractable. The intention here was to use a deterministic signal, practically free from noise, as the input when undertaking system identification, and hence to obtain an output signal having similar properties. Under these circumstances the least square criterion is appropriate [36].

Having decided on an error criterion and a suitable model, the remaining problem is that of an efficient algorithm to estimate the coefficients of the FIR filters. Such an algorithm is considered in the next section.

3.3.3 - Choice of algorithm

Figure 3.1 shows a system with an unknown impulse response. When subjected to an input excitation x(n) (where n is a integer value), it produces an output y(n). Using the model reference approach, the problem is to estimate the coefficients of the FIR model that will minimise the mean square error between the output from the real system y(n) and that of the FIR model $\hat{y}(n)$. It is of interest to consider how the coefficients of the FIR model can be calculated from the knowledge of the two signals x(n) and y(n). If the autocorrelation of the input signal x(n) and the cross correlation between the two signals x(n) and y(n) are both known, then there is an efficient recursive algorithm available [39] to compute the impulse response of the FIR model for any given order. The efficiency of the algorithm is based on exploiting the Toeplitz nature of the matrix equations that have to be solved.

However this method cannot be used for a system where the correlation statistics are unknown. The problem then becomes that of estimating the correlation functions in order to obtain an approximate solution based on a finite duration measurement of the two signals x(n) and y(n). It is important that the approximate solution is calculated in an efficient manner, because a simple minded approach to the problem lead to a cubic relationship between the number of arithmetic operations

required and the number of coefficients being estimated. An efficient algorithm has been developed by Marple [38]. He demonstrates that although the cross correlation matrix involved is no longer Toeplitz, an efficient algorithm can still be obtained that minimises the total squared error between the signals $y(n)$ and $\hat{y}(n)$, using a finite duration measurement of the signal $x(n)$ and $y(n)$. In terms of efficiency the algorithm requires computional operations proportional to the square of the order of the FIR model, and storage of variables proportional to the order. This efficiency is the same as can be obtained when the autocorrelation and the cross correlation functions are known.

Marple's algorithm, coded as a Fortran computer program, was used for the work described below. The program asks what order of model is desired, and then calculates the FIR coefficients, and outputs a value for the residual energy error.

It is important to note that the algorithm will always give an estimated model that is causal, linear and time-invariant, even if the system to be modelled is in fact non-causal, non-linear or time-varying [35]. In any of these cases the FIR model obtained will not, of course, be a good approximation to the real system. On the other hand if the real system can be represented exactly by a FIR model, then the algorithm will find the exact solution, i.e. the error signal will be zero, if

the correct order is chosen. In all other cases, the solution obtained will be optimum with respect to the least square criterion.

3.4 - EXPERIMENTAL METHOD USED FOR SYSTEM IDENTIFICATION

3.4.1 - Experimental layout

Figure (3.2) shows a real continuous system to be modelled. Given the input continuous time signal (x(t)) that will be convolved with the real system's impulse response to obtain the output signal (y(t)), the objective is to estimate the system parameters that will minimise the least square error between the real output, y(t), and the output of the FIR model.

Because the estimated model is to be realised as a sampled data system the diagram also shows the analog interface needed in the input and output sides of the sampled data system. The interface on the input side consists of an anti-aliasing filter, a sample and hold and an A/D converter. Similarly on the output side there is a D/A convecter, sample and hold and a re-construction filter. The necessity for having analog filtering present means that the influence of this filtering on any measurements will need to be compensated for, if the whole system is to be a good approximation to the real continuous system that it is modelling. The way in which this can be achieved in practice is considered next.

3.4.2 - Signals required

The characteristic required for the digital filter can be obtained by applying the principle of superposition to the block diagram shown in fig. 3.3 to get the following expressions:

$$y(t) = g(t) * x(t) \qquad (3.3)$$

$$\hat{y}(t) = w(t) * h_{AD}(t) \qquad (3.4)$$

where $w(t)$ = sampled convolution of $x_m(t)$, and $d(t)$

$x_m(t)$ = bandlimited sampled version of $x(t)$

$d(t)$ = sampled set of filter coefficients

Taking the Fourier transform of (3.4) leads to:

$$\hat{Y}(w) = F(w(t))\ F(h_{AD}(t)) \qquad (3.5)$$

$$= F(x_m(t)*d(t))\ H_{AD}(w) \qquad (3.6)$$

$$= D(z)\Big|_{z=e^{jwt}} H_{AI}(w)\ H_{AD}(w) \sum_{m=-\infty}^{\infty} X(w-m2\pi/T) \qquad (3.7)$$

where T is the sampling interval.

Assuming $H_{AI}(w) = 0$ for $w > \pi/T$

and that

$$H_{AD}(w) \sum_{m=-\infty}^{+\infty} X(w - m2\pi/T) = 0 \text{ for } w>\pi/T$$

and

$$H_{AD}(w) \sum_{m=-\infty}^{+\infty} X(w - m2\pi/T) = H_{AD}(w)\ X(w) \text{ for } w<\pi/T$$

leads to:

$$\hat{Y}(w) = D(z)\Big|_{z=e^{jw}} H_{AI}(w)\, H_{AD}(w)\, X(w) \qquad (3.8)$$

For $Y(w)$ to equal $\hat{Y}(w)$ requires that:

$$H_{AI}(w)\, H_{AD}(w)\, X(w)\, D(z)\Big|_{z=e^{jw}} = G(w)\, X(w) \qquad (3.9)$$

However it is not possible (digitally) to measure $G(w)\ X(w)$, the only thing that can be measured directly is $y_1(n)$ a sampled version of the signal whose Fourier Transform is $H_{AI}(w)\ H_{AD}(w)\ G(w)\ X(w)$

Hence it is convenient to multiply both sides of (3.9) by $H_{AI}(w)\ H_{AD}(w)$ to obtain:

$$[H_{AI}(w)\ H_{AD}(w)]X(w)\ D(z)\Big|_{z=e^{jw}} = H_{AI}(w)\ H_{AD}(w)\ G(w)\ X(w) \qquad (3.10)$$

The left hand side of this equation is equal to the Fourier Transform of the signal $x(t)$ after it has passed twice through the analog interfaces, multiplied by the complex frequency response of the digital filter. Hence if $y_1(n)$ is the captured signal resulting from $x(n)$ being passed through the D/A interface (see figure 3.4a), the system $q(t)$ and the A/D interface, and $y_2(n)$ is the captured signal resulting from passing $x(n)$ twice through the D/A and D/A interfaces (see figures 3.4b and c), then:

$$y_2(n) * d(n) = y_1(n) \qquad (3.11)$$

Hence, given experimental values for $y_2(n)$ and $y_1(n)$, $d(n)$ may be estimated using the Marple system identification algorithm discussed above.

A sampled version of the frequency response of the digital filter D may also be found by taking the Discrete Fourier Transform of equation (3.11).

3.5 - SUMMARY

In this chapter, the basic ideas behind the use of system identification have been explained. The reasons for choosing an FIR models for the real systems and then estimating the parameters of this model using system identification, to minimise a least square (in the time domain) performance criterion function, have been discussed.

The choice of type of model and the performance criterion were made on the basis of a compromise between the level of performance achievable in principle, the complexity of obtaining estimates of the parameters for the model, and the difficulty of realising the resulting sampled data system.

The development and implementation of a recursive least squares algorithm to do the FIR parameter estimation have been described, and the procedure for a practical realisation have been discussed. The way in which this can be applied to the modelling of the electroacoustic feedback path in an ANC system will be considered in the next chapter.

CHAPTER 4

MODELLING AND PARAMETER ESTIMATION OF THE FEEDBACK PATH

4.1 - INTRODUCTION

The next two chapters consider the application of the ideas discussed in the previous chapters to a real ANC system in a duct. The practical aspects of the realisation of an FIR parameter estimation procedure are discussed. Of the two filters required in the black box realisation, it is the feedback cancellation filter which is the easier to deal with, so the estimation of the parameters required for this filters is discussed first.

Experiments were conducted using a wooden duct section. Both of the ways of modelling the feedback path described in section 2.5, the hybrid and the all-digital arrangement were studied.

4.1.1 - Equipment used

Both the measurements on the system to determine the characteristics required for the digital filters and the filters themselves were made using a Texas Instrument TMS32010 digital processor chip mounted on an E.V.M. evaluation board, interfaced to the real world via an A.I.B. analog interface board. The A.I.B. board contains an A/D and D/A converter with their associated logic. A schematic diagram showing the essential apparatus layout is given in figure 4.1. The E.V.M. incorporates a monitor program (in EPROM) and a supervisory microprocessor controlling the TMS320, and enables programs and data

from the TMS320 to be uploaded and downloaded from a host computer.

It is essential to take into account the effect of A/D and D/A converters, sample-and-holds, processing time, anti-aliasing and reconstruction filters, when calculating coefficients for the digital filters. By using the same system for both the measurements and the implementation of the digital filters, then it become unnecessary to compensate separately for these effects, so that tight control of both amplitude and phase can more easily be obtained. The anti-aliasing and reconstruction filters were adjustable low pass filters, one of which was a Norwegian Electronic type 723, and the other was a Barr and Stroud type EF3. These both have an 8-pole Butterworth characteristic.

A Ferranti 860XT personal computer was used as the local host computer for the experimental work. Programs for the TMS320 were assembled using a cross assembler on the College VAX 11/780 cluster, and downloaded as required to the E.V.M. via the Ferranti.

It is necessary to be able to process the measured signals to look at the various frequency spectra and frequency responses. This was done using the commercial software signal processing package ILS, on the PC, and it was using this package that many of the graphs in this thesis were drawn.

The package is designed to run on an IBM PC (or any compatible computer). The signal data is stored in disk files and the software can be used to perform such operations as spectrum analysis and digital filtering, as well as arithmetic operations. The results can be displayed graphically on the computer monitor, and hard copy can be obtained using a printer. The system uses two different types of files, 16 bit integer format is used for storing sampled data, while a 32 bit floating point format is used for storing the results of calculations on the data. A limitation of using the system on a PC, rather than a mainframe computer, is that it is not possible to take the Fast Fourier Transform (FFT) of a signal exceeding 512 points in length. Using this software package is much less time consuming than having to program directly all the required signal processing operations using a high level computer language like Fortran.

The duct used for all the experimental work reported here was made from 22mm chipboard, and its dimensions were 0.3mx0.25mx10.9m. The monitoring and the detecting microphones and their amplifiers were B & K types 4145 and 2609 respectively. Both the primary and the secondary sources were a KEF type B.139.B loudspeakers. The power amplifier used to drive these loudspeakers was a Crown dual channel amplifier type DC150A.

4.2 - PRACTICAL IMPLEMENTATION OF THE FIR PARAMETER ESTIMATION PROCEDURE.

4.2.1 - Introduction

In this section, consideration will be given to the choices that have to be made in order to achieve a practical realisation of the FIR parameter estimation procedure discussed in the previous chapter. It is necessary to consider the following factors: input excitation signal, sampling frequency, cut-off frequency and cut-rate of the analog filters associated with the sampled data system. These will be discussed, as well as the practical problems encountered in the realisation of a digital filter to model the electroacoustic feedback path.

4.2.2 - Choice of parameters of the sampled data system

4.2.2.1 - Preliminary experiment.

When using a sampled data system to duplicate the response of a real continuous system it is important that the sampling frequency be appropriately chosen, to take into account the operational bandwidth desired for the system and the computional load on the digital processor. It is essential when making the choice of sample frequency to have some prior knowledge about the real system. This information may be obtained either from knowledge of the individual components, as in the

prediction described in section 2.6, or by conducting experiments on the complete system. In the real situation it is the latter approach that is easier, so a preliminary experiment was conducted to find approximately the time length required for the ANC system feedback filter. This then enabled an estimate to be made of the number of coefficients needed for any given sampling rate.

A schematic diagram showing the experimental set up that was employed is given in figure 4.2. A is a storage oscilloscope, B a pulse generator, C a power amplifier, D the secondary source loudspeaker, E is the detector microphone and F its microphone amplifier. The ends of the duct were terminated using acoustic wedges made of mineral wool.

A short (10ms) rectangular pulse from the generator was applied to the loudspeaker through the power amplifier, and the signal detected by the microphone inside the duct was amplified and displayed on the storage oscilloscope screen. Because of the low energy level of the input pulse it was hard to distinguish exactly the length of the significant portion of the system impulse response, on account of noise contamination. However after looking at a few time records it was concluded that it had decayed to a low level within a time of 140-180ms.

4.2.2.2 - Choice of sampling frequency and anti-aliasing filters

The sampling theorem dictates that the sampling rate must be more than twice the highest frequency present in the input signal. This implies that in any real system the input signal must be low-pass filtered, so that it is well attenuated at and above half the sampling frequency, if the effect of frequency aliasing is to be minimised. For this reason the input anti-aliasing and the output reconstruction filter of the sampled data system were chosen to be 8th order, and the cut-off frequency for these filters to be 0.29 of the sampling frequency. This means that the input signal will be attenuated by about 42dB at half the sampling frequency. Since the cut-off frequency of these filters determines the effective bandwidth of the system it must be carefully chosen. For example, consider the duct used in the preliminary experiment, which had its first order mode cut-off frequency at approximately 572Hz. It would be desirable to have an ANC system that would work well up to very near this frequency, which would mean that the sampling frequency would need to be of the order of 2KHz. However when using the TMS32010 digital processor it becomes much more complex if the convolution summation is more than 128 points long (corresponding to a time duration of 64ms at this sample rate). Easily available clock rates using the TMS32010 analog interface board are integers powers of 2 times a base frequency, and the

possible rates in the range of interest were 611Hz, 1221Hz and 2442Hz. Of these a rate of 2442Hz would only permit an impulse response duration of about 52ms, very much less than the 140-180ms found by experiment to be the duration of the real impulse response. Alternatively if 611Hz were chosen, while the impulse response duration would be more than adequate, the operational bandwidth of the system would be less than one third of the ideal. Hence the sampling rate used throughout all of the experiments subsequently described was 1221Hz and the anti-aliasing and the reconstruction filters were set to cut-off frequencies of 350Hz.

4.2.3 - Choice of excitation for system measurements

It is important that the input excitation signal x(n) is well chosen if reliable results are to be obtained. A requirement for the signal is that the frequency content should be flat over a range greater than the bandwidth of the system under investigation. An obvious choice is to make the input a very narrow pulse, so that the response from the system is its impulse response [40][45]. Another type of input signal that could be used is bandlimited random noise. However these inputs suffer from one of two defects. In the case of the short pulse, the energy content is necessarily small when the amplitude is kept sufficiently low to avoid non-linear effects, while bandlimited random noise is not repeatable, so it is not possible to use signal averaging

to improve the signal to noise ratio of the measurements. A signal that has a flat easily-controlled spectrum and also a large energy content compared with its maximum amplitude is a linearly swept sine wave describe by the following expression:

$$\sin\left[\left(2\pi\left(\frac{f_2-f_1}{2T}\right)+f_1\right)t\right] \qquad (4.1)$$

where f_1 is the start frequency, f_2 the final frequency and T the duration of the sweep. It was this signal, cosine-tapered at each end to smooth the spectrum, that was used as the primary input excitation for experiments to measure the characteristics of the system.

4.2.4 - Details of the practical realisation

There are a number of points of detail that must be considered when effecting a practical realisation of the method of system identification described in the previous chapter. Using the TMS320 system allowed simultaneous generation of the excitation signal and capture of the system response. The operational steps to do this were as follows. First of all the excitation signal (swept sinusoid, generated using a Fortran program) was downloaded from the host PC into the TMS320 EVM memory. A TMS320 program was then run that successively output to the D/A and captured from the A/D, 512 samples. This procedure was repeated sixteen times

and the results averaged so as to enhance the signal to noise ratio. The captured response was subsequently uploaded from the TMS320 memory back to the host computer.

It is necessary to be careful when choosing the duration of the excitation and the duration of the capture of the response. If the input digital signal is of length N samples, and this signal is then convolved with a system whose impulse response is of duration M samples, the overall length of the output signal is M+N-1 samples. If the length of this signal exceeds the time duration of the capture, then it will be truncated, leading to distortion of the system frequency response [42]. In order to ensure that this does not happen, it is necessary to have some prior information about the duration of the impulse response of the system, in order that an appropriate length for the input transient swept sinusoid can be selected. It is also important that the system should return to a quiescent state before the capture process is repeated.

Based on the information obtained from the preliminary experiment the primary excitation was chosen to be a swept sinusoid with lower and upper cut-off frequencies of 50Hz and 350Hz respectively, and time duration of 210ms. This is shown, together with its spectrum, in figure 4.3. Since the sampling frequency was set to 1221Hz, and therefore the time duration of the

capture was 512/1221 = 419ms, the duration of that of the excitation was one half of the capture.

4.3 - INDEPENDENT REALISATION ("HYBRID SYSTEM")

4.3.1 - Introduction

This section contains the results of a study of the hybrid system configuration for the cancellation of the effect of feedback. An analysis is carried out, using a block diagram approach, to show which signals are required in order to calculate the model parameters for the electroacoustic feedback path. The way in which the signals were measured using the experimental duct is described. These signals were then used to predict the feedback cancellation performance that would be obtained using an FIR filter of lengths 61, 128 and 256 points respectively. Finally a comparison was done between the predicted and actual performance of a system using a 61 point filter.

4.3.1.1 - Choice of signals to be measured.

Figures 4.4 and 4.5 show the relationship between the sampled data system and the feedback path that it is intended to model.

The various steps required to capture signals from which coefficients for the digital filter of the

sampled data system may be obtained are shown in figures 4.6(a), (b) and (c). The signals $Y_{ss}(z)$, $Y_{s4}(z)$, $Y_{12}(z)$ in figure 4.6 are equivalent to $X(z)$, $Y_1(z)$ and $Y_3(z)$ respectively in figure 3.4. Hence substituting into equation [3.10], the following expresssion can be written down directly.

$$\left[H'_{A1}(w)H'_{A0}(w)\right]^{-1}Y_{ss}(w)D_{FB}(z) \Big|_{z=e^{jwT}} = H'_{A1}(w)H'_{A0}(w)H_{s1}(w)Y_{ss}(w) \quad (4.2)$$

Where $H'_{A1}(w)$ and $H'_{A0}(w)$ are the transfer functions of the analog interfaces and $H_{s1}(w)$ is the transfer function for the system electroacoustic feedback path. Substituting into equation [3.11] gives

$$y_{12}(n) * d_{FB}(n) = y_{s4}(n) \quad (4.3)$$

and by taking the Discrete Fourier Transform of equation (4.3), the transfer function of the digital filter required in the feedback cancellation sampled data system can be found. This sampled data system is required to model the duct electroacoustic path between the points 2 to 1 in figure 4.4. The frequency response of this can also be estimated directly from the sampled versions of the two signals $Y_{s2}(n)$ and $Y_{s3}(n)$ (Figure 4.6a), by computing their Discrete Fourier Transforms and dividing one into the other. This can then be compared with the response actually achieved by the finite duration response of the sampled data system.

4.3.1.2 - Experimental measurement of the signals.

The purpose of this section is to describe the signals obtained from measurements using the set up shown

in figure 4.7, details of which are given in table 4.1. The figure shows the various ways in which signals were injected into and captured from the real system in order to acquire all the signals shown in figure 4.6a-c.

Table 4.1
(with reference to figure 4.7)

Sampling frequency fs = 1221Hz
Duct cross section area A = 0.25x0.30m
Duct anechoically terminated at both ends
Microphones 1" B & K type 4145
Microphone amplifers B & K type 2609 Gain=20dB
Power amplifier DC150A Gain = -6dB
Primary and secondary source loudspeakers KEF type B139.B
Input low pass filter gain = 1.0 Cut-off frequency = 350Hz
Output low pass filter gain = 1.0 Cut-off frequency = 350Hz
Analog filter cut-off rate -48dB/octave

Duct Transfucers Spacing	(m)
L_1	0.93
L_2	0.80
L_3	6.85
L_4	1.27
L_5	1.05
L	0.91

where the various L's are as shown on figure 2.1.

Equation 4.3 shows that the transfer function of the digital filter is given by the ratio of the Discrete Fourier Transforms of the two signals $y_{e4}(n)$ and $y_{1e}(n)$ the transfer function of the physical system that is to be duplicated in inverted form by the complete sampled data system is given by the ratio of the discrete Fourier transforms of the two captured signals $y_{e3}(n)$

and $y_{22}(n)$. The four signals $y_{12}(n)$, $y_{22}(n)$, $y_{23}(n)$ and $y_{24}(n)$ are shown, together with their frequency spectra, in figure 4.8. These captured signals were then used to compute the required frequency responses for (a) the digital filter ($D_{FB}(z)$) needed in the feedback sampled data system, and (b) the duct electroacoustic feedback path that the feedback sampled data system is required to model. These frequency responses are shown in figures 4.9(a) and (b) respectively.

4.3.1.3 - FIR parameter estimation for the feedback filter.

In order to estimate digital filter coefficients suitable for putting in a finite length filter, the two signals $y_{24}(n)$ and $y_{12}(n)$ were used as input to the FIR algorithm, and estimates were found for the coefficients for filters of lengths 61, 128 and 256 points. These are shown in figure 4.10 together with their corresponding frequency responses. These frequency responses can be compared to the ideal frequency responses shown in figure 4.9(a). The difference between the responses is a measure of the error introduced by the finite duration of the impulse response estimate, and hence a measure of the quality of performance of the system.

The impulse and frequency responses for the total sampled data system using digital filters of

lengths 61, 128 and 256 points are shown in figure 4.12. These can be compared with figure 4.9(b) to see how well the sampled data system succeeds in modelling the feedback path that it is intended to cancel. The shortest filter model is too smooth in nature, but the 256 point model is almost indistinguishable over the passband. This is further demonstrated in the feedback cancellation responses shown in figure 4.11 (residual feedback/original feedback). Since the response is always less than 0dB it implies that even with the shortest filter reasonable modelling is obtained; with the longest filter typical feedback cancellation is around -40dB over the passband, meaning that the modelling is very good indeed.

The stability of the complete system will depend also on the gain of the feedforward path multiplied by that of the residual feedback path. Provided the feedforward gain is less than the attenuation shown in these results (and one would expect it to be typically of the order of 0dB) the whole ANC system will be stable.

The results so far give a prediction of how well a parallel compensating FIR filter could work; the next section describes the implementation of such a filter in a real system and thus gives an idea of the extent to which the predicted performance can be realised.

4.3.1.4 - Experimental implementation of a 61-point filter.

This section describes the experimental implementation of a 61 point FIR filter in a sampled data system to cancel the feedback path measured in the experiment of section 4.3.1.2. The extent of feedback cancellation actually achieved is compared to that predicted in the previous section. The experimental set up that was used is shown in figure 4.13.

The H.P. spectrum analyzer was used to generate random noise, bandlimited to the range 0-500Hz, which was fed through a power amplifier to the loudspeaker to produce a sound field inside the duct. The transfer function for the electroacoustic path was measured by capturing the signals at the terminals 2 and 1 using the spectrum analyzer and is shown in figure 4.14. Next the random noise signal was fed to the input of the sampled data system and the transfer function of the sampled data system was determined by comparing the signals at terminals 2 and 3. The result is shown in figure 4.15. If the system were perfect then these two transfer functions should be identical in amplitude and 180° different in phase. The two amplitude responses are shown super-imposed in figure 4.16, and can be seen to be very similar while it can be seen from figures 4.14(b) and 4.15(b) that the two phase responses do indeed differ by about 180°. The extent of the error was investigated by measuring the output from the summing amplifier (terminal

4). First of all the spectrum of the signal at terminal 4 was recorded with channel B of the summing amplifier disconnected (i.e. the output from the sampled data system disconnected), then the level at this point was again recorded but now with the sampled data system connected to channel B. The difference between the two frequency spectra (shown in figure 4.17) is a measure of the degree of cancellation achieved.

It can be seen that with the system working the reduction in the level of the captured signal is of the order of 15-20dB across the passband. This should be compared with the predicted level of 20-30dB (see figure 4.11(a). This is probably due to small differences between the conditions when the measurements were taken and when this implementation was done. It should also be noted that the predicted level was calculated using floating point arithmetic whereas the sampled data system used fixed point arithmetic.

The figures quoted for the amount of feedback cancellation were based on visual inspection of the graphs to determine an average value for the amount of cancellation across the design bandwidth of 50Hz and 350Hz.

The conclusion that can be drawn from this experiment is that, since cancellation is significant across the entire passband of the system, it might well

be adequate to ensure that a system that also included a feedforward filter would be stable and produce the desired level of attenuation of the unwanted noise in the duct.

4.3.2 - All-digital realisation

4.3.2.1 - Introduction

As described in Chapter 2, there are two possible implementation for the parallel feedback filter. The realisation described and tested in the previous section was the "hybrid" one; the alternative approach, to be described now, is the "all-digital" one. In this approach the parallel feedback filter modelling the electroacoustic feedback path also has to incorporate the analog filtering of the sampled data system associated with the feedforward filter.

4.3.2.2 - Measurement procedure.

Figure 4.18 shows the experimental set up used to measure the signals required in order to calculate coefficients for the feedback filter for this realisation. Initially the swept sine wave was output through one of the low pass analog filter to obtain a captured bandlimited digital signal $y_{BF}(n)$. This captured signal was then used to excite the system by injecting the analog reconstruction of this signal at terminal 2. The response to this signal was captured via terminal 1, giving the digital signal $y_{21}(n)$. The

digital transfer function for the electroacoustic feedback path is given by the ratio of the z-transform of these two captured signals. The impulse response and the transfer function obtained from the measured signals by direct FFT processing are shown in figure 4.19.

4.3.2.3 - Effect of filter length.

Once again estimates of the feedback filter impulse response for the filter length 64, 128 and 256 points, the two captured time series ($y_{BA}(n)$ and $y_{AF}(n)$) were obtained and are shown in figure 4.20. The predicted feedback cancellation is shown in figure 4.21.

The results for the all-digital case are similar in kind to those obtained for the hybrid realisation, but the modelling is less good for the same length of filter. This is due to the need for the digital filter to duplicate the response of the analog filters; this means that some of their length is already "occupied", and a given length filter is therefore less well able to model the electroacoustic path. This is discussed more fully in Chapter 6.

4.4 - SUMMARY

The results of using the FIR system identification method described here indicate that it can be used in practice to estimate the parameters of a real system, and also that this estimate can be used for control purposes. This use has been illustrated by applying the method to nullify the presence of the electroacoustic feedback path in a real duct.

The next chapter considers the design of the feedforward filter using the same FIR system identification method described in this chapter.

CHAPTER 5

MODELLING AND PARAMETER ESTIMATION OF THE FEEDFORWARD PATH

5.1 - INTRODUCTION

The previous chapter showed how the method of FIR system identification can be used to model a real system, the electroacoustic feedback path in a duct. This method is further developed here, to show how it can be applied to the design of the feedforward filter in the black box. The problem of the causality of this filter is addressed.

5.2 - EXPERIMENTAL MODELLING AND FIR ESTIMATION OF THE FEEDFORWARD PATH

5.2.1 - Causality constraint in feedforward path modelling

The need to make sure that a physical system being modelled by a sampled data system has a delay in excess of that due to the analog filtering of the sampled data system is discussed in appendix [C] ("Implication of causality for a digital based system"). The consequence of this for the feedforward filter in an ANC system in a duct is considered next.

The problem is to design the feedforward digital filter to be connected between the terminals (1) and (2) in figure 5.1 so that the acoustic signal received at terminal (3) is attenuated as much as possible. Provided

that there is sufficient distance (and hence delay) between the detector microphone and the secondary source, then the necessary digital feedforward filter will be causal and therefore physically realisable. In a duct ANC system it is possible to some extent to alter the distance, which is an advantage because it implies that the delay in the electroacoustic path may be chosen such as to ensure the causality of the filter. The major causes of delay in the electrical feedforward path are the anti-aliasing and reconstruction low pass filters. For the filters employed here (8th order, cut-off frequency equal to 0.29 of the sampling frequency) this causes a delay of the order of 8 sample periods. The detector microphone and secondary source loudspeaker also contribute to the delay; their contribution is about 2ms, ie. around 2 sample periods at the clock frequency used. Knowing the transducer spacings it is possible to compute approximately the delays in the acoustic system. For the test duct the acoustic delay between the detector microphone and the secondary source loudspeaker was about 24 sample periods; since this was much greater than the 10 period delay of the electrical components, the required filter was indeed causal.

5.2.2 - Choice of signals to be measured

We wish to specify the digital filter $D_{FF}(z)$ which when connected between points 1 and 2 in figure 5.1 will reduce the error signal to zero.

From figure 5.1 and 5.2, we can define the following discrete transfer functions analogous to the continuous transfer functions of equations 2.1, 2.2 and 2.4:

$$H_{o1}(z) = \frac{Y_{1o}(z)}{Y_{ss}(z)} \quad \text{with } Y_{ss} \text{ as input to PS and no input to SS} \qquad (5.1)$$

$$H_{o3}(z) = \frac{Y_{3o}(z)}{Y_{ss}(z)} \quad \text{with } Y_{ss} \text{ as input to PS and no input to SS} \qquad (5.2)$$

$$\text{and } H_{e3}(z) = \frac{Y_{3e}(z)}{Y_{1o}(z)} \quad \text{with } Y_{1o} \text{ as input to SS and no input to PS} \qquad (5.3)$$

To reduce E(z) to zero requires that

$$H_{o1}(z)\, D_{FF}(z)\, H_{e3}(z) = -H_{o3}(z) \qquad (5.4)$$

$$\text{Hence} \quad D_{FF}(z) = \frac{-H_{o3}(z)}{H_{o1}(z)\, H_{e3}(z)} \qquad (5.5)$$

This is directly analogous with equation 2.13 for the continuous system.

Substituting from equations (5.1-5.3) gives

$$D_{FF}(z) = \frac{-Y_{3o}(z)}{Y_{3e}(z)} \qquad (5.6)$$

Therefore measurement of the two signals $Y_{3o}(z)$ and $Y_{3e}(z)$ is all that is required in order to determine the digital filter characteristic for the feedforward filter.

5.2.2.1 - Experimental measurements of signals

The signal $Y_{ss}(z)$, is the same swept sinusoid used in the determination of the characteristic for the

feedback cancelling filter described in the previous chapter. This signal was passed through the duct between terminals 0 and 3 in figure 5.3 (the secondary source loudspeaker not being energised), to obtain the signal $Y_{30}(z)$. The same input signal $Y_{33}(z)$ was then passed through the duct between the terminals 0 and 1 to obtain the signal $Y_{10}(z)$, again with the secondary source not being energised. Finally, this signal $Y_{10}(z)$ was passed between terminals 2 and 3 (with the primary source not being energised) to obtain the signal $Y_{32}(z)$.

5.2.2.2 - Results

The captured digital signals (both time series and spectras) used in the determination of the feedforward filter are shown in figure 5.4. The impulse response and the transfer function for $D_{FF}(z)$ determined from the signal $Y_{30}(z)$ and $Y_{32}(z)$ by direct FFT processing are shown in figure 5.5(a). The impulse responses and transfer functions for FIR approximations to $D_{FF}(z)$ of order 256, 128 and 61 are shown in figures 5.5(b), (c) and (d) and can be compared to the response shown in figure 5.5(a).

The attenuation achievable with a given approximation to $D_{FF}(z)$, say $\hat{D}_{FF}(z)$, can be calculated from the expression

$$ATTN(z) = 20 \log_{10} \left[1+\hat{D}_{FF}(z) \left(\frac{Y_{32}(z)}{Y_{30}(z)} \right) \right] \qquad (5.7)$$

Predicting the attenuation achievable for filters of orders 256, 128 and 61 points, gave the results shown in figure 5.6(a), (b) and (c). These show that for a filter with 61 coefficients the attenuation is of the order 10-15dB across the pass-band of the system. Increasing the order of the filter to 128, the attenuation across the pass-band is approximately 25dB, and when further increased to 256, is of the order of 30dB.

5.2.3 - Conclusions

The results for all the filter lengths show that there is attenuation over the entire width of the pass-band of the system. Since the system is strongly bandlimited by the anti-aliasing and reconstruction filters (25dB down at 400Hz, and with a slope of -96dB/octave), outside the pass-band any signal passing through the feedforward system is very heavily attenuated and does not contribute to the sound field at the monitor.

5.3 - CAUSALITY CONSTRAINT ON FEEDBACK PATH MODELLING

It is convenient at this point to observe that the hybrid system for feedback cancellation (described in chapter 2) also imposes a causality constraint on the feedback filter. This is due to it having to compensate

for the anti-aliasing and reconstruction filters (section 2.5.2.3). However, unlike the feedforward filter, it does not have to compensate for the secondary source loudspeaker and detector microphone. Hence the constraint on the feedback filter is less severe than on the feedforward filter. Thus, provided the system parameters are chosen such that the feedforward filter characteristic is causal, then the feedback characteristic will be causal also. Note that the problem only arises with the hybrid system; with the all-digital one there is no causality problem at all as the digital filter is required to model directly a physically real, and hence necessarily causal, system.

5.4 CONCLUDING REMARKS

The causality constraint in the design of a digital filter on a sampled data system modelling the feedforward filter has been discussed.

It has been shown how, for an ANC system in a duct, sufficient delay can be incorporated into the physical system by suitable positioning of the detecting microphone relative to the secondary source loudspeaker. Similar arguments apply to the realisation of the feedback filter in a hybrid implementation sampled data system, but for an all-digital realisation there is no causality constraint on the feedback filter.

How good an approximation to the feedforward response required can be achieved in practice will depend on the length of FIR filter specified and the complexity of the acoustic system's response. In the case of an ANC system in the experimental duct the predicted level of performance using a feedforward FIR filter of lengths 128-256 points, was attenuation of the order 20-30dB across the frequency range of interest.

It has already been shown that by choosing the appropriate order of FIR filter to model the electroacoustic feedback path a significant level of cancellation of the electroacoustic feedback path can be achieved. However the system stability depends on the system open loop response, which incorporates the feedforward filter, so this feedforward filter will have an effect on system stability. Because of the non-ideal characteristic of the feedforward and feedback filter due to the necessity for truncation, the effect will depend on the length of each filter. This question of system stability is considered in the next chapter.

A similar argument can be applied to the level of attenuation that is achievable using a given feedforward filter, as the overall performance of the system will depend also on the effectiveness of the feedback filter. Here again there will be an effect due to truncation of the feedforward and feedback filter that will depend on their lengths; this is also considered in the next chapter.

CHAPTER 6

EVALUATION OF THE OVERALL SYSTEM PERFORMANCE

6.1 - INTRODUCTION

In the previous two chapters consideration was given as to how to realise an ANC system in a duct using two FIR filters. It has been explained in detail how to design the digital filters using FIR system identification and the way in which they can be realised has also been demonstrated. The predicted performance of the system incorporating a parallel feedback filter has indicated good system stability. The performance of the feedforward filter has been assessed assuming perfect cancellation of the feedback path and it has been predicted that the level of attenuation that can be achieved in the experimental duct using an FIR filter of length 128-256 points anechoically terminated at each end, is of the order of 20-30dB.

What will be considered in this chapter is the extent to which the non-ideal characteristics of the filters affect the system stability, and the level of attenuation that is achievable when they are taken into account. The stability is assessed by looking at the open loop response of the complete system while the attenuation is studied by considering the closed loop response and the sensitivity of this closed loop response to change in either feedforward or feedback transfer functions.

6.2 - DERIVATION OF EQUATIONS

6.2.1 - Introduction

The closed loop and open loop transfer functions of the system, and hence the level of attenuation, can be calculated in terms of the measured signals and the actual transfer functions of the feedforward and feedback filters.

6.2.2 - All-digital system

Figure 6.1 (which uses the same nomenclature as before), shows the transfer functions and the signals involved.

$H_{01}(z)$, $H_{03}(z)$ and $H_{23}(z)$ are as defined in equations 5.1-5.3 while $H_{21}(z)$ is defined (analogously to equation 2.3) as the ratio of the digital signal captured at terminal 1 in figure 5.1 to the digital signal injected at terminal 2 (with no input to terminal 0). Hence if the swept sinusoid $Y_{33}(z)$ is used as the input and the resulting captured output is $Y_{24}(z)$, then:

$$H_{21}(z) = \frac{Y_{24}(z)}{Y_{33}(z)} \qquad (6.1)$$

The block diagram shown in figure 6.1 can be simplified by presenting the overall transfer function of the system shown inside the dotted box as:

$$G_A(z) = \frac{\hat{D}_{FF}(z)}{1 - \hat{D}_{FF}(z)\,[\hat{D}_{FB}(z) + H_{21}(z)]} \qquad (6.2)$$

$\hat{D}_{FF}(z)$, and $\hat{D}_{FB}(z)$ are the actual transfer functions for the "black box" feedforward and feedback paths respectively, the approximations to the ideal $D_{FF}(z)$ and $D_{FB}(z)$.

Hence the following expression can be written down for the closed loop transfer function of the lower limb of figure 6.1:

$$G_{CL}(z) = \frac{H_{01}(z)\,\hat{D}_{FF}(z)\,H_{23}(z)}{1 - \hat{D}_{FF}(z)\,[\hat{D}_{FB}(z) + H_{21}(z)]} \qquad (6.3)$$

Substituting equations 5.1-5.3 and 6.1 into this gives:

$$G_{CL}(z) = \frac{\left(\dfrac{Y_{32}(z)}{Y_{33}(z)}\right)\hat{D}_{FF}(z)}{1 - \hat{D}_{FF}(z)\left[\hat{D}_{FB}(z) + \dfrac{Y_{24}(z)}{Y_{33}(z)}\right]} \qquad (6.4)$$

From equation 6.4, the system open loop response is:

$$G_{OP}(z) = \hat{D}_{FF}(z)\left[\hat{D}_{FB}(z) + \frac{Y_{24}(z)}{Y_{33}(z)}\right] \qquad (6.5)$$

The level of attenuation is given by:

$$ATTN(z) = 20\log_{10}[1+G_{CL}(z) / H_{03}(z)] \qquad (6.6)$$

so substituting from 5.2 and 6.4,

$$ATTN(z)=20\ LOG_{10}\left[1+\frac{\left(\frac{Y_{SP}(z)}{Y_{SO}(z)}\right)\hat{D}_{FF}(z)}{1-\hat{D}_{FF}(z)\left[\hat{D}_{FB}(z)+\frac{Y_{24}(z)}{Y_{SS}(z)}\right]}\right] \qquad (6.7)$$

Hence it is possible to predict the actual performance of the all-digital system designed on the basis discussed so far.

6.2.3 - Hybrid system

Similar expressions to 6.4, 6.5 and 6.7 may be obtained for the hybrid system and are as follows:

Closed loop response:

$$G_{CL}(z)=\frac{\left(\frac{Y_{SP}(z)}{Y_{SS}(z)}\right)\hat{D}_{FF}(z)}{1-\hat{D}_{FF}(z)\left[\frac{Y_{AR}(z)}{Y_{SS}(z)}\hat{D}_{FB}(z)+\frac{Y_{24}(z)}{Y_{SS}(z)}\right]} \qquad (6.8)$$

Open loop response:

$$G_{OP}(z)=\hat{D}_{FF}(z)\left[\frac{Y_{AR}(z)}{Y_{SS}(z)}\hat{D}_{FB}(z)+\frac{Y_{24}(z)}{Y_{SS}(z)}\right] \qquad (6.9)$$

Level of attenuation:

$$ATTN(z)=20\ log_{10}\left[1+\frac{\left(\frac{Y_{SP}(z)}{Y_{SO}(z)}\right)\hat{D}_{FF}(z)}{1-\hat{D}_{FF}(z)\left[\frac{Y_{AR}(z)}{Y_{SS}(z)}\hat{D}_{FB}(z)+\frac{Y_{24}(z)}{Y_{SS}(z)}\right]}\right] \qquad (6.10)$$

$Y_{AR}(z)$ is the signal obtained by passing $Y_{SS}(z)$ through the cascaded combination of the analog filtering associated with both the feedforward and

feedback sampled data system. This is because for the hybrid case $\hat{D}_{FB}(z)$ has to compensate for the feedback sampled data system analog filtering.

6.2.4 - Sensitivity

An ANC system should be assessed not only in terms of stability and attenuation, but also in terms of the sensitivity of the closed loop response to small changes in parameters in the feedforward and feedback paths.

We can define the term sensitivity as a measurement of the extent to which variation in the transfer function of a component part of a feedback system affects the closed loop transfer function of the complete system. The system sensitivity function for small changes in the system feedforward transfer function is defined as:

$$S_{HFF}(w) = \frac{\text{Percentage change in closed loop transfer function}}{\text{Percentage change in the feedforward transfer function}}$$

This section considers the evaluation of the sensitivity functions for the feedforward, residual feedback, and the real system feedback transfer function.

The closed loop transfer function for the ANC system can be written as (equation (2.5))

$$G_{CL}(w) = \frac{H_{O1}(w)\, H_{RR}(w)\, H_{P3}(w)}{1 - H_{RR}(w)\, H_{P1}(w)} \qquad (6.11)$$

Substituting for $H_{FB}(w)$ using equations 2.6, 2.12 and 2.13 and representing the residual feedback transfer function ($H_{FB}(w) + H_{21}(w)$) by T(w), this can be rewritten as:

$$G_{CL}(w) = \frac{H_{O1}(w)\ H_{FF}(w)\ H_{23}(w)}{1 - H_{FF}(w)\ T(w)} \qquad (6.12)$$

Using the analysis given in reference (32) (page 63), the system sensitivity functions for small changes in the two transfer functions $H_{FF}(w)$ and T(w) can be written down directly and are:

Feedforward sensitivity function:

$$S_{HFF}(w) = \frac{1}{1 - H_{FF}(w)\ T(w)} \qquad (6.13)$$

Residual feedback sensitivity function:

$$S_{T}(w) = \frac{-H_{FF}(w)\ T(w)}{1 - H_{FF}(w)\ T(w)} \qquad (6.14)$$

The same approach as used in (32) to derive these equations can also be used to obtain an expression for sensitivity to small changes in the acoustic feedback transfer function:

$$S_{H21}(w) = \frac{-H_{FF}(w)\ H_{21}(w)}{1 - H_{FF}(w)\ T(w)} \qquad (6.15)$$

Note that in the first two cases $H_{FF}(w)$ and T(w) only appear as the ANC open loop response, the product $H_{FF}(w)T(w)$, so the open loop transfer function is all that is needed in order to calculate closed loop sensitivity functions for both these cases. The results of doing this for attenuations between 1 and 50dB are shown in Table 6.1 and indicates how sensitive the ANC system will be to these parameters.

TABLE 6.1

EVALUATION OF SENSITIVITY FUNCTIONS

ATTN (dB)	$S_{HFF}(w)$	$S_T(w)$
1	9.195	8.195
2	4.862	3.862
3	3.424	2.424
4	2.710	1.710
5	2.285	1.285
6	2.005	1.005
7	1.807	0.807
8	1.661	0.661
9	1.550	0.550
10	1.462	0.462
20	1.111	0.111
30	1.033	0.033
40	1.010	0.010
50	1.003	0.003

For a system with very low residual feedback the open loop response will tend to zero, and therefore the system sensitivity function $S_{HFF}(w) \longrightarrow 1$, and $S_T(w) \longrightarrow 0$. This means that the system become directly sensitive to small changes in parameters in the feedforward transfer function and insensitive to small changes in the residual feedback transfer function.

A knowledge of all of $H_{FF}(w)$, $T(w)$ and $H_{FB}(w)$ is required to calculate the acoustic feedback sensitivity function, $S_{HFB}(w)$, and both $H_{FF}(w)$ and $H_{FB}(w)$ are dependent on the properties of the specific system. This means that, unlike the other two sensitivity functions, it is not possible to calculate values for

this sensitivity on the basis of attenuation alone. However it is possible for any given system to calculate this sensitivity function, as sampled versions of the three transfer function ($H_{FF}(w)$, $H_{FB}(w)$, and $T(w)$ can be obtained from the measured signals.

For the special case where there is very little residual feedback ie $H_{FF}(w)T(w) \longrightarrow 0$, then from equation 6.15 it can be seen that the system sensitivity function to small changes in the acoustic system feedback transfer function ($H_{FB}(w)$), tends to the value $-H_{FF}(w)H_{FB}(w)$.

6.3 CALCULATIONS ON EXPERIMENTAL DATA

6.3.1 Introduction

A series of calculations was performed in order to gain insight into the effect of filter length on the overall performance of the ANC system. Calculations, based on the equations in Section 6.2, were made for both the hybrid and all-digital implementations, and for three different types of duct terminations, anechoic/anechoic, anechoic/open and open/open.

It has already been shown that the end terminations influence the responses needed for the feedforward and feedback filters. It is the duration and

the detailed composition of the impulse responses that will determine what order of FIR filter will be needed for good modelling.

There are two extreme end termination conditions for a duct namely a) anechoic, b) perfectly reflecting. In practice it is not possible to have a perfectly anechoic termination, however acoustic wedges made from fibrous material can be used to reduce substantially the reflections from the end. This was done to the duct investigated previously to achieve an approximation to an anechoic termination. The other termination condition that was investigated was leaving the end of the duct open. Three different combinations of these terminations were used, namely anechoic/anechoic, open/open, and anechoic at the primary source end with the other end open.

The measuring procedure described in chapters 4 and 5 was used to capture the appropriate signals needed for FIR system identification. The same transducer arrangements were used as previously (table 4.1) and the gain settings of the microphone and power amplifiers were kept unaltered throughout all the measurements. This was done so that the results obtained would be directly comparable, in that the only difference between each set of measurements would be in the way that the ends of the duct was terminated. A complete set of measurements were taken one after the other for all three different duct

terminations to minimise the effects due to any time varying properties of the electroacoustic system (e.g. temperature, background noise level etc.).

6.3.2 Anechoic/anechoic terminations

6.3.2.1 Hybrid system

6.3.2.1.1 Open loop response

The FIR approximations for the feedback filter are shown in fig. 6.2 (b), (c) and (d) for filter lengths 256, 128 and 61 points respectively. The feedforward filter together with the various FIR approximations to it (already shown in Figure 5.6) are repeated here as Figure 6.3.

The system open loop response was calculated using equation 6.9, for various different length filters in the feedforward and feedback paths. If there were perfect cancellation of the electroacoustic feedback, the open loop gain would be zero (ie. $-\infty$dB) for all frequencies; the results actually obtained are shown in Figure 6.4. They show that using filters of lengths 256, 128 and 61 to model both the feedforward and the feedback paths, then the system maximum loop gain , given by the difference between the highest peak in the passband and 0dB, was of the order of -30, -25 and -18dB respectively, i.e. the gain is in each case much less than unity. Only

the gain of the open loop transfer function is important for assessing the stability of the system as the large amount of phase shift associated with the electroacoustic feedback path means that there will be a large number of frequencies where the phase shift around the loop is 180°, satisfying the phase condition for potential instability. When a feedforward filter of length 256 was combined with a 61 coefficient feedback filter the maximum open loop gain stability was of the order of -18dB.

6.3.2.1.2 Closed loop response

The closed loop response of the entire ANC system should be equal but opposite to that of the acoustic system alone. The computed closed loop response for systems employing feedforward and feedback filters both of lengths 256, 128 and 61 are shown in figure 6.5 (b), (c) and (d) and can be compared with the ideal response shown in figure 6.5(a).

6.3.2.1.3 Attenuation

The calculated attenuation graphs for the duct investigated (computed from Equation 6.10) are shown in figure 6.6 (b), (d) and (f) for feedforward and feedback filters both of lengths 256, 128 and 61. These graphs can be compared with those for feedforward filter lengths 256, 128 and 61 points but assuming perfect feedback cancellation (figures 6.6 (a), (c) and (e)).

The predicted level of attenuation achievable from an ANC system employing a feedforward filter of length 256, and a feedback FIR filter of length 61 is shown in figure 6.7.

6.3.2.1.4 Sensitivity

Using equation 6.13-6.15, it is possible to calculate values for the system sensitivity function ($S_{HFF}(w)$, $S_T(w)$ and $S_{H21}(w)$), using sampled versions of the transfer functions involved. These can be calculated using the measured signals and the feedforward and feedback filter responses. The calculated sensitivity functions for 256 point filters in the feedforward and feedback paths are shown in figure 6.8.

Note that the frequency responses shown for $S_{HFF}(w)$ and $S_T(w)$ do verify the argument advanced in section 6.24 that, for a system with little residual feedback, the two sensitivity function $S_{HFF}(w)$ and $S_T(w)$ will tend towards 1 and 0 respectively. It is interesting to compare the values for $S_{HFF}(w)$ and $S_T(w)$ in these graphs with those calculated from the open loop gain using equations 6.13 and 6.14. Table 6.2 (figure 6.14) shows the maximum values for the two sensitivity functions calculated from the worst case values of the open loop gain. There is good agreement between the values quoted in table 6.2, and the maximum values read off directly from figure 6.8.

The acoustic feedback sensitivity function $S_{H_{ae}H_{ae}}(w)$ shown in figure 6.8(c) is seen to show much greater variation with frequency compared with the feedforward and residual feedback sensitivity functions. Within the system passband the maximum value of this sensitivity function is 1.7, compared to 1.03 and 0.03 for the feedforward and residual feedback sensitivity functions.

6.3.2.1.5 Summary

For the duct investigated, having anechoic terminations and with the feedback filter realised as a separate independent FIR sampled data system, the maximum open loop gain is in the range -18 to -30dB, depending on the length of filter used. This means that significant changes in the feedforward and feedback paths can be tolerated without the system going unstable. However the effect on the system closed loop performance will depend on precisely what these changes are.

It was found that the sensitivity functions for small changes in the feedforward and residual feedback transfer functions were approximately 1 and 0 respectively. For small changes in the acoustic feedback transfer function the sensitivity function was seen to vary significantly with frequency, having a maximum value of 1.7, when employing filters of lengths of 256 points.

The predicted closed loop performance of the system shows achievement of a level of attenuation comparable to that which would be achieved if the feedback cancellation were perfect. The results indicate that for the duct investigated a feedback filter of length 61 may be sufficient to ensure a stable system (maximum open loop gain of the order -18dB) and similar attenuation will still be achieved to that which would be obtained using a much longer feedback filter.

6.3.2.2 All-digital system

6.3.2.2.1 Open loop response

A similar series of calculations were done for an all-digital implementation of the ANC system. The open loop responses using similar filter lengths (256/256, 128/128 and 61/64) are shown in figures 6.9 a, b and c. The maximum gain is of the order of -18, -12 and -8dB respectively.

The open loop gain for a system having a feedforward filter of length 256, and feedback filter length 64 is shown in fig. 6.9(d).

6.3.2.2.2 Attenuation

The calculation attenuations are shown in figures 6.10 (a), (b), (c) for feedforward/feedback filters of lengths 256/256, 128/128 and 61/64 points.

The attenuation from a system employing 256 coefficients for the feedforward filter and 64 coefficients for the feedback filter is shown in figure 6.10 (d).

6.3.2.2.3 Sensitivity

Carrying out the calculations discussed in section 6.3.2.1.4, but how for the all-digital system, gave the results shown in figure 6.11 for the three sensitivity functions. Notice that the maximum values of all three sensitivity functions are greater than their equivalents for the hybrid realisation.

6.3.2.2.4 Summary

For the all-digital system the predicted attenuation with filters of lengths 256/256, 128/128 and 61/64 is never less than 20, 15 and 3dB respectively. For the system using a 256 point filter in the feedforward path and a 64 point filter in the feedback path the attenuation is in excess of 15dB. Hence once again the attenuation achieved with a relatively short feedback filter is comparable to that which would be obtained if the feedback filter were very much longer, showing that all these lengths of feedback filter are able to model the feedback path sufficiently well to reduce significantly the influence of the feedback path on the closed loop system.

The maximum open loop gain of the system is of the order of -18, -12 and -8dB respectively, significantly poorer than in the hybrid realisation.

Using feedforward and feedback filters with only 61 and 64 coefficients respectively the level of attenuation is poor (figure 6.10(c)), and also the maximum open loop gain (8dB) is such that the residual feedback sensitivity function is relatively large, so the actual performance may differ significantly from the predicted. The 128 point feedforward/128 point feedback case is not vastly better, but for filters of length 256/256, the maximum open loop gain (-15dB) is at a more acceptable level and attenuation is in excess of 20dB.

As in the hybrid case, the system was found to have sensitivity function $S_{HFF}(w)$ and $S_T(w)$ approaching 1 and 0 respectively. The acoustic feedback sensitivity function $S_{HFB}(w)$ had a maximum value of 1.9, when using filter lengths of 256 or 128 points in the feedforward and feedback paths.

6.3.2.3 Comparison between the two realisations

For the duct investigated, anechoically terminated at both ends and employing the hybrid arrangement of filters, the length of filters required is of the order 128-256 points in order to achieve a satisfactory level of performance (i.e. capable of both giving a useful level of attenuation and also being reliably stable).

When the whole system is implemented as an all-digital filter, the lengths of filters needed in the modelling of the feedforward and feedback paths is of the order of 256 coefficients to achieve satisfactory performance. Thus the filters need to be longer for this configuration than for the hybrid system in order to achieve the same performance. A similar message may be obtained by looking at the sensitivity functions. For filters of the same length the sensitivity functions for the all-digital implementation are greater than for the hybrid case.

This difference in performance can be explained using the ideas in Appendix D which considers FIR models of an all-pole system and of the inverse of an all-pole system. For the all-digital realisation the feedback filter is required to duplicate the impulse response of an electroacoustic feedback path that includes the anti-alias analog filters and this adds 16 poles to the response being modelled. However in the hybrid realisation the feedback filter has to duplicate the convolution of the electroacoustic feedback path and an impulse response equal to the inverse of the analog filters. Hence the system contains 16 extra zeros rather than 16 extra poles, and hence the filter impulse response is shorter in duration, implying the need for less coefficients (see figure 6.12).

The same line of reasoning can be extended to the modelling of the feedforward path, where the filter is required to compensate not only for the analog filtering of the sampled data system, but also for the presence of the other analog elements needed in the feedforward path (microphone, amplifiers and loudspeaker).

6.3.3 Open/open terminations

A similar set of measurements to those carried out in the duct with anechoic terminations were repeated with the wedges removed. The open ends to the duct meant that there was more reflection of sound from the ends, and therefore the sound field inside the duct was more reverberant. It was thought that this would be a better approximation to a real duct.

Some of the recorded signals from the duct with open end termination are shown in figure 6.13. The system performance was assessed in the same way as previously using filters of lengths 256 and 128 points for the feedforward and feedback paths.

The system performance was predicted both for the hybrid filter arrangement and also for the all-digital system.

The results obtained are summarised in the table in Figure 6.14. The single figures quoted for the attenuation levels are typical figures for within the passband of the system obtained by visual inspection of the attenuation/frequency graphs. The figures for the sensitivity functions ($S_{HFF}(w)$ and $S_T(w)$) were obtained by substituting the values for maximum open loop gain into equations 6.13 and 6.14 and hence represent worst cases. The figures quoted for the sensitivity function ($S_{HFF}(w)$) were obtained by evaluating equation 6.15, as described in section 6.3.2.1.4 and looking for the maximum value.

6.3.4 Open end/anechoic termination

A third set of measurements were taken with the duct having one end open and the other (nearest the primary source) anechoically terminated using acoustic wedges of fibrous material. This was done in order to study a situation intermediate between the two previous cases. The system performance in terms of stability (open loop response) system sensitivity and level of attenuation (closed loop response) for both ways of implementing the feedback filter are summarised in Figure 6.14.

6.4 DISCUSSION OF ALL THE RESULTS

6.4.1 Open and closed loop responses

The results indicate that the performance of the ANC system deteriorated when the acoustic wedges were removed from the ends of the duct. This was to be expected on account of the more reverberant sound field inside the duct, which causes the ideal form for the impulse responses of the feedforward and feedback filters to be more complicated in nature and longer in duration. However for the duct investigated it transpired that for all three terminating conditions the impulse responses to be modelled were more or less contained within a time corresponding to 256 sample periods at the clock rate used, indicating that this number of points was adequate to achieve an acceptable level of performance. "Acceptable" here means a value for the system maximum open loop gain of -15dB, and a level of attenuation greater than 15dB.

6.4.2 Sensitivity functions

With one or both ends open the sensitivity functions tend to be larger, implying that the system is more sensitive to small changes in the feedforward and feedback electroacoustic transfer functions.

What one would like for an ANC system would be for all the sensitivity functions to be zero, making the system very insensitive to external parameter changes. However for the design discussed here the best that is possible is for the system to have a sensitivity function of unity for the feedforward path and zero for the residual feedback path. For the acoustic feedback sensitivity function it is not possible to give an "ideal" value for this realisation as it depends on the precise reverberation characteristics of the duct.

6.5 SUMMARY

It has been found that system performance was more significantly affected by the way in which the electroacoustic feedback path was modelled (i.e. as a hybrid or an all-digital system), than by the way that the ends of the duct were terminated.

To achieve satisfactory performance, the filters in the ANC system need to be quite long. The all-digital system had greater maximum values for the sensitivity function than the hybrid system for the same lengths of filters. This meant not only that such a system would be less stable but also that its real-life performance was more likely to differ significantly from that predicted.

Though the detail of the results presented here (for example the absolute lengths of the filters required to achieve a certain performance) relate only to the particular duct investigated, the general conclusions may be applied to any duct. The same approach can also be applied to any duct in order to specify the complexity of filters needed in order to achieve a given performance. Hence the methods described here may be used as a design tool to test the ability of a system of a given complexity to meet a given performance specification.

CHAPTER 7

CONCLUDING CHAPTER

7.1 INTRODUCTION

In this thesis the performance of a minimal ANC system consisting of a single loudspeaker and detecting microphone in a duct has been analysed and evaluated using FIR system identification. In section 7.2 the basic ideas behind the design and implementation of the ANC system are reviewed. The practical application of these ideas to a real system is then considered. The main conclusions from the experimental investigation of the system are discussed, in order to highlight the advantages and limitations of this method in producing a reliable stable working ANC system, capable of producing a guaranteed level of performance in a given situation. The chapter concludes with proposals for further work, extending and building on the work reported.

7.2 BASIC IDEAS

It has been shown that the basic problem is to specify the requirements of the 'black box' between the detecting microphone and the secondary source loudspeaker. Because the system has inherent feedback there is the possibility of instability, so the 'black box' must compensate for the effect of this feedback, whilst also ensuring that the system will have the transfer function needed for cancellation of the unwanted noise. In chapter 2 it was shown how control theory could

be used to design the black box. It was recognised that the black box had the characteristic of a closed loop system containing both a feedforward and a feedback path. This led to the idea of independently modelling the feedforward and feedback paths, and connecting these two paths in a feedback loop to synthesise the black box.

The stability of the ANC system is of major practical importance. The problem of stability is overcome by incorporating into the black box feedback path an inverted model of the real system feedback path to nullify the presence of the feedback. The real system feedback path was modelled using an FIR filter. Providing that sufficient cancellation of the feedback path is obtained the system will be guaranteed stable and the presence of the feedback path can be ignored. This means that the filter in the feedforward path (to achieve cancellation at the monitoring microphone position) can be designed under the assumption that there is no feedback at all.

If two independent sampled data systems (hybrid configuration) are used, to model separately the feedforward and feedback paths, there is a causality constraint on the realisation of both the filters. If an all-digital configuration is used then there is no causality constraint on the feedback filter, because it is modelling a completely causal system.

The overall performance of the system will depend on the complexity of the physical systems to be modelled, which will determine the order of FIR filters needed to obtain satisfactory performance. The complexity and the unknown nature of the transfer functions involved means that they can only be determined by carrying out measurements on the system. A measuring system was developed using the TMS320 processor. This same processor could be used for the implementation of the two FIR filters. The measuring system was used to measure signals for input to the FIR system identification algorithm.

7.2.1 Practical application (real duct)

7.2.1.1 Experimental work

In chapter 6, the results obtained from the experimental investigation into the performance of a minimal ANC system were analysed and evaluated in terms of system attenuation, stability, and sensitivity to uncertainty, for various orders of FIR filters. The performance of the system was assessed for the two different possible configurations (all-digital or hybrid). An idea of the effect of different end terminations on the order of FIR filters needed was obtained by evaluating the results obtained when the duct had three different end terminations (anechoic/anechoic, open/open and anechoic/open).

7.2.1.2 Main conclusions

The main conclusion to be drawn from the results presented in chapter 6 is that the system does work but in order to achieve a satisfactory level of performance the length of FIR filter needed in the feedforward and parallel feedback paths is long. The performance of the system is dependent on the way in which the duct is terminated, but the effect of different end terminations is less significant than the configuration used for the realisation of the feedback filter. It was found that for the hybrid system the performance is better than the all-digital system for the same lengths of FIR filters. Though these conclusions were derived from the particular experimental duct used, the following generalisation may be made: provided the feedback path to be modelled by the digital filter in a hybrid system is causal, then better performance will be achieved for the same length filters for a hybrid rather than an all-digital system.

7.2.1.3 Advantages and limitations of the system.

In this section, consideration will be given to some generalisations that can be deduced about the advantages and the limitations of an ANC system of the type described in this thesis.

7.2.1.3.1 Portability

One major advantage of the scheme and apparatus described is its portability, in that it can be used to assess the potential of using an ANC system before any costly installation work is done. The order of FIR filters needed for accurate modelling of both the feedforward and feedback paths can be obtained. The time varying properties of the real system can be assessed by repeating the measuring procedure several times to see how much the feedforward and feedback paths change with time.

It may be that the order of the FIR filters needed to achieve any worthwhile real time control for certain practical applications are found to be prohibitively high. It should however be noted that the speed and the amount of addressable memory of single chip digital signal processors are constantly being improved. For example the TMS32010, which was capable of doing a 128 point convolution within one sample period at the sampling rate of 1221Hz and was used for the work described in this thesis, has now been superseded by the TMS32020 which is able to implement a 256 point filter within the same sampling period. Texas Instruments, the manufacturer of the TMS320 series, have announced the development of another processor TMS32030, that will be more than three times as fast as the TMS32020. This processor is due on the market within the next year or so. The implications are that, in the not too distant

future, it will be possible to implement cheaply much higher order FIR filters in real time than is currently the case. Hence the system described in this thesis has the potential for future development as a stand-alone system for ANC application where the system is not significantly time varying.

7.2.1.3.2 Suitable model

As mentioned in chapter 3, for linear time invariant systems there are three possible models that can be used for the purposes of system identification. The model chosen for the work done in this thesis, was a Moving Average (MA) or FIR (all-zero) model. The choice of model depends on the complexity of the physical system to be modelled, and on how much prior knowledge there is available about the system. It may be that for applications where FIR modelling will lead to excessive demand on the processing power of the microprocessor system to be used, that the use of one of another type of model (AR or ARMA) should be considered. It should be noted that the use of an Autoregressive Moving Average Model of the "correct" order, will give the minimum number of parameters needed to completely describe that system. This can be a significant saving in terms of the digital processing requirements on the microprocessor to be used, in comparison to FIR modelling. Whether an AR or ARMA model should be chosen will depend on other factors beside that of the computational load on the microprocessor. One of these is the need to constrain

these models to be stable, whereas the FIR model is unconditionally stable. The choice of a suitable algorithm is also important. The point to be made here is that for situations where the order of FIR filters needed is excessively high, then the captured signals used here in the FIR algorithm can be used instead in either an AR or ARMA system identification algorithm. Thus the same captured signals can be used in different algorithms to assess the relative performance of each in modelling the required filters.

7.2.1.3.3 System sensitivity

A major practical limitation of using a system modelling approach is the sensitivity of the system to small parameter changes. This can mean that even with initially accurate models for transfer functions involved, the actual system performance may deviate quite significantly from what has been predicted.

For the ANC system used in this thesis, it was found that, with perfect cancellation of the electroacoustic feedback path, the system has a sensitivity functions of unity for the feedforward path. This implies that small changes in the feedforward path directly affect the output from the system and hence the level of attenuation achievable. Because the sensitivity to the residual feedback path was close to zero, however the system will be less sensitive to small changes in this. However the experimentally observed values of the

order of unity for the acoustic feedback sensitivity function imply a similar sensitivity to changes in this path as to the feedforward path.

7.2.1.3.4 Adaptive filtering

If the physical system has slowly time varying properties then the possibility exists of repeating the FIR system identification measuring procedure at intervals to take account of variations in the system dynamics. This type of off-line data analysis can be used to update the system to maintain the performance of the system near to its optimum designed level, provided that the system parameters vary slowly enough. An example of the application of this principle of self-adaptive system to the ANC problem is given in the references [20] [21] [22]. The ANC system used in this thesis is directly amenable to development as such a self-adaptive system.

If the system to be modelled has properties that are highly time varying, then it may be possible to track these properties by using adaptive filter(s) with coefficients altering in a continuous fashion [29]. There are however a number of practical problems that need to be overcome if continuous adaptive filtering is to be used in ANC systems [21] [25] [30].

The necessity to carry out some measurements on the acoustic system for the purposes of estimation is a common feature of both the fixed digital filter

realisation used in this thesis and of adaptive systems. It is another advantage of the measurement method described here that it can be used in order to estimate the order of FIR filter needed in an adaptive system.

7.2.2 Future work

The following section contains proposals for future work, based on the work already described.

(a) On-site (away from the laboratory) evaluation of the system performance for the solution of some real practical problems (e.g. an industrial air conditioning duct, etc.).

(b) Extending the method of FIR system identification to the control of three dimensional acoustic sound fields (e.g. small enclosures and free space).

(c) Evaluation of the performance of the system described for controlling mechanical vibrations and periodic noise sources.

(d) Assessment of the use of different time invariant models (i.e. different system identification algorithms) for ANC applications.

(e) Development of continuously or block adaptive systems.

7.2.3 Summary

FIR system identification for designing an ANC system has been successfully applied to an experimental wooden duct. The two FIR filters needed to model the system feedforward and feedback paths were found to be relatively long due to reverberation, in order to achieve a satisfactory level of performance from the system. The constraints on the realisation of the two filters in terms of causality and stability have been discussed in some detail. The performance of the system has been evaluated and assessed in term of level of attenuation, stability, and system sensitivity to parameter variations.

The advantages and the limitations of the use of such an ANC system for widespread application have been discussed. It has been concluded that the ANC system used in this thesis is worthy of further development for applications where the system properties do not significantly change with time. For systems where the properties do change significantly, it has been proposed that the method should be further developed to make the system adaptive to take account of these changes, and so maintain the performance of the system near its optimum level.

APPENDIXES

APPENDIX A

Loudspeaker transfer function

A.1 Frequency response

The transfer function relating the input voltage to the output volume velocity for a loudspeaker is given by the Laplace Transform expression [34]:

$$H_{LS}(s) = \frac{s(ABl)}{(Z_E Z_m)+(Bl)^2} \qquad A.1$$

where $Z_E = R_E + sL_E$, $Z_m = R_m + R_r + s(m+m_r) + K/s$. The expression for the mechanical impedance can be simplified by assuming that the radiation impedence $Z_R = Rr+sMr$ is so small that it can be neglected, so that $Zm = R_m + sm + K/s$. By substituting back into expression (A.1) it can be shown that the loudspeaker transfer function is given by:

$$H_{LS}(s) = \frac{s(U)}{s^3 a + s^2 b + sc + d} \qquad (A.2)$$

where $U = A\ Bl$

$a = mL_E$

$b = R_m L_E + R_E m$

$c = L_E K + R_E R_m + (Bl)^2$

$d = R_E K$

In this expression the denominator is a cubic equation. Equating the denominator to zero and calling the roots of

the equation d_1, d_2 and d_3 then the expression for H_{LS} can be re-written as:

$$H_{LS}(s) = \frac{s(U)}{(s+d_1)(s+d_2)(s+d_3)} \qquad (A.3)$$

This expression for the loudspeaker transfer function introduces the idea of using poles and zeros to describe the frequency behaviour of a system in the s plane. The loudspeaker is an example of a third order system, containing three poles and three zeros (one at the origin and two at infinity). Known values of the loudspeaker's parameters can be used in the system characteristic equation (denominator equated to zero) to find the positions in the s plane of the system poles. Taking as an example the K.E.F. loudspeaker B139.B and using the data specification sheet (no. SP1044) to obtain numerical values for the system parameters, a computer program was used to evaluate the roots of the characteristic equation and gave the following results: d_1=-11232rad/sec, d_2=-534rad/sec, and d_3=-49rad/sec. Hence all the poles are simple and distinct. Their positions in the s-plane are shown in Figure A.1.

Knowing the positions of the poles and zeros the steady state frequency response of the system can be evaluated by substituting $s = jw$ in the system transfer function. This turns the Laplace transform into a Fourier transform. For the KEF loudspeaker the results are shown in figure A.2. This transfer function is seen to be far

from ideal as it introduces a significant amount of distortion of both the amplitude and the phase.

The graph also indicates the nature of system inverse transfer function that would be required for perfect compensation or equalisation of the loudspeaker response. The compensating network transfer function is given by $\frac{1}{H_{LS}(s)}$, implying that the inverse transfer function is required to locate zeros at the precise location of the system poles and poles at the system zeros. The problem here is that the inverse transfer function required is non-rational as the degree of the numerator exceeds that of the denominator. This type of transfer function cannot be synthesised by a physical system. However very often satisfactory pole-zero compensation can be achieve by incorporating extra poles into the non-rational transfer function to make it rational. The extra poles that are required to make the inverse system physically realisable should be located far enough from the system dominant poles so as not to alter significantly the performance of the system. Thus it is possible in practice to make a good approximation to the inverse of a system transfer function using the method of pole-zero matching. One drawback on this method is that is that the exact location of the real system poles and zeros need to be found, and then it must be assumed that these position are fixed and will not vary with time.

A.2 - Impulse response

The system behaviour can also be described in the time domain by its impulse response, which is the inverse Laplace transform of the system transfer function i.e. $h_{LS}(t) = L^{-1}H_{LS}(s)$. Hence the loudspeaker impulse response is given by the Inverse Laplace Transform of:

$$h_{LS}(t) = L^{-1}\left[\frac{s(U)}{(s+d_1)(S+d_2)(s+d_3)}\right] \qquad (A.4)$$

The 3rd order transfer function, containing three simple distinct poles, can be re-written as the sum of three first order terms:

$$\frac{s(U)}{(s+d_1)(s+d_2)(s+d_3)} = \frac{A}{(s+d_1)} + \frac{B}{(s+d_2)} + \frac{C}{(s+d_3)} \qquad (A.5)$$

It can be shown that the coefficients A, B and C are given by the following expressions:

$$A = \frac{-d_1 U}{(-d_1+d_2)(-d_1+d_3)} \qquad (A.6)$$

$$B = \frac{-d_2 U}{(-d_2+d_1)(-d_2+d_3)} \qquad (A.7)$$

$$C = \frac{-d_3 U}{(-d_3+d_1)(-d_3+d_2)} \qquad (A.8)$$

so now the loudspeaker impulse response is given by:

$$h_{LS}(t) = L^{-1}\frac{A}{(s+d_1)} + L^{-1}\frac{B}{(s+d_2)} + L^{-1}\frac{C}{(s+d_3)} \qquad (A.9)$$

The inverse Laplace transform for each term can be obtained from tables to give the following expression for

loudspeaker impulse response:

$$h_{l\_s}(t) = Aexp(-d_1 t)+Bexp(-d_2 t)+Cexp(-d_3 t) \qquad (A.10)$$

Hence the system impulse is the sum of three exponential terms. For the KEF loudspeaker the following expression for the impulse response was calculated:

$$h_{l\_s}(t)=-0.409\times10^{-4}exp(-11232t)+0.448exp(-534t)-0.389exp(-49t) \qquad (A.11)$$

A plot of this is shown in figure A.3.

APPENDIX B

Digital Filtering and Sampled Data System

A continuous system transfer function can be approximated to a good degree of accuracy using a sampled data system incorporating a digital filter. The digital processor is the central part of any sampled data system. It is required to operate on digital input samples to produce the correct output samples.

The need to sample the input signal and convert this into numbers for operation on by the digital processor necessitates the use of analog hardware. This consists of two parts:

a) an input section consisting of an anti-aliasing filter followed by a sampler and coder,

b) a decoder and reconstruction filter to eliminate the effect of the sampling process.

For a causal digital filter the system transfer function is given by the following expression:

$$D(z) = \frac{a_0+a_1z^{-1}+a_2z^{-2}+.....a_mz^{-M}}{1+b_1z^{-1}+b_2z^{-2}+.....b_nz^{-N}} \quad \text{where } N>M \qquad (B.1)$$

The above expression is analoguous with the continuous system where the transfer function was written in terms of poles and zeros. In the digital case the a's and b's specify the system transfer function zeros and

poles respectively. Consider the case where the digital filter has no poles (except at the origin in the z-plane (trivial poles). These do not alter the magnitude of the filter response but do introduce a linear phase shift corresponding to extra delay). All the b's will be equal to zero and hence the transfer function is given by

$$D(z) = a_0+a_1z^{-1}+a_2z^{-2}.....a_mz^m \qquad (B.2)$$

and will contain only zeros.

Taking the inverse z transform of the above expression gives the following expression for the filter impulse response coefficients:

$$a_0(0T),\ a_1(1T),\ a_2(2T).....a_m(mT) \qquad (B.3)$$

where T is the sampling interval.

Since the impulse response of such a filter is bounded in time, it is called a finite impulse response (FIR) filter. Such a filter is unconditionally stable.

APPENDIX C

IMPLICATION OF CAUSALITY FOR A DIGITAL BASED SYSTEM

C.1 - INTRODUCTION

The purpose of this appendix is to illustrate some of the constraints that causality imposes on the use of sampled data systems for real time control. Sampled data systems have to employ analog filters for anti-aliasing and reconstruction and these introduce unavoidable delay. It is shown here that one can in a simple way get an approximate value for the delay due to the analog filtering. The necessity of incorporating sufficient delay into the physical system to be controlled is illustrated by an experiment involving the modelling, by a sampled data system, of a pure time delay.

C.1.1 - Calculation of the time delay through an n-pole analog filter

The phase delay and group delay of a linear system are defined by the following expressions:

$$\text{Phase delay} \quad t_p = \frac{-\theta(w)}{w} \qquad \text{(C.1)}$$

$$\text{Group delay} \quad t_g = \frac{-d\theta(w)}{dw} \qquad \text{(C.2)}$$

If the phase shift is linear with frequency, tp and tg will both be constant, and equal to each other.

Since each pole in a filter's response introduces an extra $-\pi/4$ phase shift at the pole frequency, it follows that an n-pole filter, all of whose poles are around angular frequency w_c, the total phase shift across the frequency range $0-w_c$, will be of the order of $-n\pi/4$.

Hence, from equations C.1 and C.2, the group delay

$$t_g = \frac{+ n \pi/4}{w_c} = \frac{+ n}{8 f_c} \qquad (C.3)$$

where f_c is the cut-off frequency of the filter.

This expression can be used to give an approximate value, for the delay through an n-pole low pass analog filter. It should be appreciated that in a practical filter the phase shift is not strictly linear, especially near the cut-off frequency, but a useful estimate of the delay introduced by the filter across its passband may be obtained.

C.1.2 - Calculations for the experimental system used

The input and output analog filters were both 8th order and had the same cut-off frequency of 350Hz. Substituting these values into equation C.3, gives a

value for the delay of about 5.7ms, or about 7 sample periods for a system with a sampling frequency of 1221Hz.

Delays of up to 1 sample period will also arise from the sample and hold and A/D converter, and there will also be a processing delay associated with the digital processor which must also be allowed for.

Hence if such a sampled data system is to be capable of providing a good model of a certain physical system, that physical system must have an inherent delay greater than 8 sample periods.

C.2 - MODELLING AND FIR ESTIMATION OF A SIMPLE TIME DELAY

C.2.1 - Introduction

This section describes an experiment carried out to test the ideas advanced in the previous section. The system to be modelled was a pure time delay and the sampled data system employed a finite length filter. The experimental results demonstrate that there is a range of delay values over which good performance can be expected from such a system.

C.2.2 - Choise of signals required

Figure C.1 shows the various transfer functions and measured signals.

$G_t(z)$ is the transfer function of the discrete time delay system to be modelled, $H_{AI}(w)$ and $H_{AO}(w)$ are the transfer functions of the analog filtering associated with the sampled data system, and H_{AD} is the transfer function for the analog to digital conversion.

In order to reduce the error signal E(z) to zero, it is required that the two signals input to the summing junction should be equal but inverted with respect to each other. If $Y_{32}(z)$ is the result of passing $Y_{33}(z)$ through H_{AO}, H_{AI}, H_{AO} and H_{AD} and $Y_{30}(z)$ of passing Y_{33} through H_{AO}, H_{AD} and G_t, then the digital filter to be connected between terminals 1 and 2 must have a transfer function given by:

$$F(z) = -Y_{30}(z)/Y_{32}(z) \qquad (C.4)$$

The attenuation of $Y_{30}(z)$ obtained by employing a system of response $\hat{F}(z)$, approximating F(z), can be calculated from:

$$ATTN(z) = 20 \log_{10} [1+\hat{F}(z)\, Y_{32}(z)/Y_{30}(z)] \qquad (C.5)$$

C.2.2.1 - Experimental method.

The sequence of measuring operations was similar to that described in section 5.2.2.1. Figure C.2 illustrates the measurement sequence.

1) The swept sinusoid ($Y_{ss}(z)$) was downloaded to the TMS 320 digital processor memory and output through the sampled data system D/A converter, reconstruction filter and A/D converter to obtain the signal $Y_o(z)$.

2) Next the swept sinusoid $Y_{ss}(z)$ was passed through the D/A, analog reconstruction and anti-aliasing filters the A/D converter to give $Y_{1o}(z)$.

3) This signal, $Y_{1o}(z)$, was output through the D/A converter, reconstruction filter only, (not the anti-aliasing filter) and A/D converter to give the signal $Y_{2e}(z)$. (Note that the operation carried out on the signal in step 3 is identical to that in step 1, but carried out on $Y_{1o}(z)$ rather than $Y_{ss}(z)$.

4) Finally the effect of a perfect discrete time delay was produced by preceding $Y_{1o}(z)$ with an appropriate number of zeros to produce $Y_{3o}(z)$.

The signals Y_{3o} and Y_{2e} were then input to the FIR algorithm described in Chapter 3 to obtain values for the digital filter coefficients.

C.2.2.2 - Results.

The order of FIR filter in the sampled data system was chosen to be 256 coefficients. The different time delays used were 0, 4T, 6T, 8T, 12T, 16T, 32T, and 128T. The impulse and frequency responses obtained as approximations to the delay are shown in figures C.3, C.4 and C.5. Ideally the frequency responses should be flat in amplitude, while the phase should be linear with frequency, with a slope corresponding to the pure delay of n sample periods. How well the sampled data system modelled the different time delays can be seen from the graphs showing the level of attenuation (calculated using equation C.5) achievable by the system; these are shown in figure C.6.

They show that in order to achieve any useful attenuation the delay incorporated into the physical system needed to be of the order 6-8 sampling periods. For time delays less than six sampling periods little attenuation was achieved, and at certain frequencies there was enchancement.

The delay due to the analog filtering was estimated from the transfer function shown in figure C.5(c). It shows a phase shift of about -4π in 320Hz, which corresponds well to the figure of about 8 sample periods estimated in section C.1.2 from the simple arguments advanced there.

The attenuation graph for the modelling of a system with an 8 sample period delay is of the order 20dB across the passband of the system; increasing the delay to 12 sample periods increased the attenuation to approximately 30dB. Further increase in the pure time delay to 16, 32 and 128 sampling periods did not significantly alter the overall level of attenuation any further.

Thus, the introduction of excess delay into the physical system over and above the minimum needed to ensure that the requisite digital filter would be reasonably causal did not lead to significantly improved performance.

C.2.3 - Conclusions

If a sampled data system is to be used to model a real system, the delay in the real system must be greater than the delay from the analog filtering of the sampled data system, so that the digital filter will only need to model a causal system. A highly non-causal system can be modelled by modelling the causal part of the system impulse response only, but the performance of such a system will be poor. In a real situation two methods exists for improving matters; either the time delay in the real system must be increased or the delay through the analog filtering of the sampled data system must be decreased. This latter can be achieved by increasing the

bandwidth of the low pass analog filters, providing the clock frequency of the system is suitably increased, but it is not possible to alter the amount of delay through the parts of the real system whose bandwidth is fixed. This is true in particular, for example, for a loudspeaker.

Also increasing the sampling rate will mean that there is less time available to do the convolution summation required for the digital filter, so the order of filter attainable may be so restricted that its performance is severely reduced. Hence there is a compromise between sampling rate and the computional speed of the digital processor used to implement the filter.

APPENDIX D

Normal and inverse modelling of all-pole systems using FIR filters

D.1 Introduction

The purpose of this appendix is to demonstrate that to obtain good modelling of an all-pole system using an FIR filter will, in general, require a high order filter, whereas to model the inverse of such a system will in general only require a filter of low order. To show this, we take as an example [31] a second order low pass analog filter (i.e. a system containing two distinct poles, and two zeros at infinity), such as that shown in Figure D.1.

The Laplace transform for the filter is given by:

$$H_{L.P.}(s) = \frac{w_c^2}{(s + w_c)^2} \qquad (D.1)$$

where w_c is the filter cut-off frequency.

By using the method of partial fractions or a look-up table it is possible to transform the above continuous transform directly to the z-transform to obtain the following discrete transfer function for an equivalent discrete low pass filter having the same cut-off frequency $w_{c_d} = w_c$.

$$D_{LP}(z) = \frac{T^2 w_c^2 z e^{-w_0 T}}{(z - e^{-w_0 T})^2} \quad \text{where } T = \text{sampling period} \qquad (D.2)$$

Choosing w_c to be $\pi/2T$, (i.e. choosing the cut-off frequency to be equal to a quarter the sampling rate)

$$D(z) = \frac{\pi^2/4 \; z \; e^{-\pi/2}}{(z - e^{-\pi/2})^2} \qquad (D.3)$$

Letting $C = \pi^2/4$ and $a = e^{-\pi/2}$, this can be represented as:

$$D_{LP}(z) = \frac{C a z}{(z - a)^2} \qquad (D.4)$$

The characteristic equation for this is:

$$z^2 - 2a z + a^2 = 0 \qquad (D.5)$$

and the roots of this quadratic equation will give the positions of the system poles in the z-plane. It can easily be shown that the roots are:

$p_1, p_2 = a$ where $a = e^{-\pi/2}$

Hence the system transfer function can be represented in the z-plane as the pole-zero diagram shown in Figure D.2.

D.2 FIR Modelling of an all-pole system

Consider the modelling of the two pole low pass filter using an FIR filter.

The (causal) transfer function of the two pole

filter considered here can be synthesised by an FIR filter whose coefficients can be obtained by long division:

$$D_{LP}(z) = \frac{C\,a\,z}{(z-a)^2} \qquad (D.6)$$

$$D_{LP}(z) = ca\,z^{-1} + 2ca^2\,z^{-2} + 3ca^3\,z^{-3} + 4ca^4\,z^{-4} + \ldots\ldots\infty \qquad (D.7)$$

This illustrates the point that to model exactly an all pole system using an FIR filter requires an infinite number of coefficients in the impulse response.

D.3 Inverse modelling of an all-pole system

A partial inverse for any causal system can be always found, providing that there is sufficient delay between the input and output signals [(X(z) and Y(z) in Figure D.3], whether the real system is minimum or non-minimum phase.

To demonstrate what is meant by this, we take as an example the inverse modelling of the all-pole second order low-pass filter considered in the previous section. The system inverse is given by the reciprocal of the z-transform of the filter, i.e.

$$D_{LP}(z) = \frac{(z-a)^2}{C\,a\,z} \qquad (D.8)$$

This inverse transfer function is non-causal, requiring time advance. The system can be made causal by placing an extra pole at the origin in the z-plane. In the time domain this has the effect of introducing extra

delay into the system response. This is why the block diagram shown in the Figure D.3 has delay between the input and output signals. Providing the extra delay needed to obtain a causal inverse transfer function is acceptable in practice, then good results can be obtained. This system with the extra pole at the origin has the pole-zero pattern shown in Figure D.4..

The system frequency response is given by:

$$D_{LP}(z) = (z^2 - 2az + a^2)/caz^2 \Big|_{z=e^{jwT}} \qquad (D.9)$$

Taking the inverse discrete Fourier transform gives the following expression for the inverse filter impulse response:

$$h(nT) = h(0)\ (0T) - h(1)\ (-T) + h(2)\ (-2T) \qquad (D.10)$$

with $h(0) = 4/\pi^2 e^{-\pi/2}$, $h(1) = 8/\pi^2$, and

$h(2) = e^{-\pi/2}\ 4/\pi^2$

This is shown in Figure D.5. It can be realised exactly as an FIR filter as shown in Figure D.6.

D.4 Comments

It has been demonstrated that using an FIR filter to model exactly a system containing poles would require an infinite number of terms in the filter impulse response. In contrast, it has been shown that for a

system containing only poles, then the system inverse contains a finite number of zeros (equal to the number of poles), plus trival poles needed to make the system causal. The effect of these trivial poles is that the system will have extra delay.

FIGURES FOR CHAPTER 1 TO 6

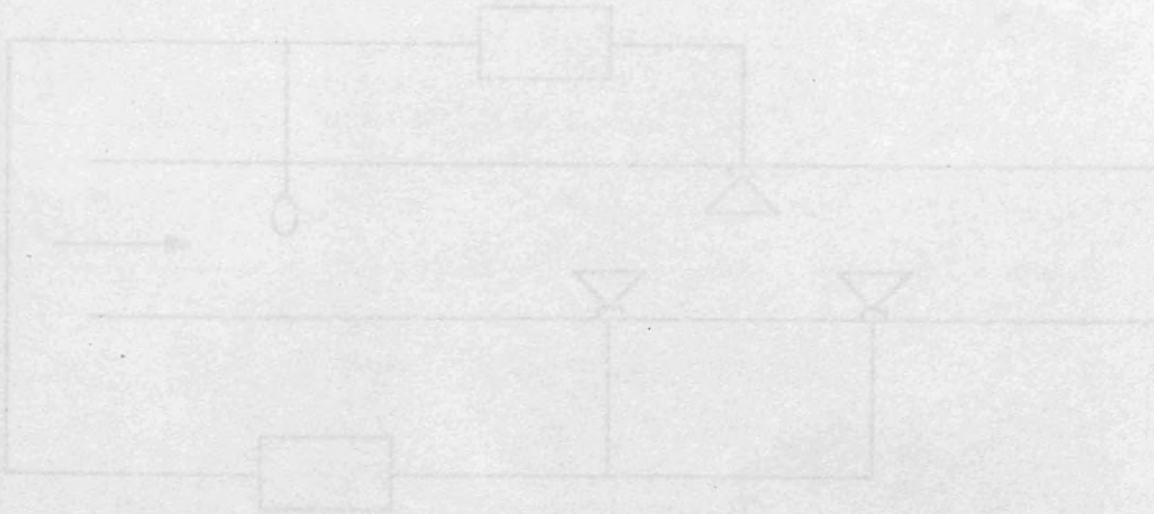

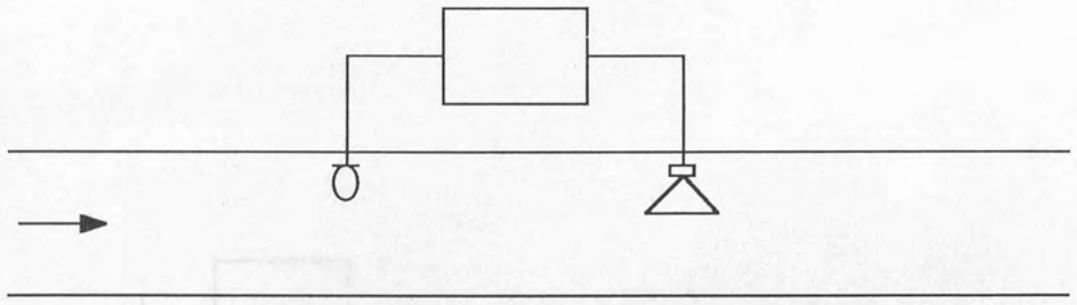

Figure 1 (a) Monopole system

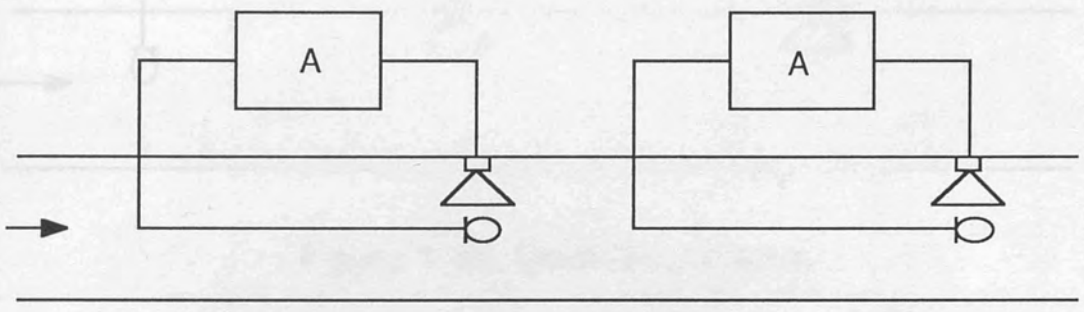

Figure 1(b) Tight coupled tandem monopole system

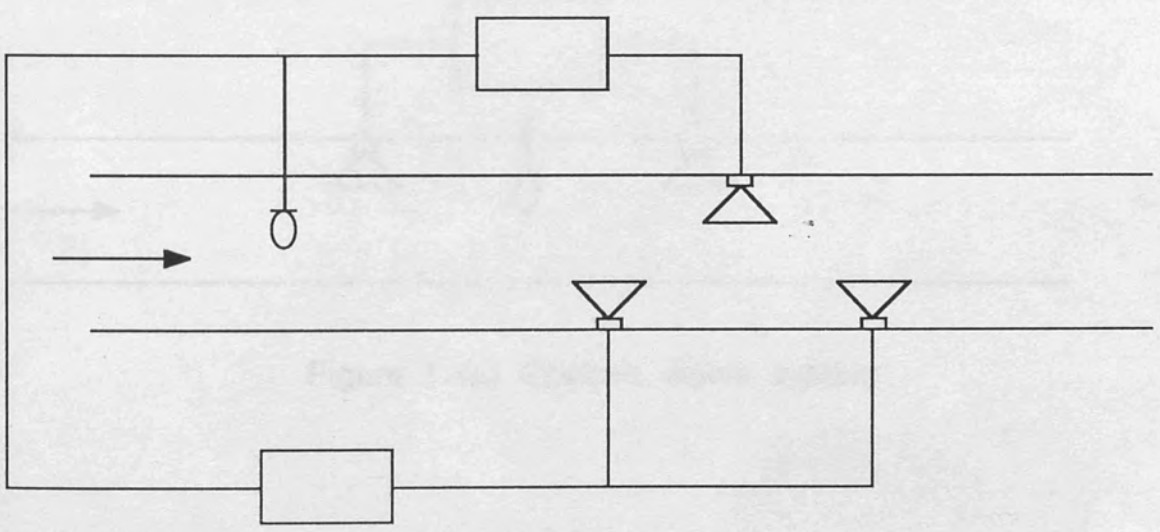

Figure 1(c) Jessel system

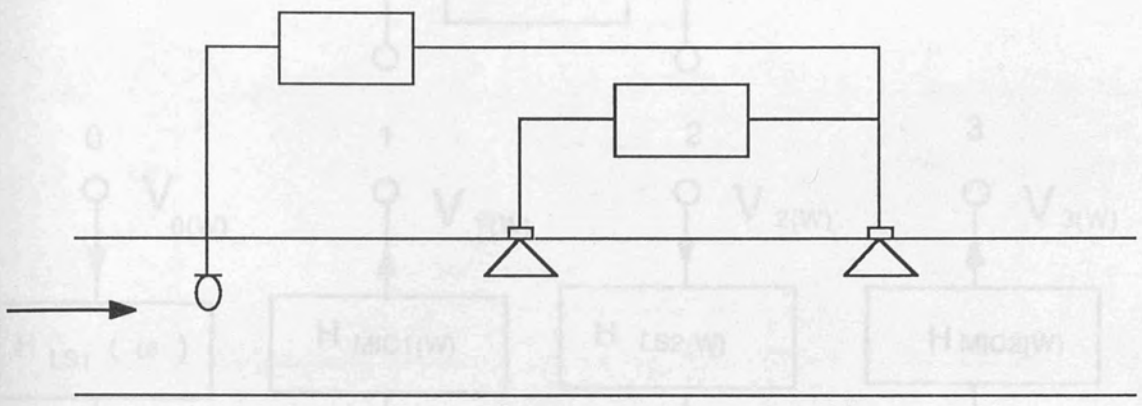

Figure 1 (d) Swinbanks system

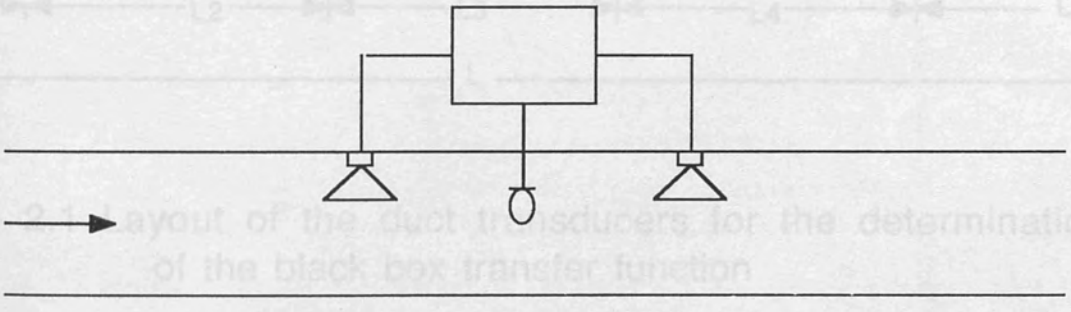

Figure 1 (e) Chelsea dipole system

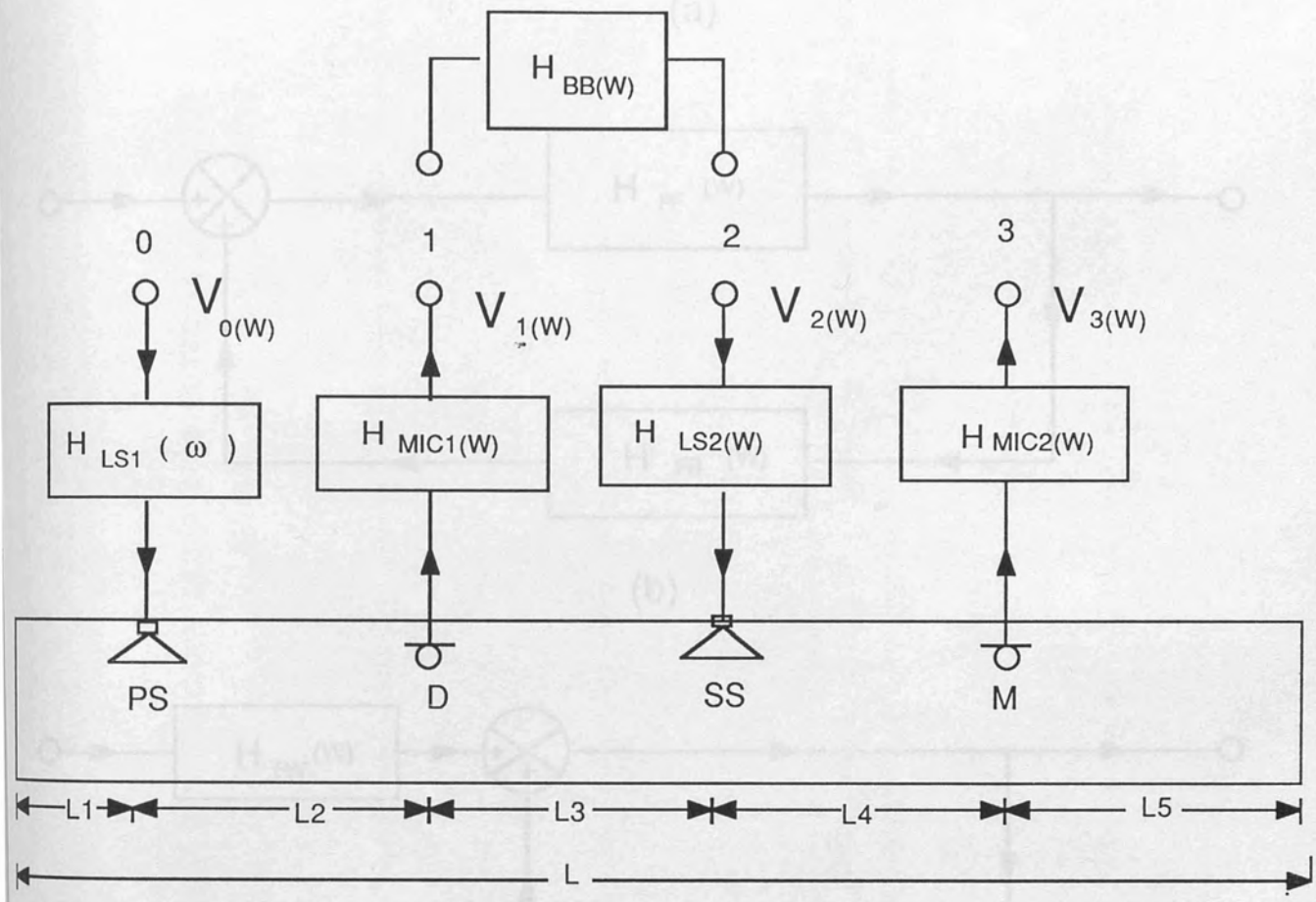

Figure 2.1 Layout of the duct transducers for the determination of the black box transfer function

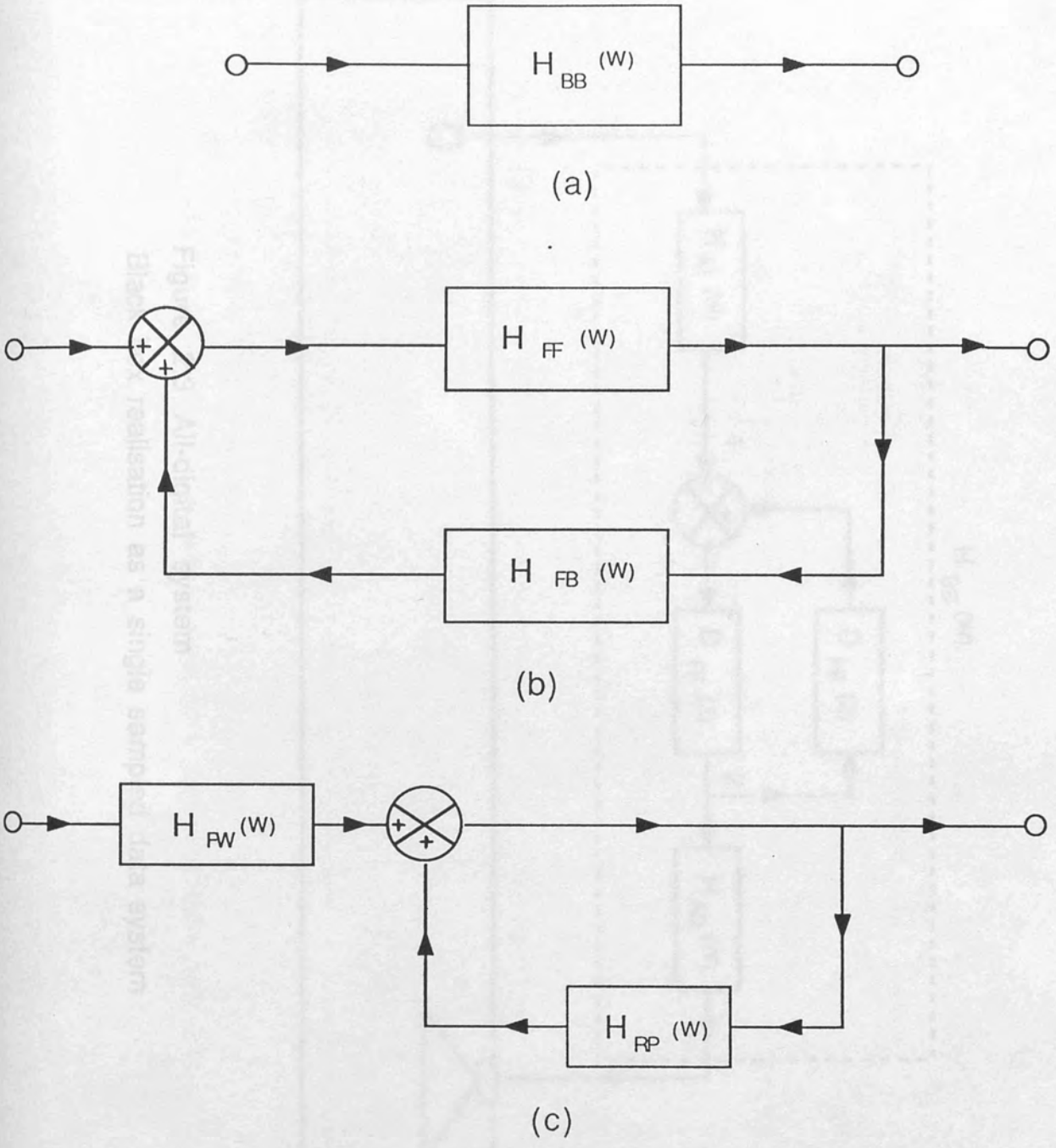

Figure 2.2 Alternative ways of implementing the black box transfer function (a) feedforward filter ,(b) feedforward and feedback filter combination,and (c) different recursive realisation to (b)

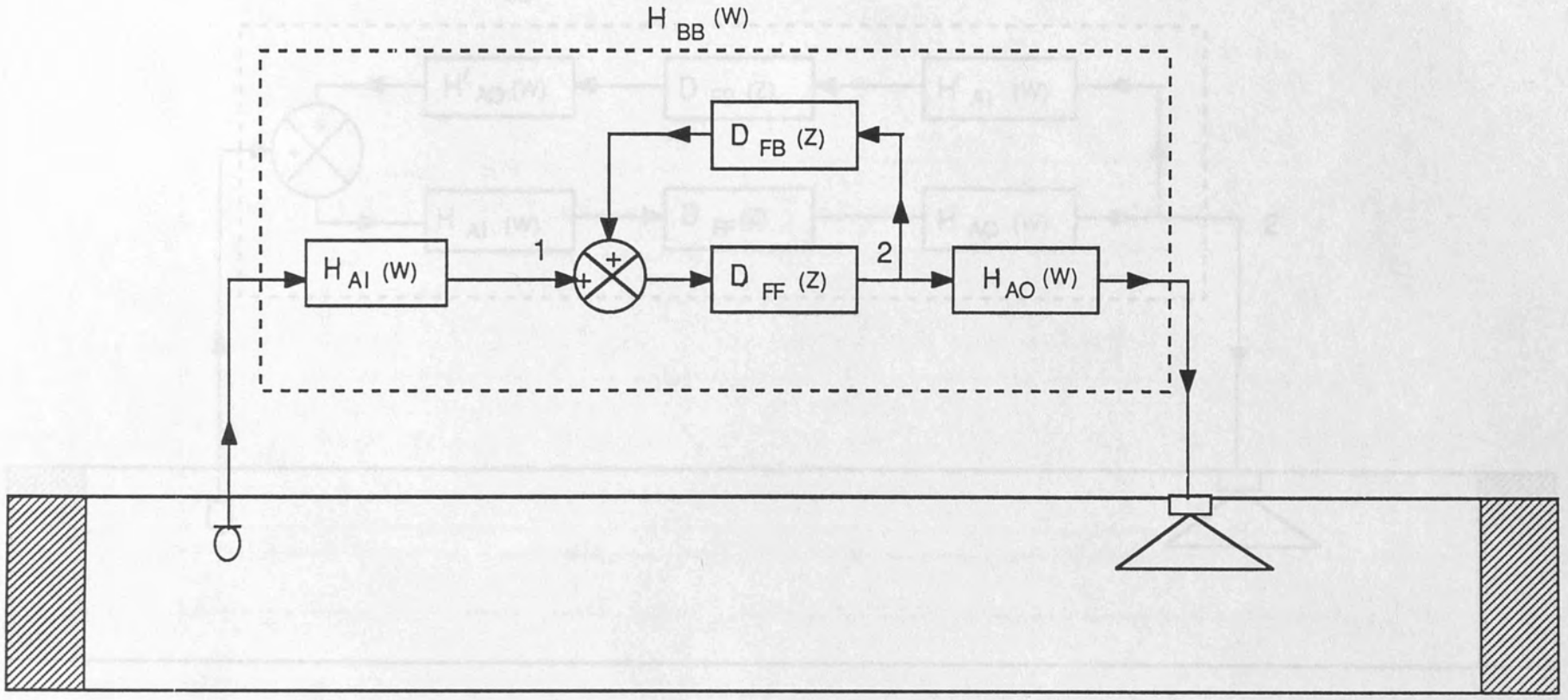

Figure 2.3 All-digital system
Black box realisation as a single sampled data system

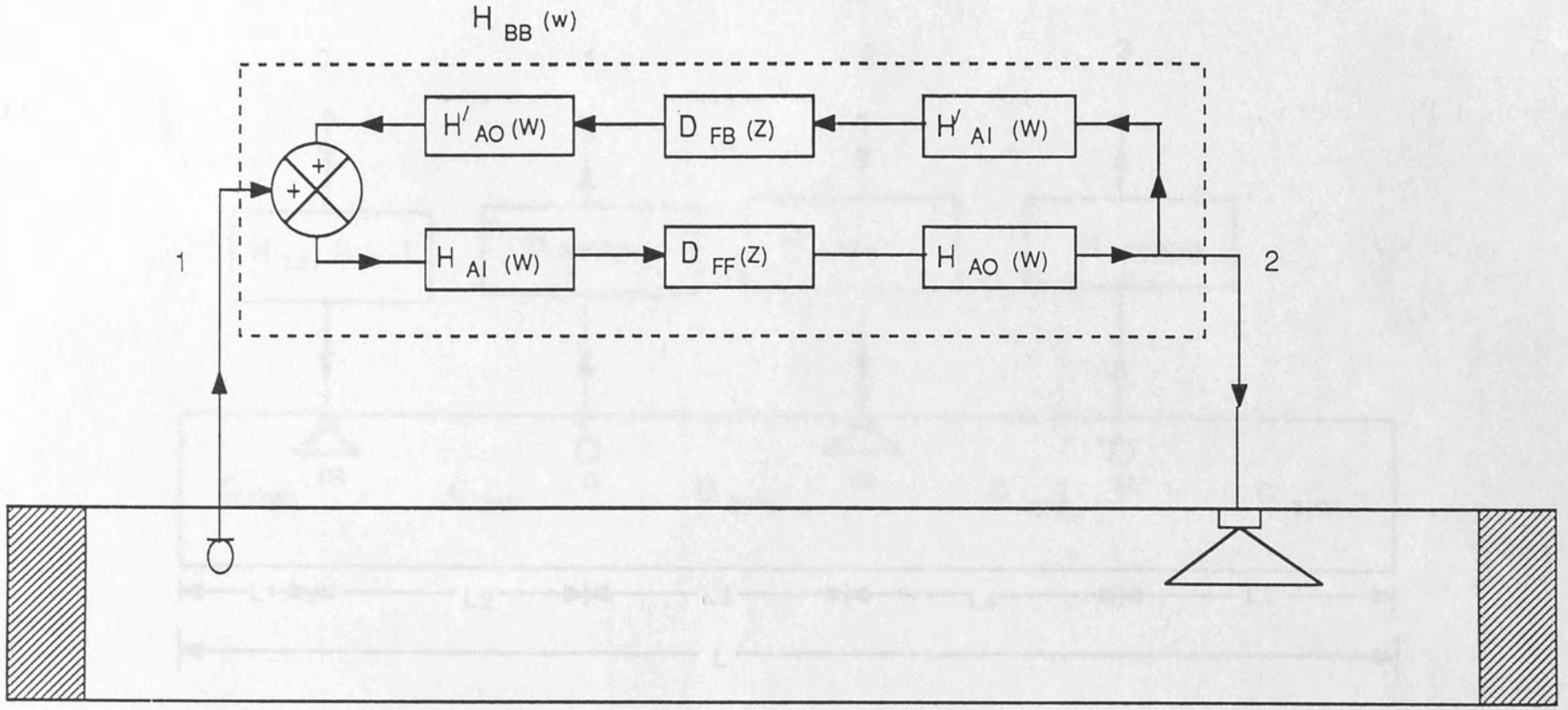

Figure 2.4 Hybrid system
Black box realisation as two independent sampled data systems

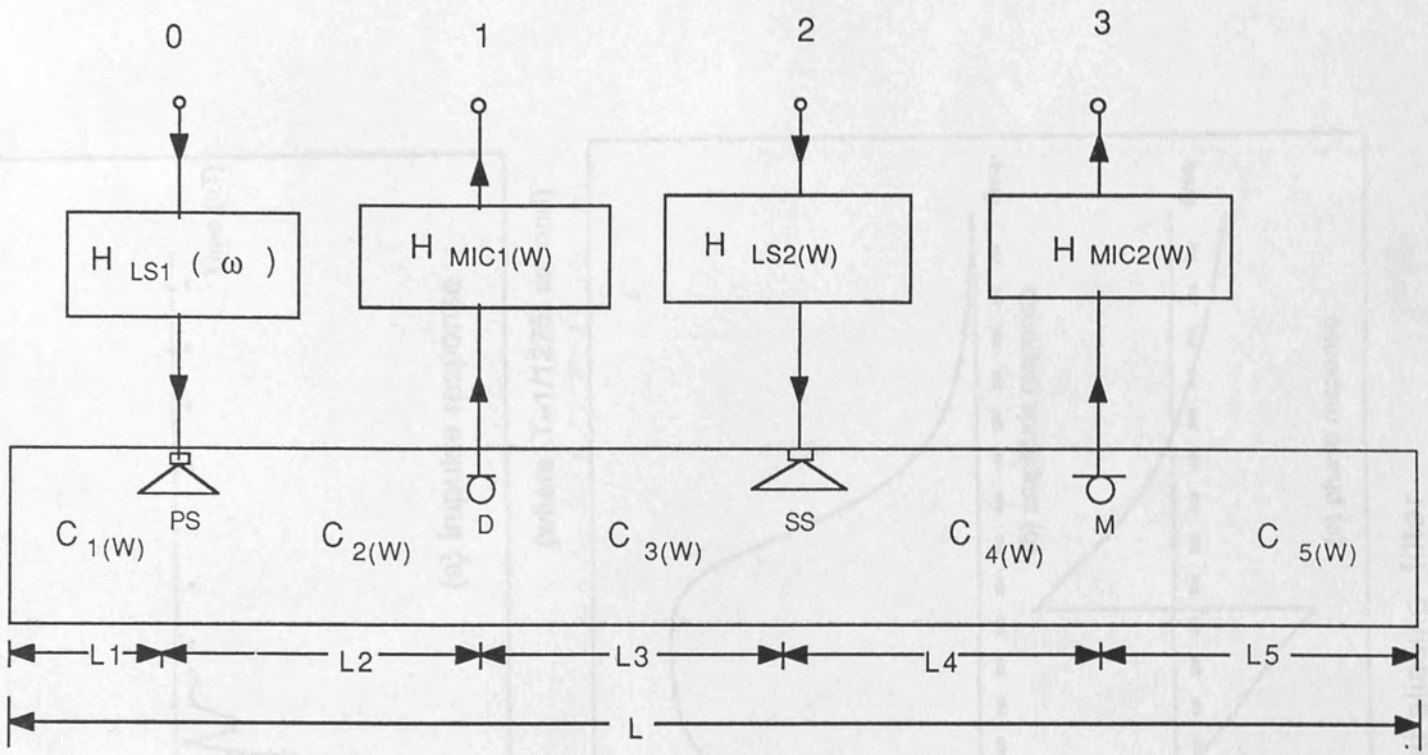

Figure 2.5 Modelling of the four electroacoustic transfer functions $H_{01}(W)$, $H_{03}(W)$, $H_{23}(W)$, and $H_{21}(W)$

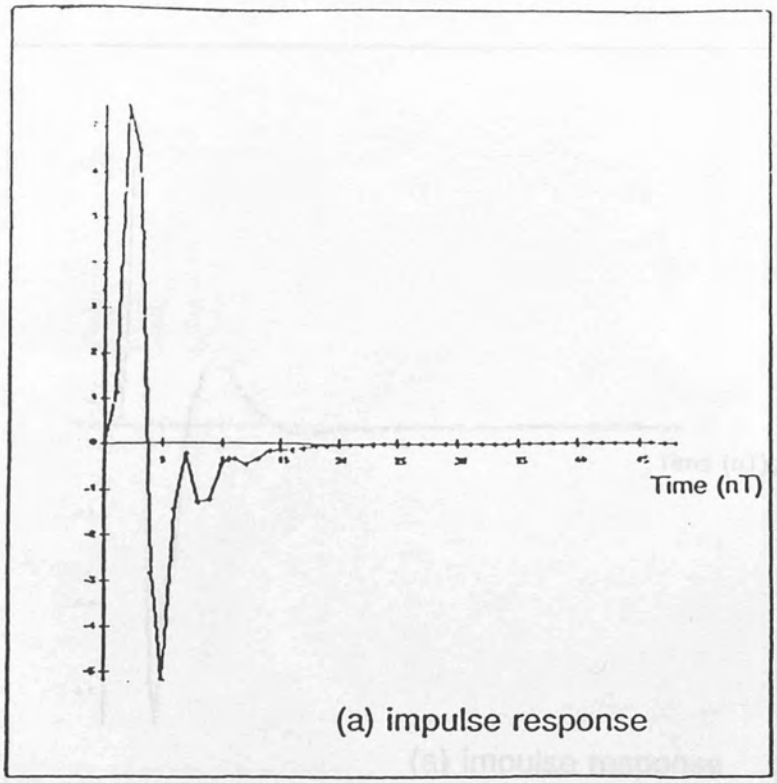

(where T=1/1275 second)

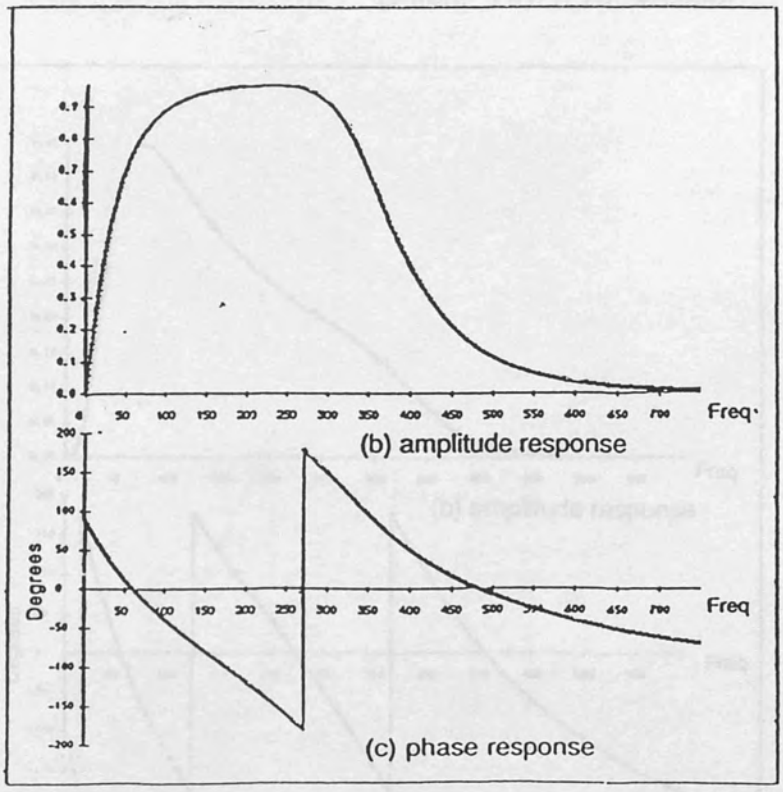

Figure 2.6 Anti-aliasing filter

Impulse and frequency responses for analog bandpass filter of the sampled data system

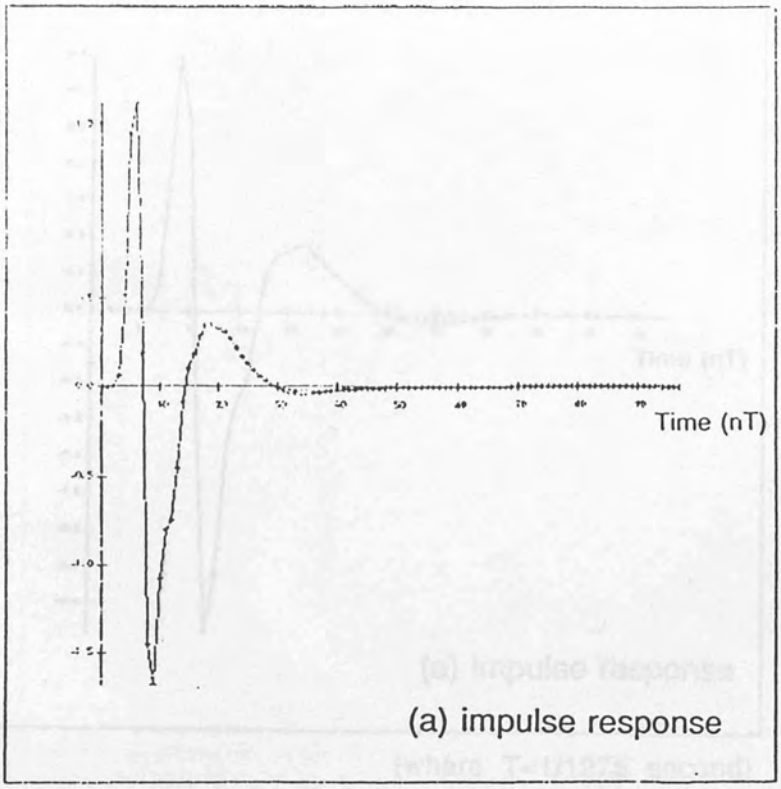

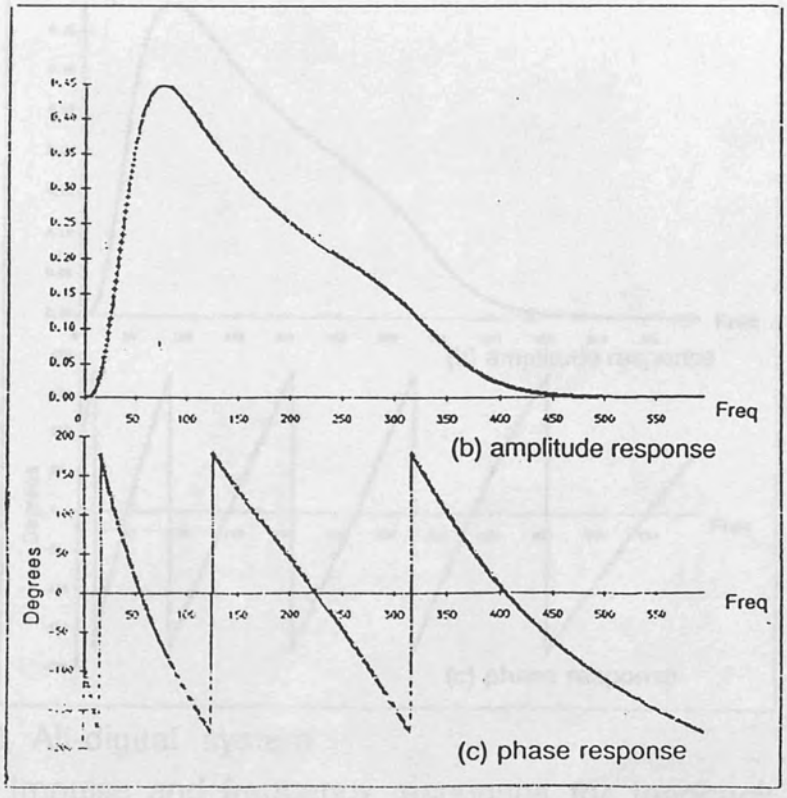

Figure 2.7 Impulse and frequency responses of the feedforward path, including microphone, bandpass filters, and loudspeaker

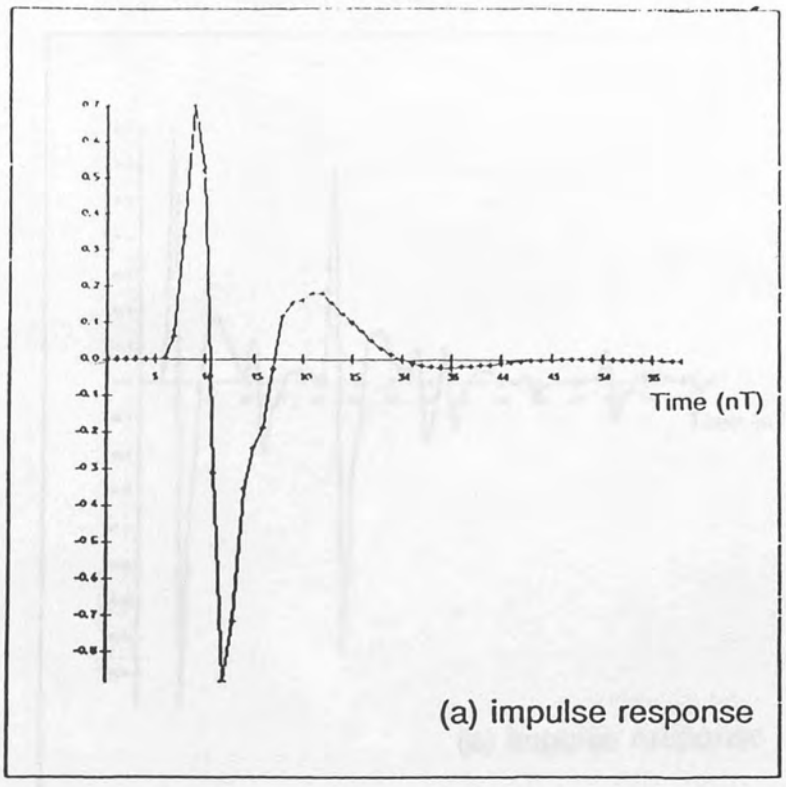

(where T=1/1275 second)

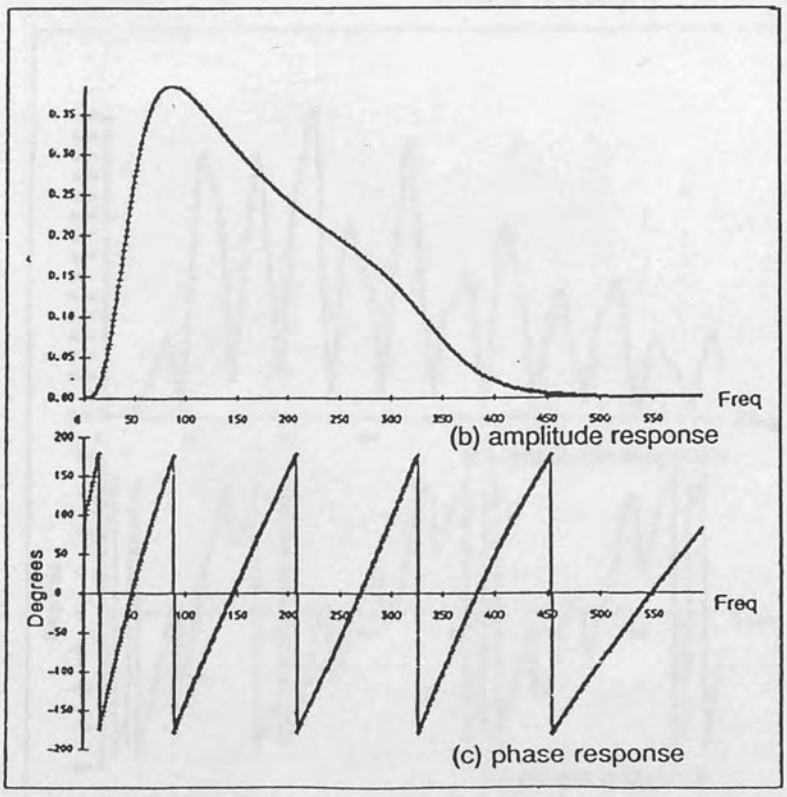

Figure 2.8 All-digital system
Impulse and frequency responses for feedback filter for a non-reflective duct

Note: the phase responses in figures 2.8, and 2.9 were calculated using the exp(-jwt) convention rather than the exp(+jwt) convention used every where else in this thesis.Hence in these figures a positive slope corresponds to a time delay.

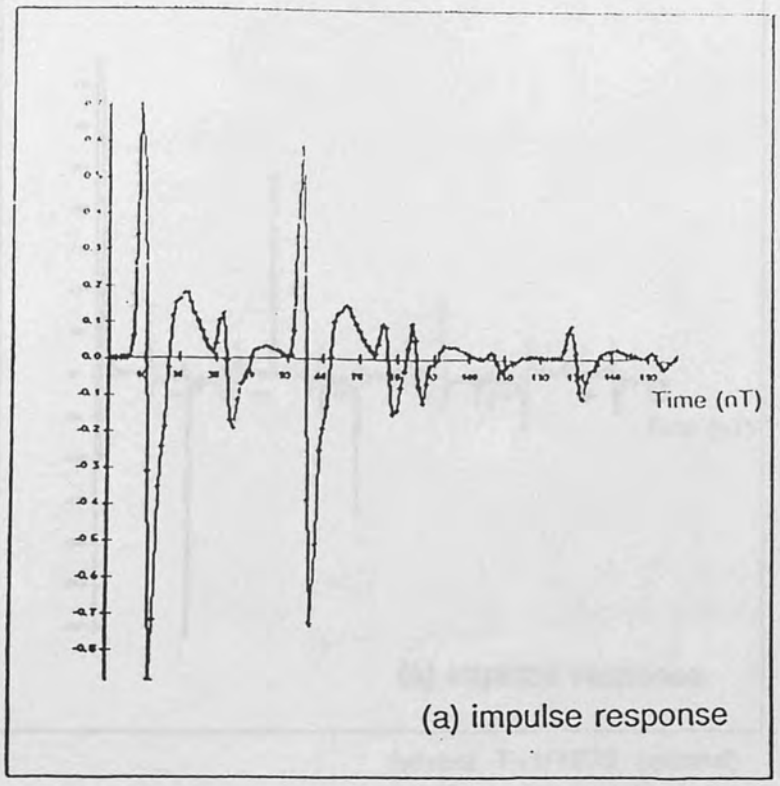

(where T=1/1275 second)

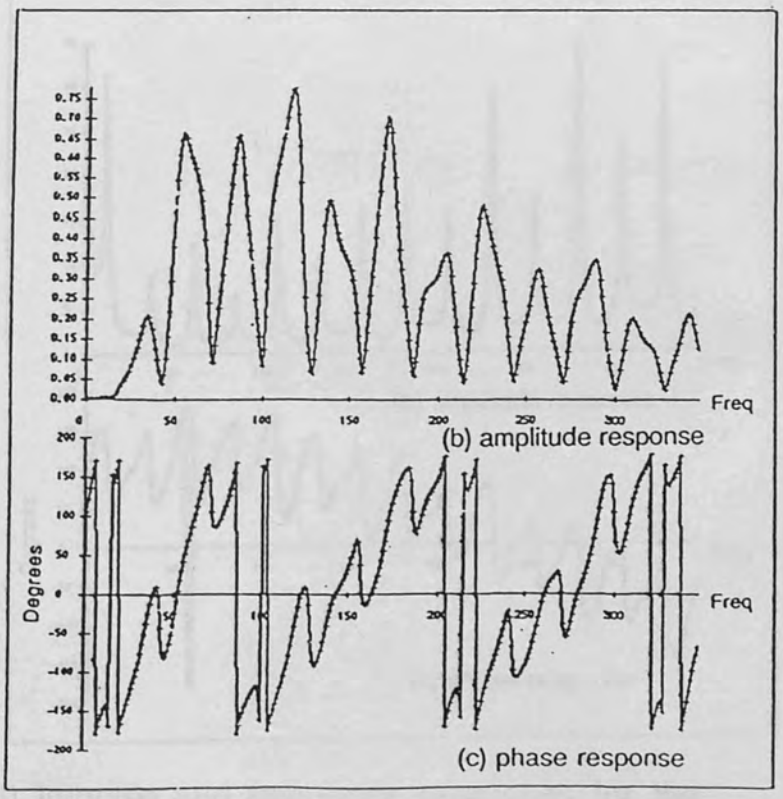

Figure 2.9 All-digital system

Impulse and frequency responses for a feedback filter with reflection coefficients shown in table 2.2

Note: the phase responses in figures 2.8, and 2.9 were calculated using the exp(-jwt) convention rather than the exp(+jwt) convention used every where else in this thesis.Hence in these figures a positive slope corresponds to a time delay.

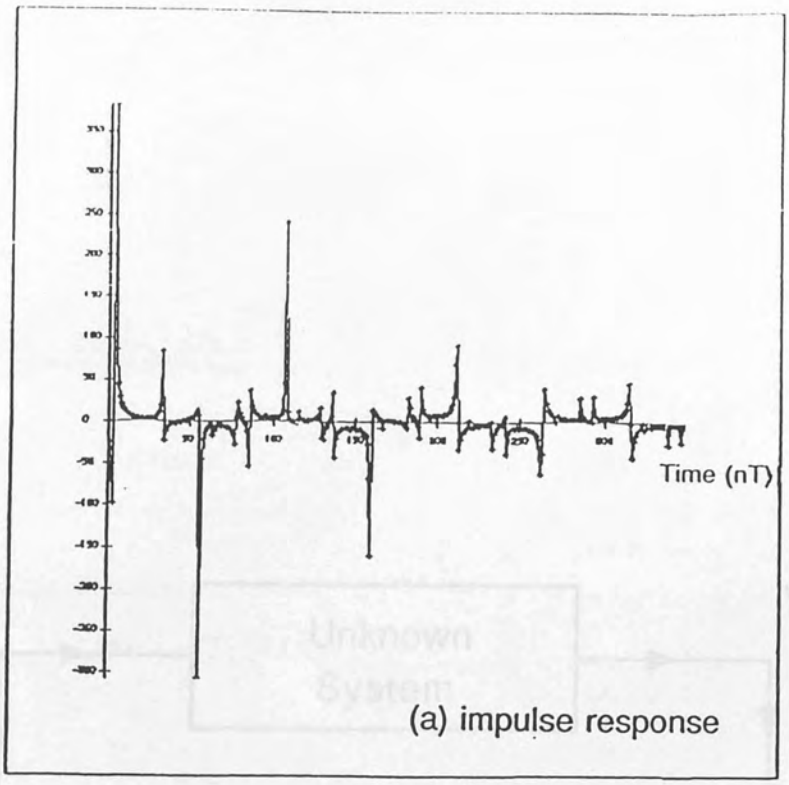

(where T=1/1275 second)

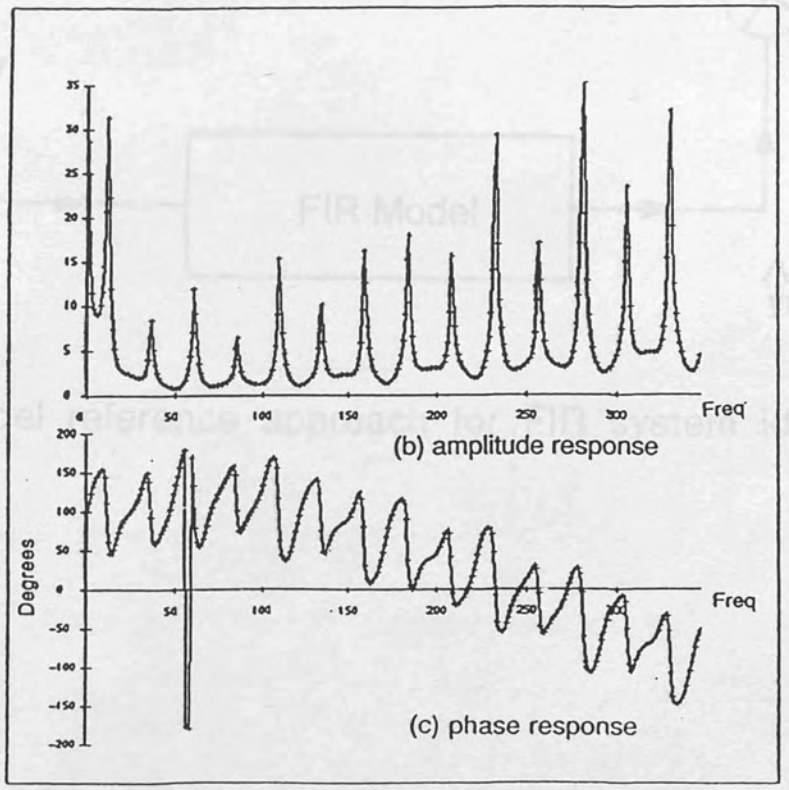

Figure 2.10 Impulse and frequency responses for the feedforward filter (assuming perferct analog elements in the feedforward path)

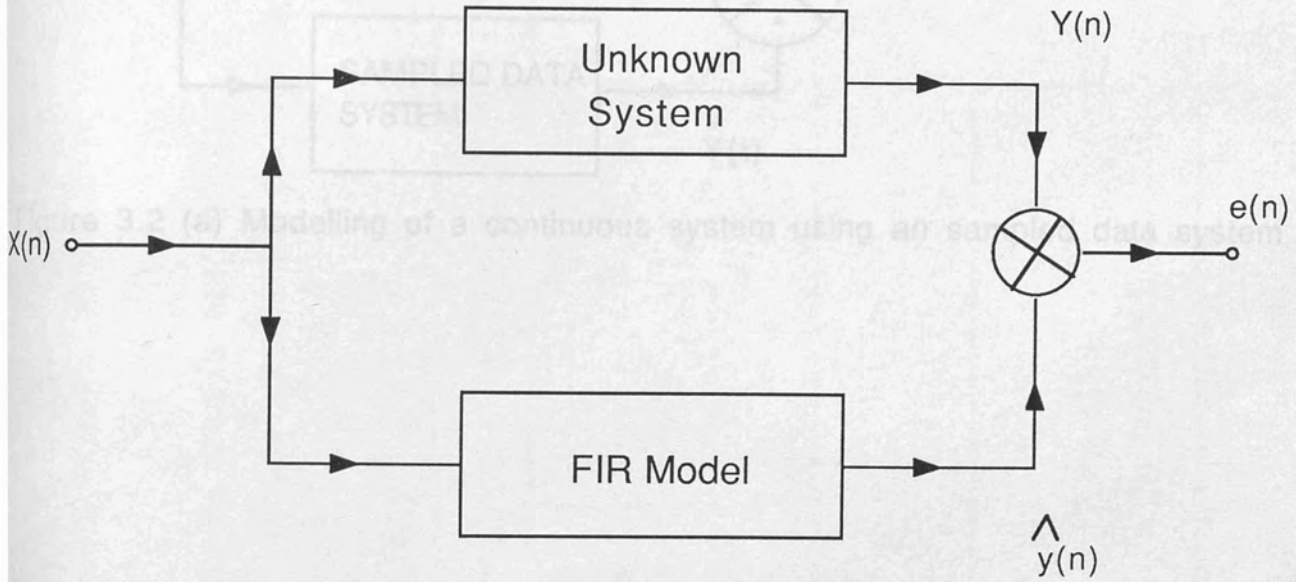

Figure 3.1 Model reference approach for FIR system identification

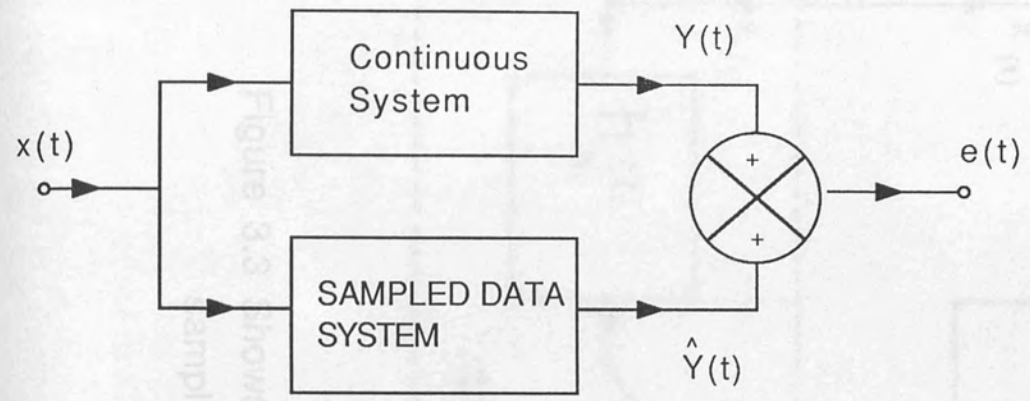

Figure 3.2 (a) Modelling of a continuous system using an sampled data system

Figure 3.2 (b) F I R sampled data system

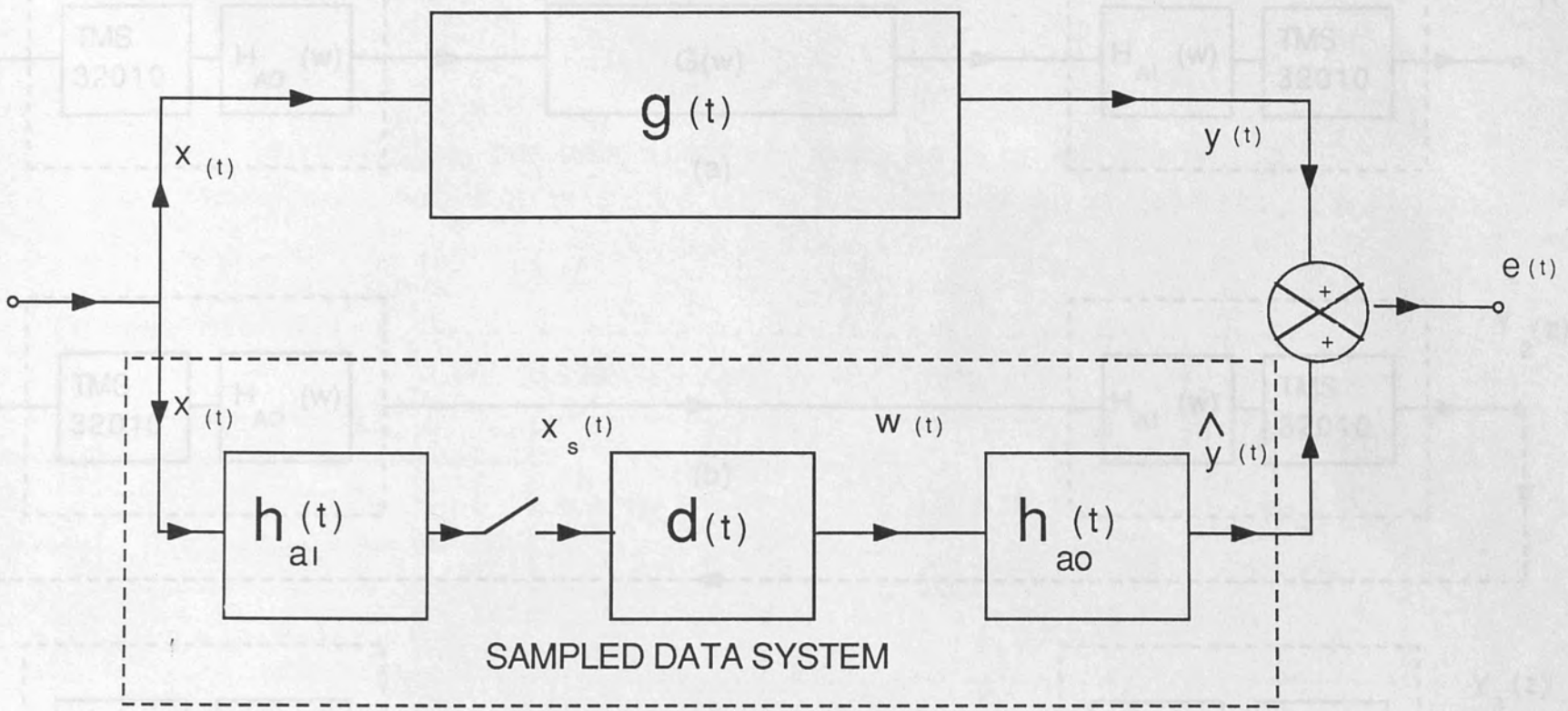

Figure 3.3 Shows the signals and impulse responses involved in using an sampled data system to model a continuous system

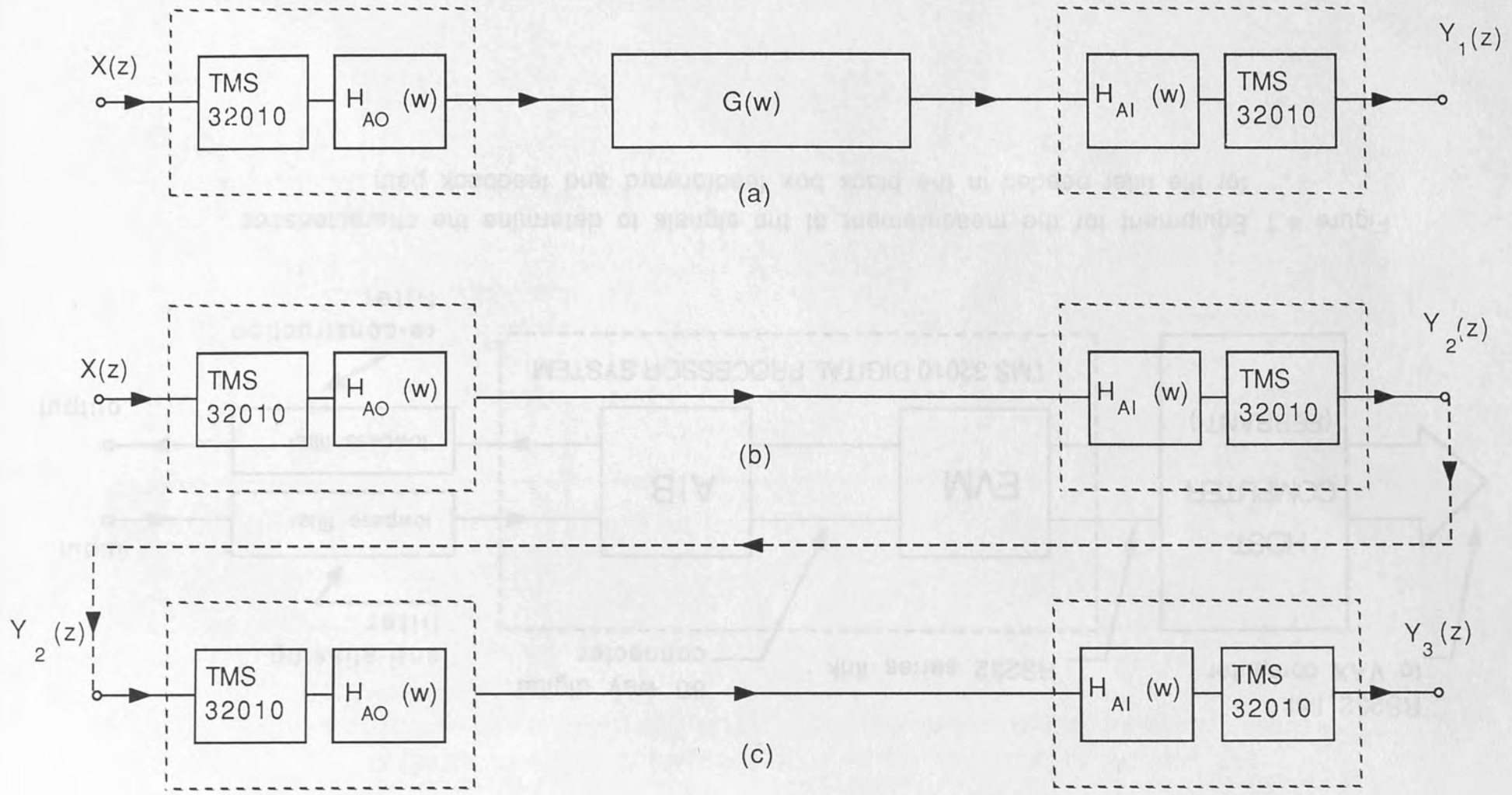

Figure 3.4 (a),(b) and (c) Shows the measuring procedure for the modelling of the continuous system G(w) by a sampled data system

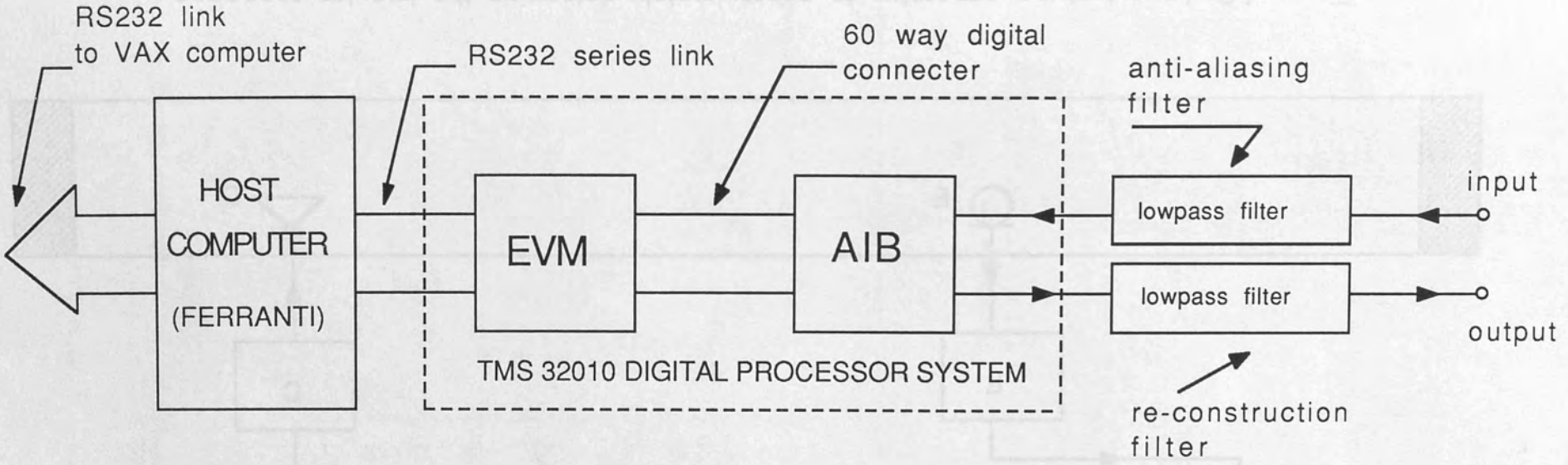

Figure 4.1 Equipment for the measurement of the signals to determine the characteristics for the filter needed in the black box feedforward and feedback path

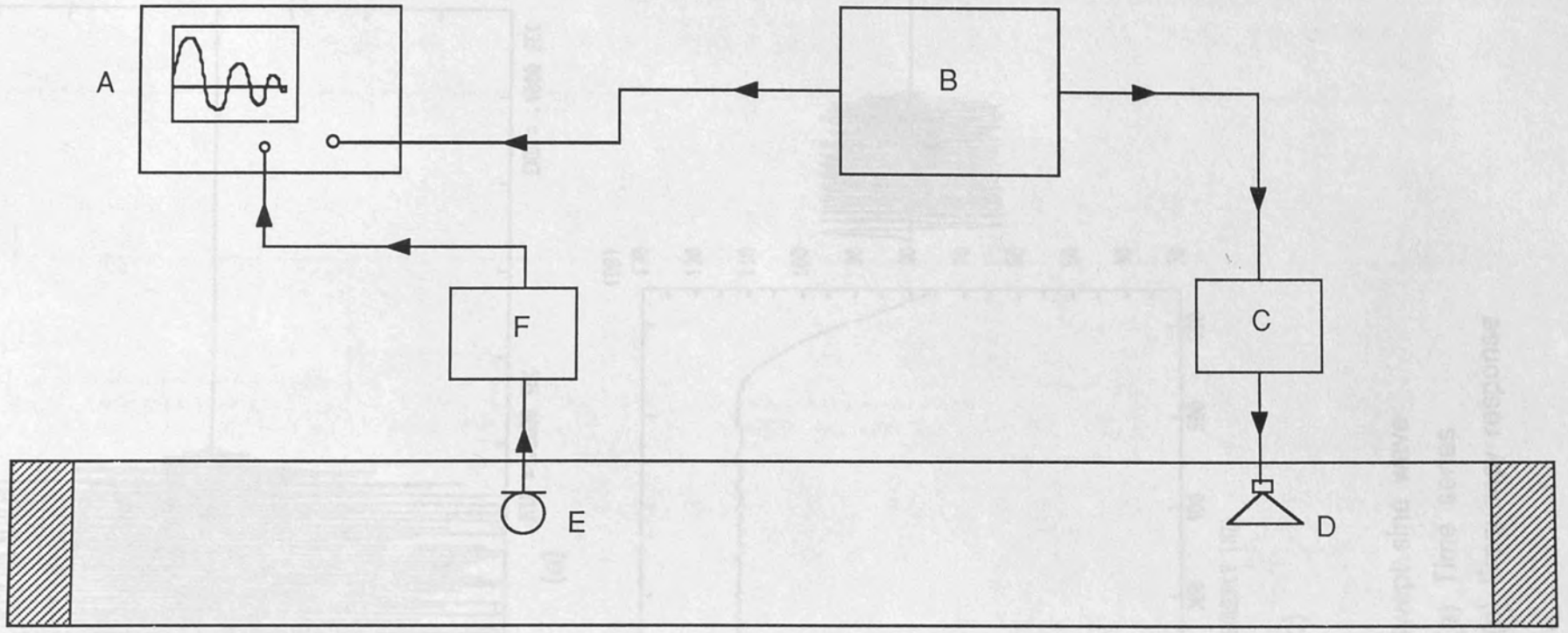

Figure 4.2 Layout of the apparatus to approximately determine the impulse response of the electroacoustic feedback path in the experimental wooden duct

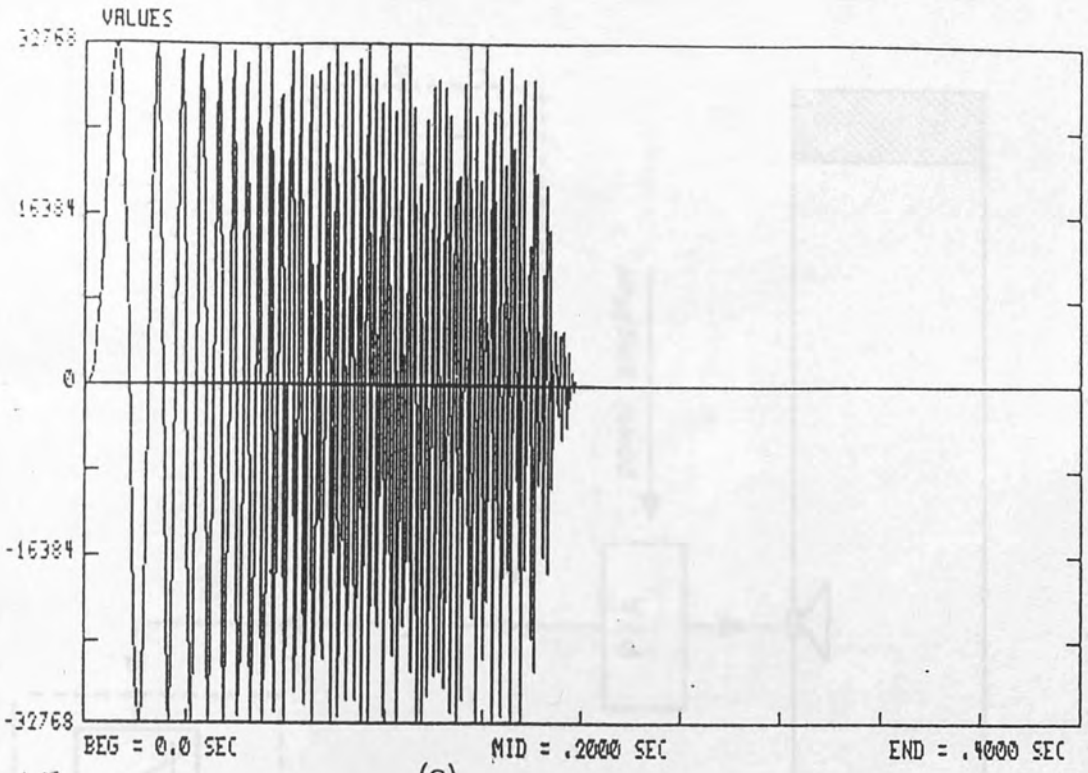

(a)

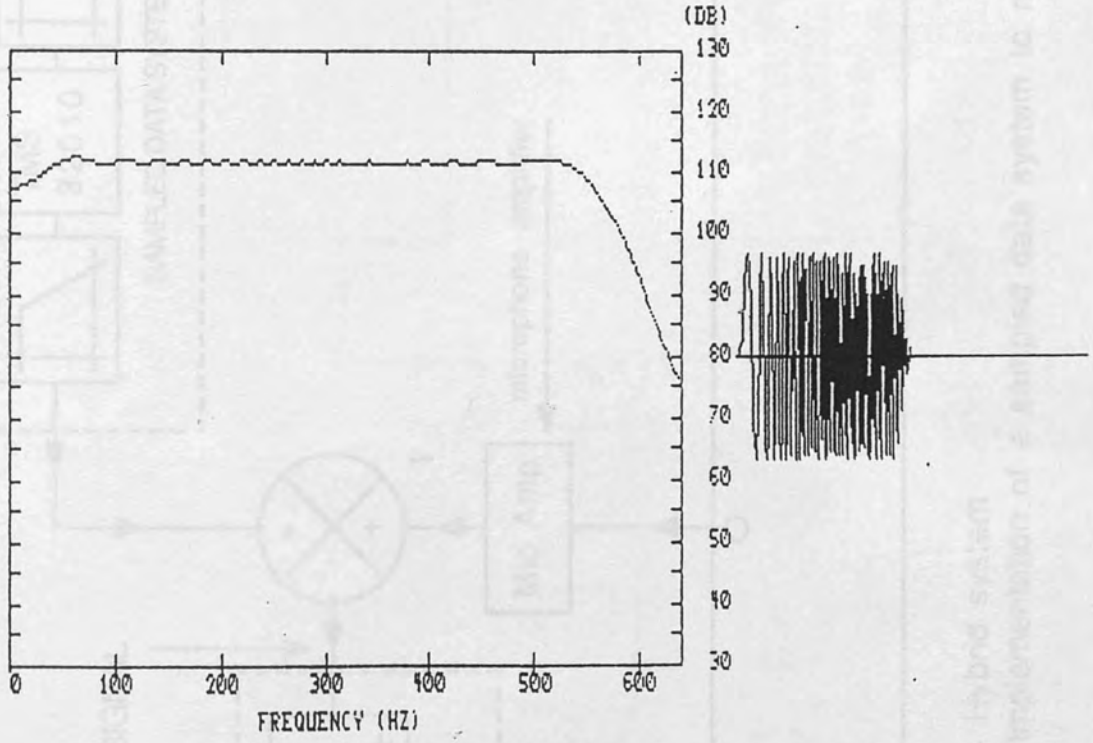

(b)

Figure 4.3 Swept sine wave
(a) Time series
(b) Frequency response

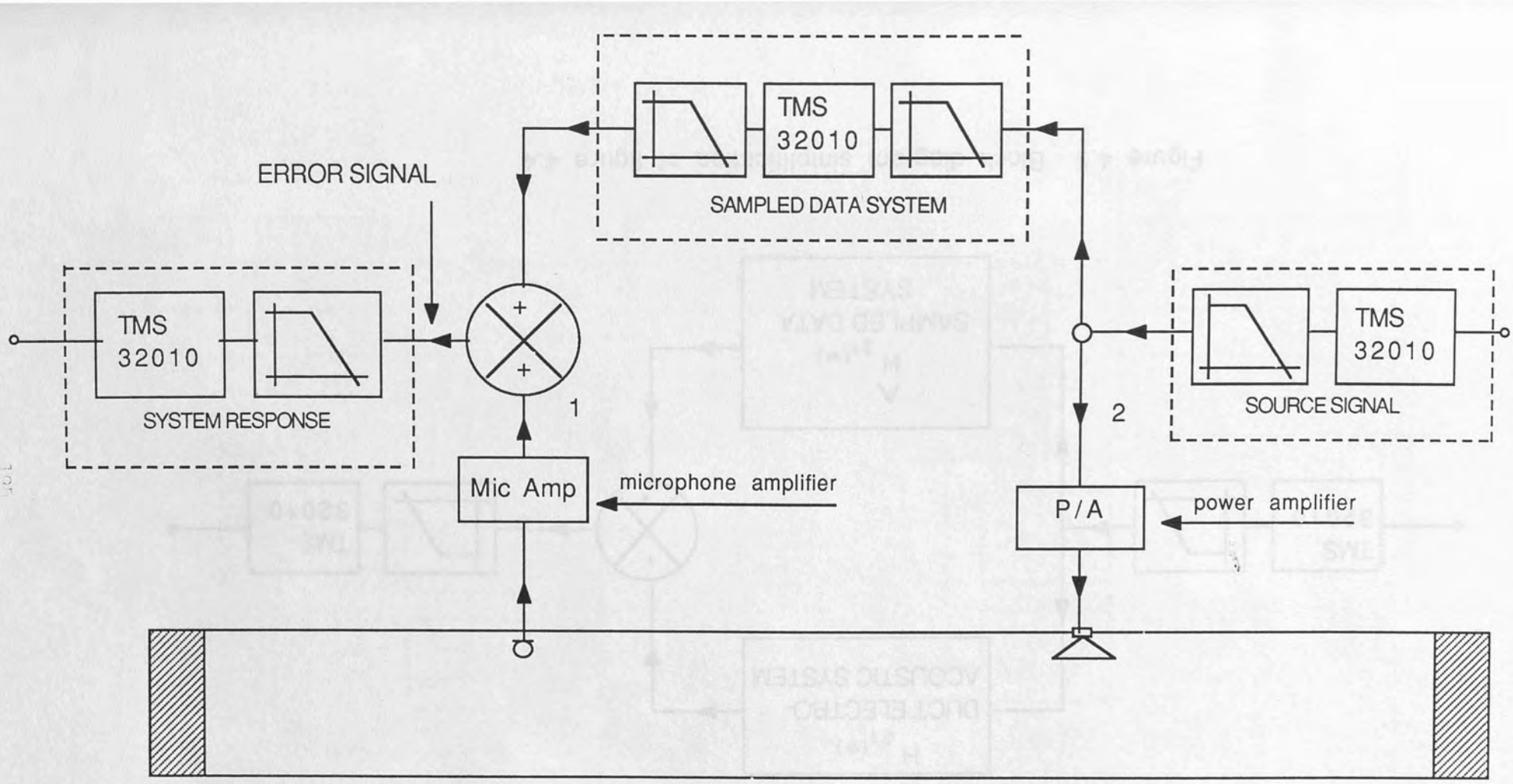

Figure 4.4 Hybrid system
Implementation of a sampled data system to model the electroacoustic feedback path

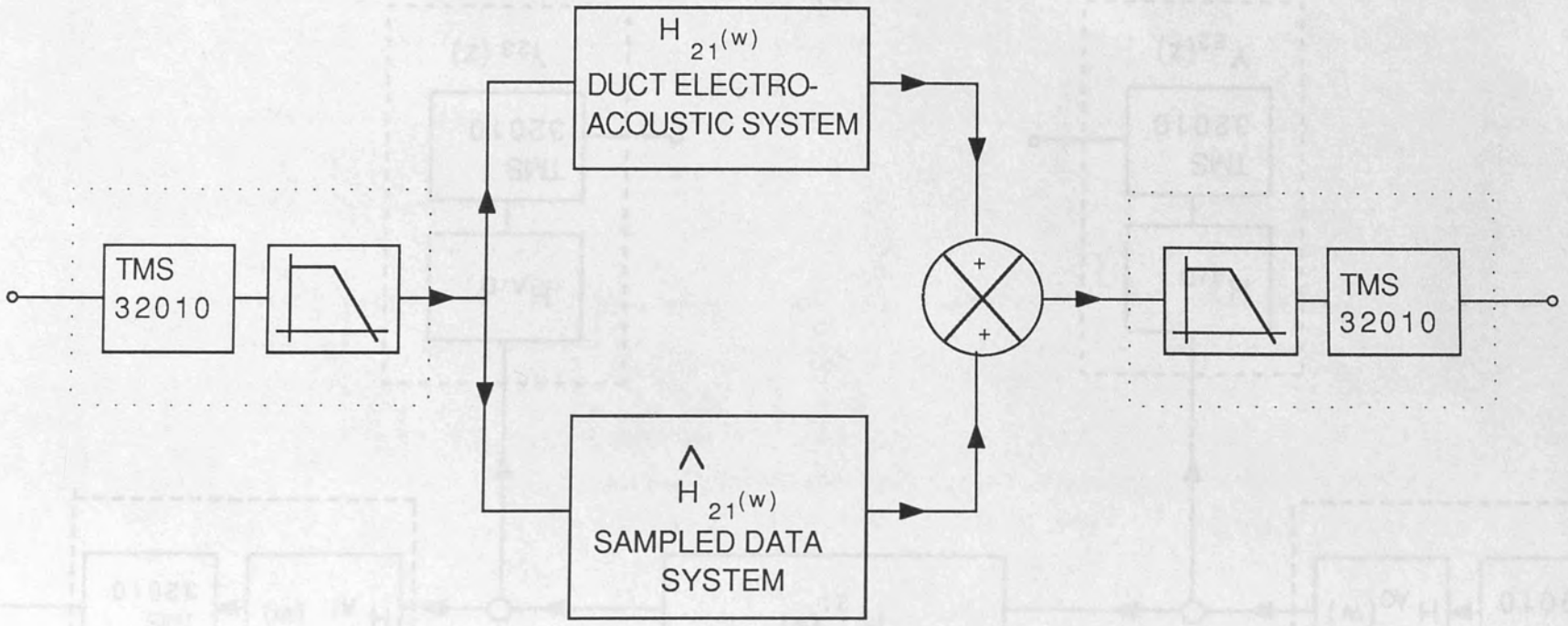

Figure 4.5 Block diagram simplification of figure 4.4

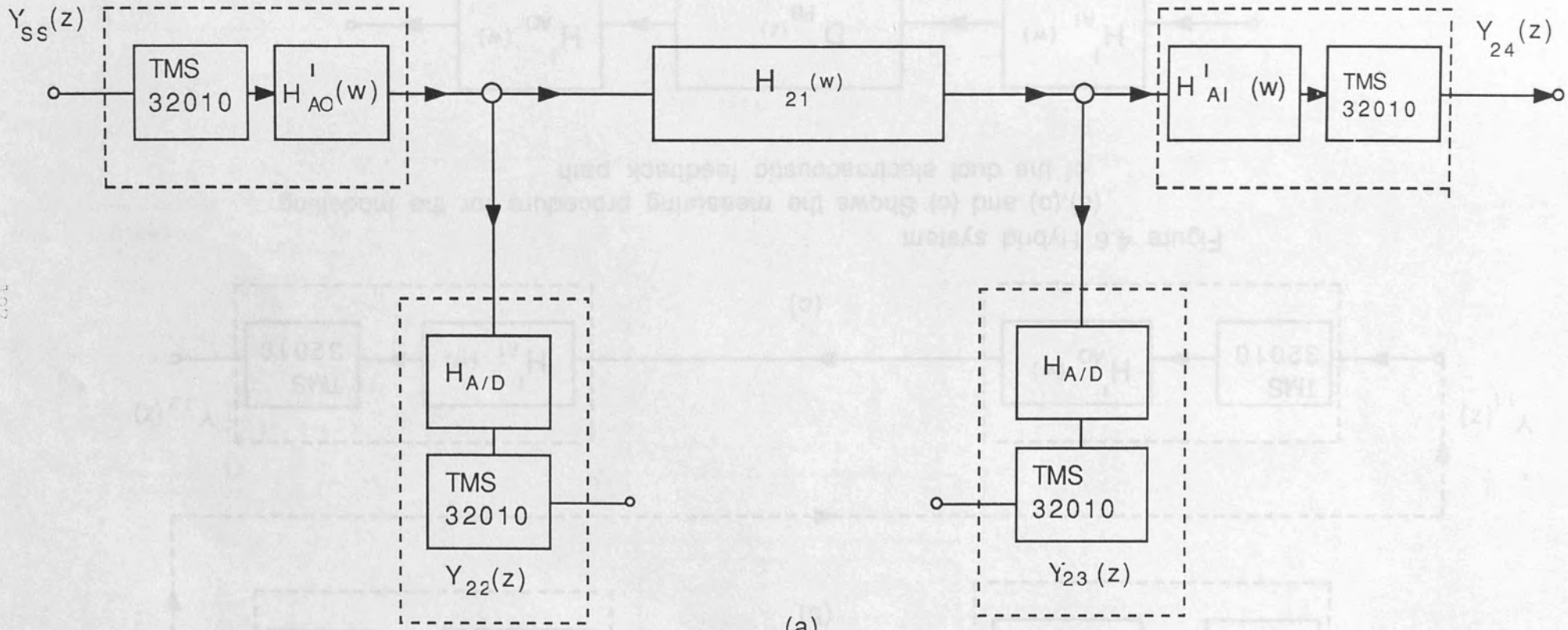

Figure 4.6 Hybrid system
Measurement of signals for the modelling of the electroacoustic feedback path

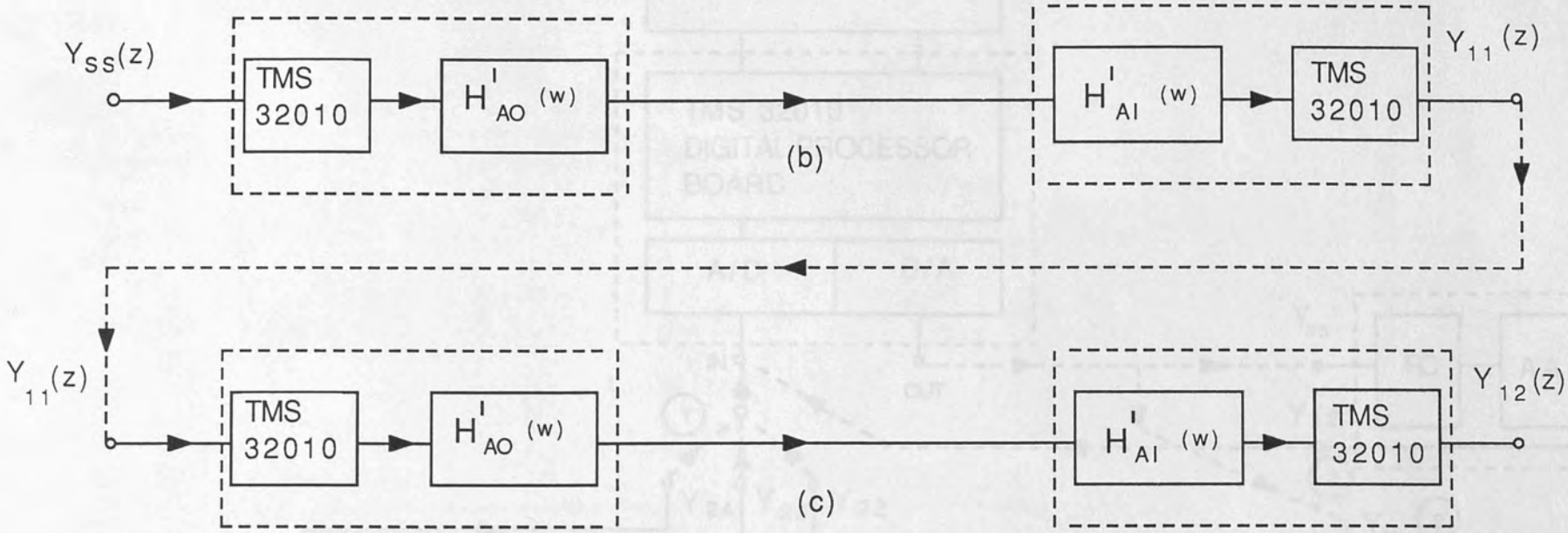

Figure 4.6 Hybrid system

(a),(b) and (c) Shows the measuring procedure for the modelling of the duct electroacoustic feedback path

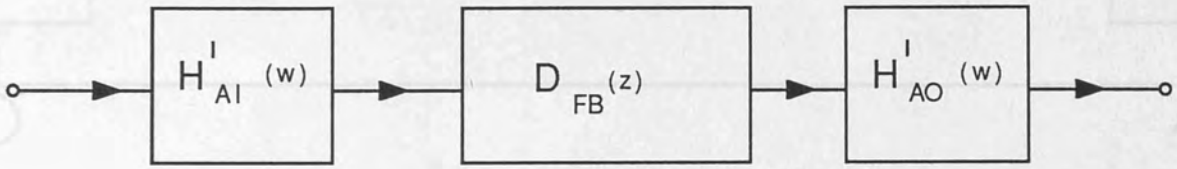

Figure 4.6 (d) Hybrid system compensating parallel feedback sampled data system

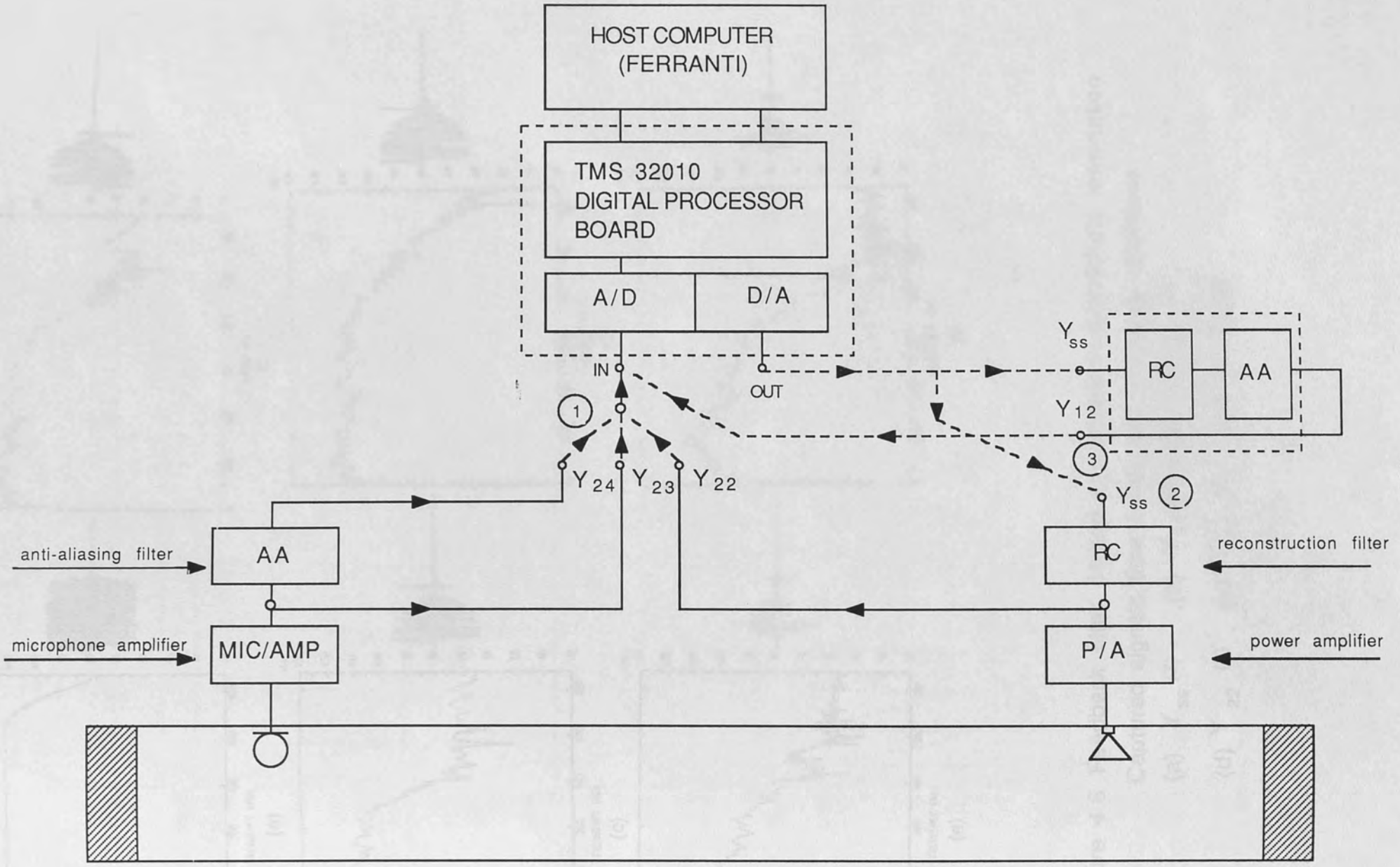

Figure 4.7 Hybrid system. Measuring system to determine the characteristic for a digital filter in an sampled data system for parallel feedback cancellation

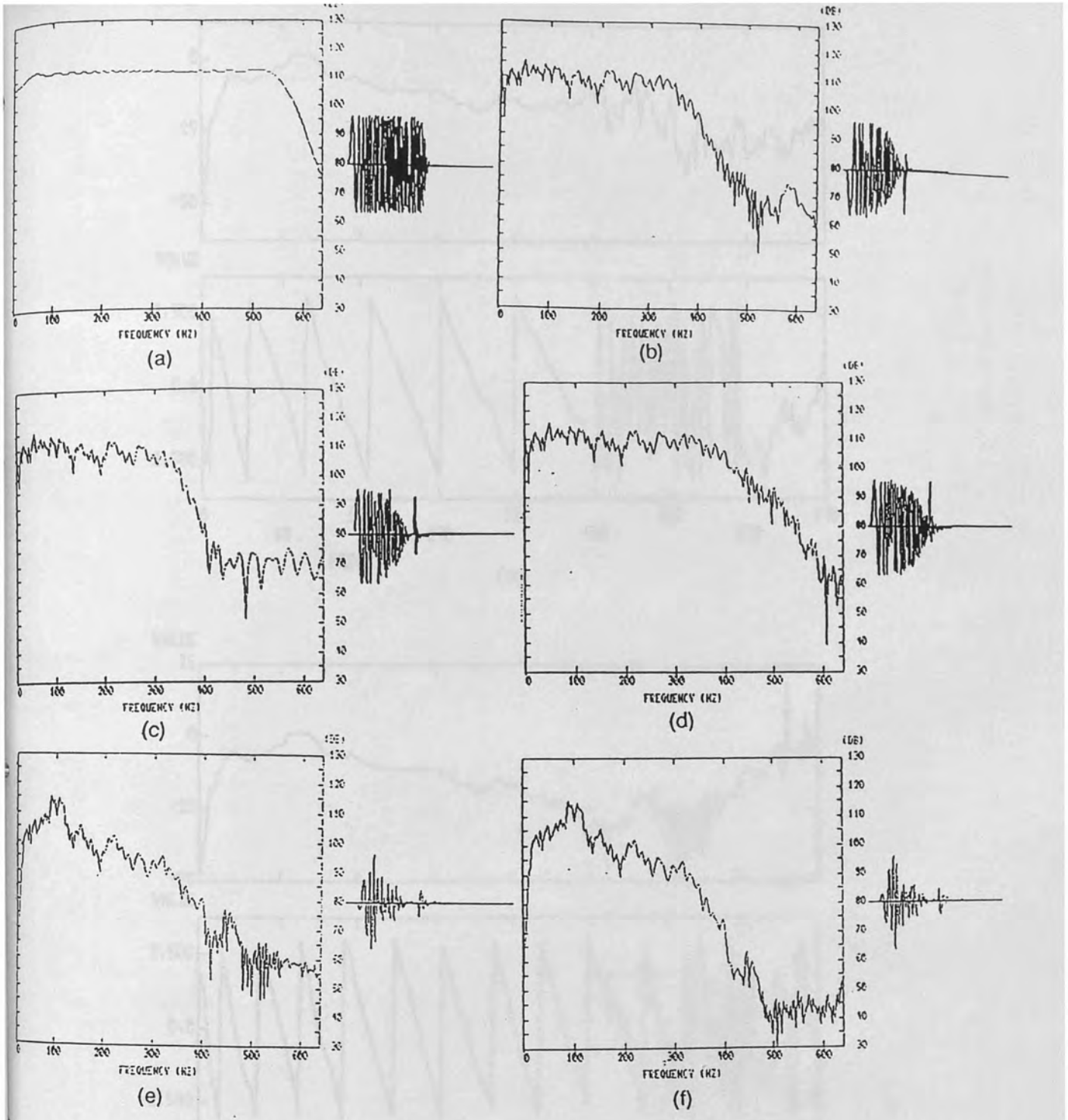

Figure 4.8 Feedback filter. Hybrid system,anechoic/anechoic termination
Captured signals time series and frequency responses
(a) $Y_{ss}(Z)$,(b) $Y_{11}(Z)$, (c) $Y_{12}(Z)$,
(d) $Y_{22}(Z)$, (e) $Y_{23}(Z)$, and (f) $Y_{24}(Z)$

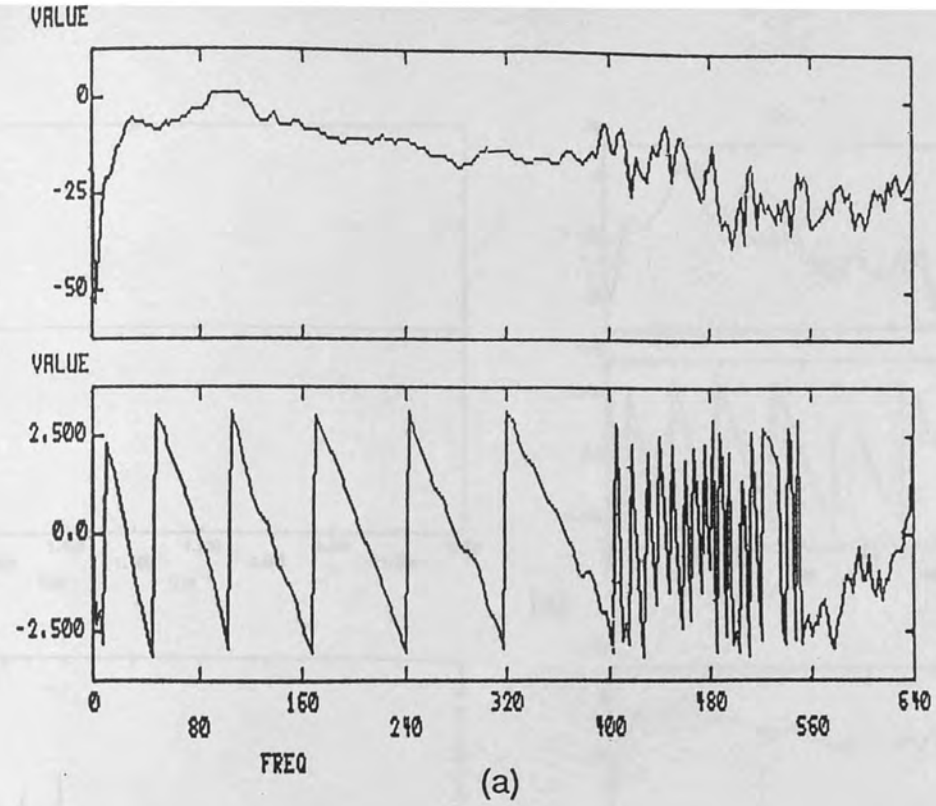

(a)

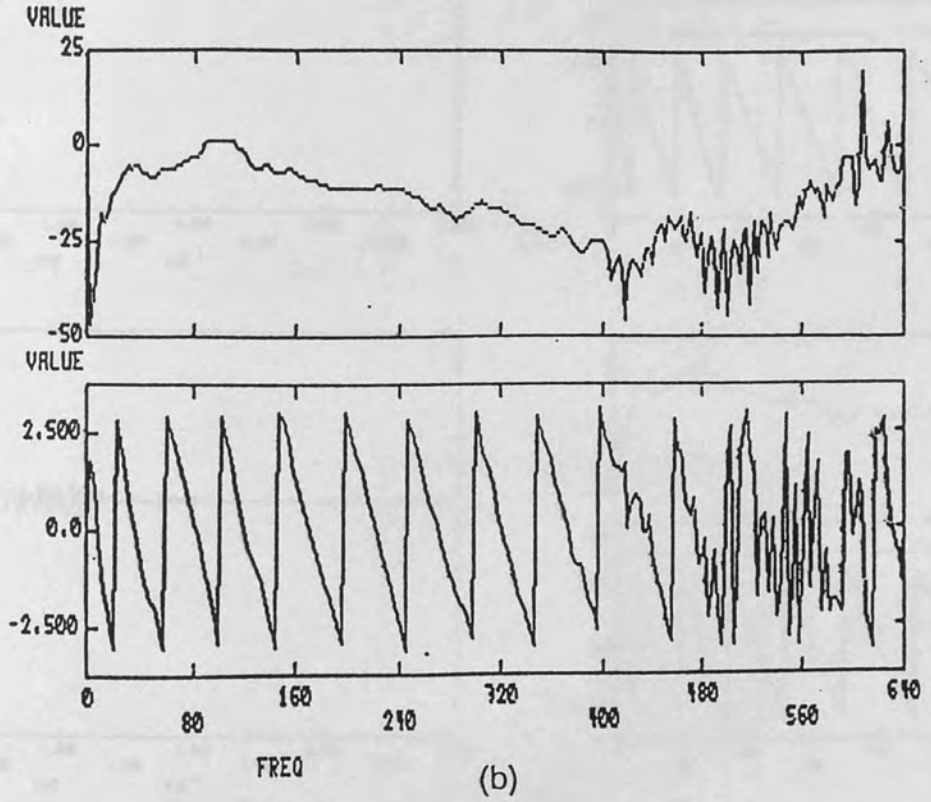

(b)

Figure 4.9 Hybrid system,anechoic/anechoic termination

Computed frequency responses from measured signals for the feedback path

(a) required digital filter response needed in the sampled data system

(b) electroacoustic feedback path to be modelled by the feedback sampled data system

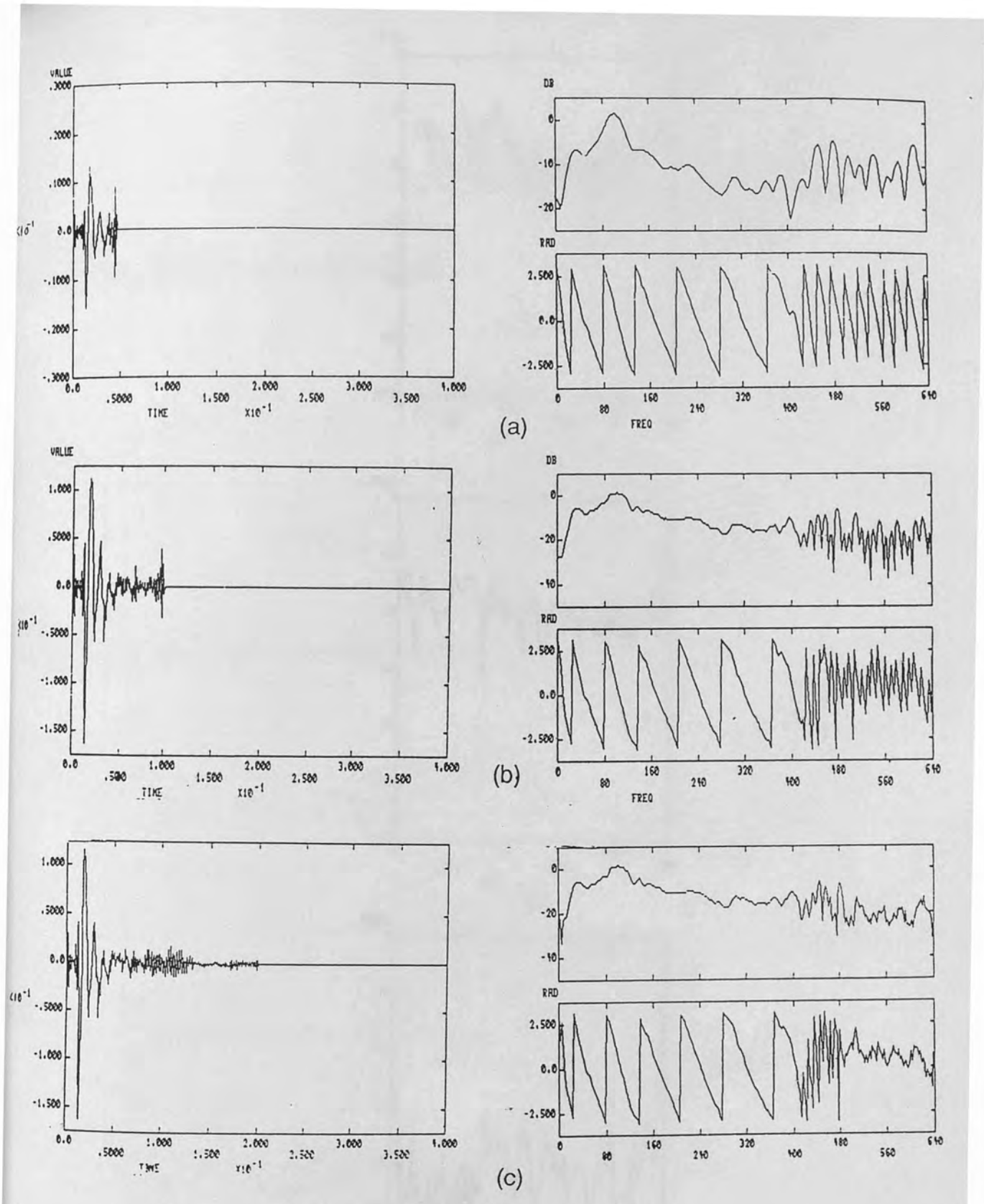

Figure 4.10 Hybrid system, anechoic/anechoic termination
FIR approximation for the digital feedback filter impulse and frequency response using the following number of coefficients (a) 61,(b) 128 and (c) 256

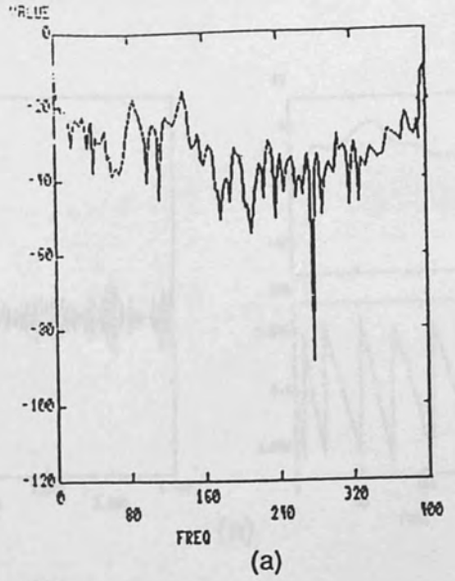

(a)

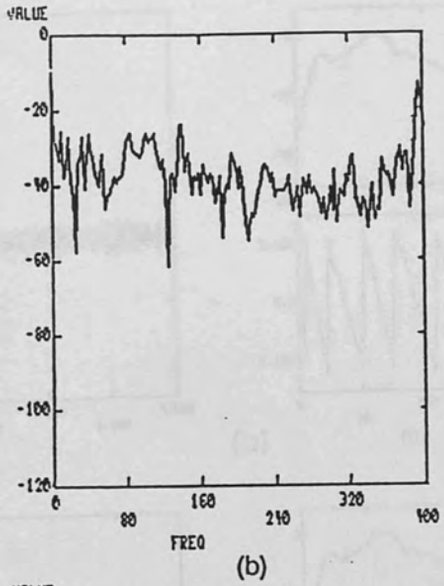

(b)

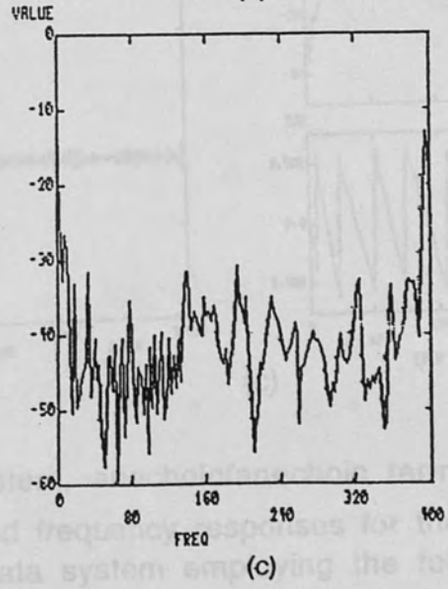

(c)

Figure 4.11 Hybrid system, anechoic/anechoic termination

Feedback cancellation using the following number of FIR coefficients in the parallel feedback sampled data system (a) 61, (b) 128, and (c) 256

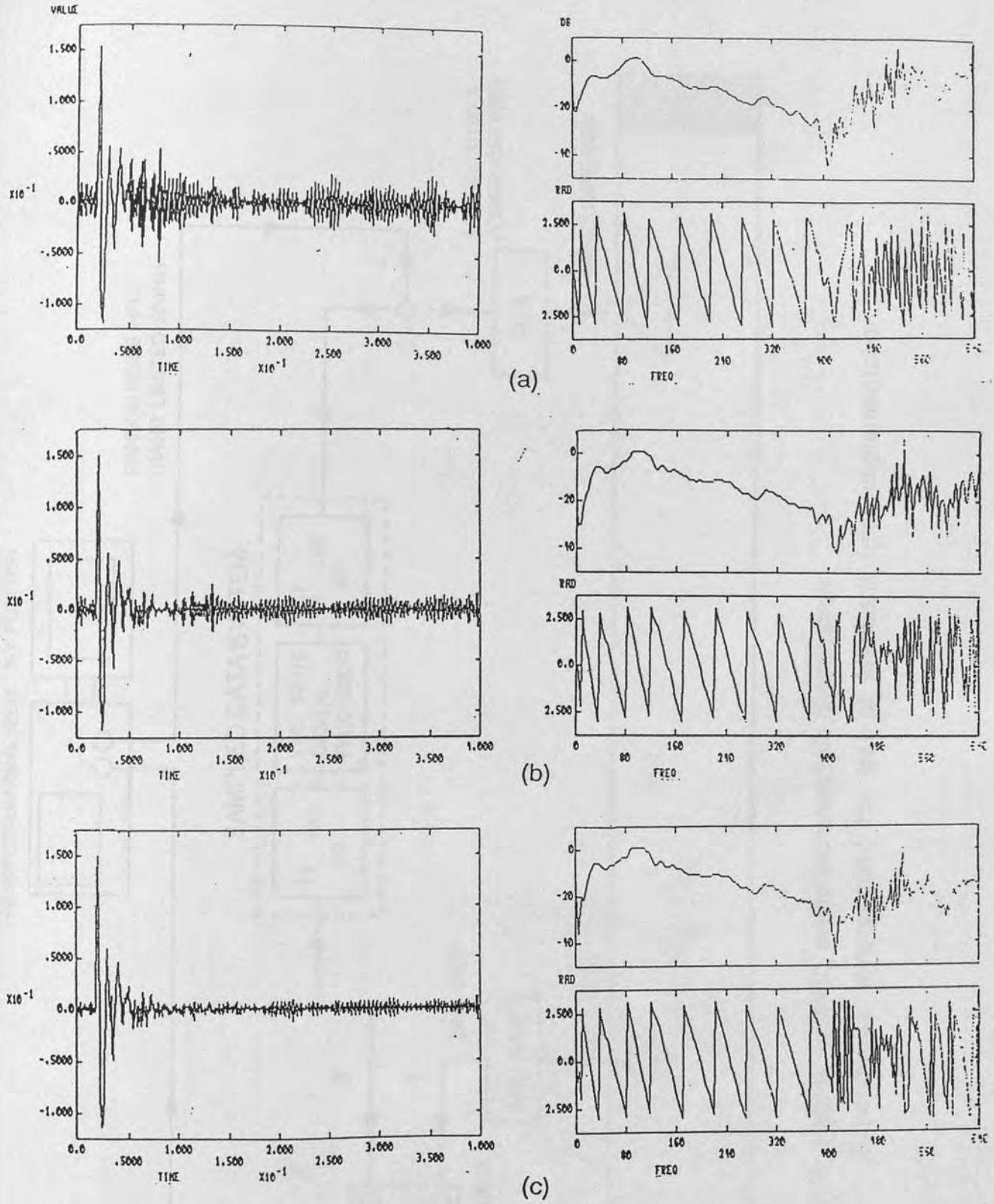

Figure 4.12 Hybrid system, anechoic/anechoic termination

Impulse and frequency responses for the feedback sampled data system employing the following number of FIR coefficients (a) 61, (b)128, and (c) 256

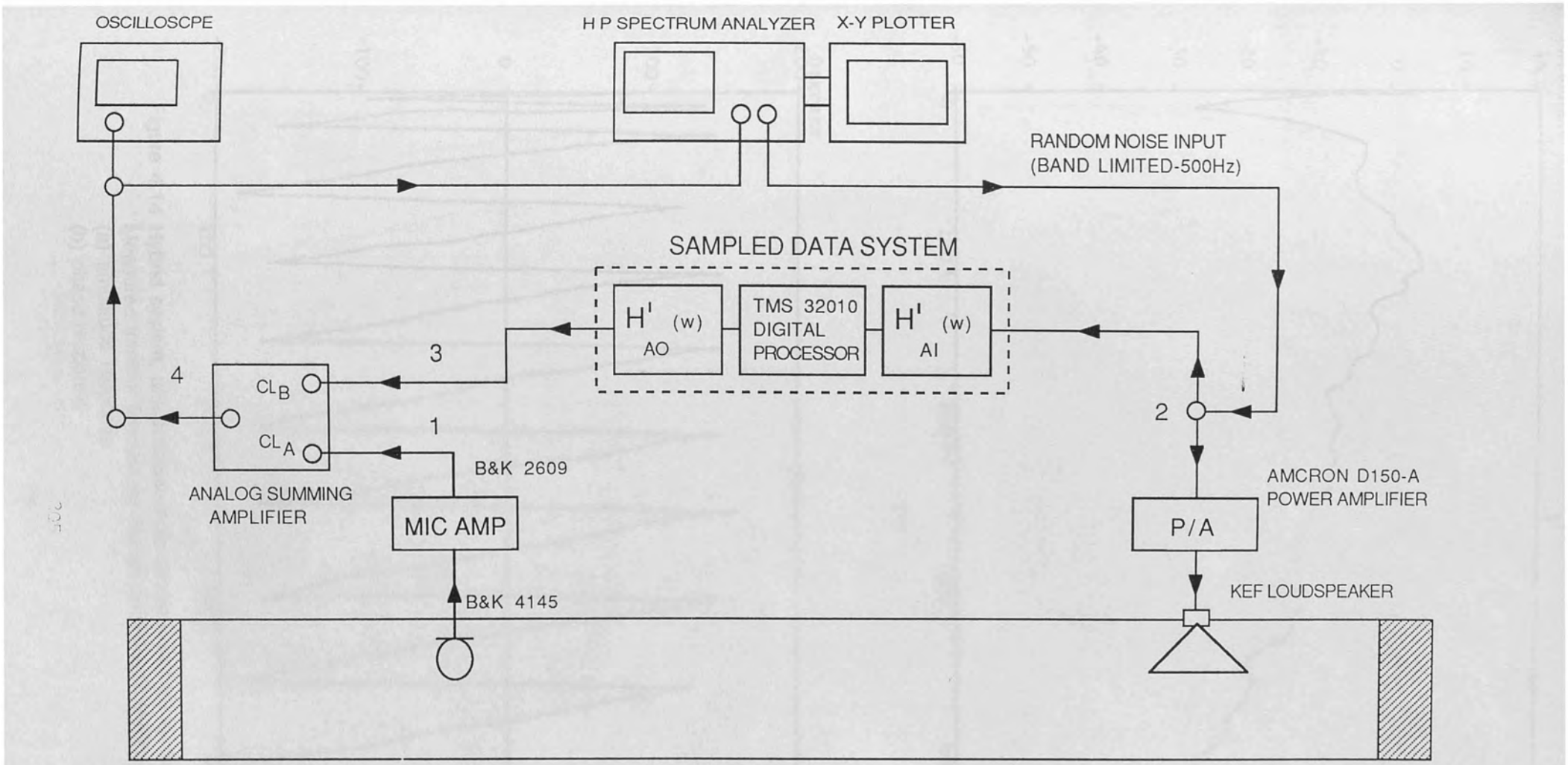

Figure 4.13 Hybrid system, anechoic/anechoic termination

Experimental arrangement for test of feedback filter implementation.

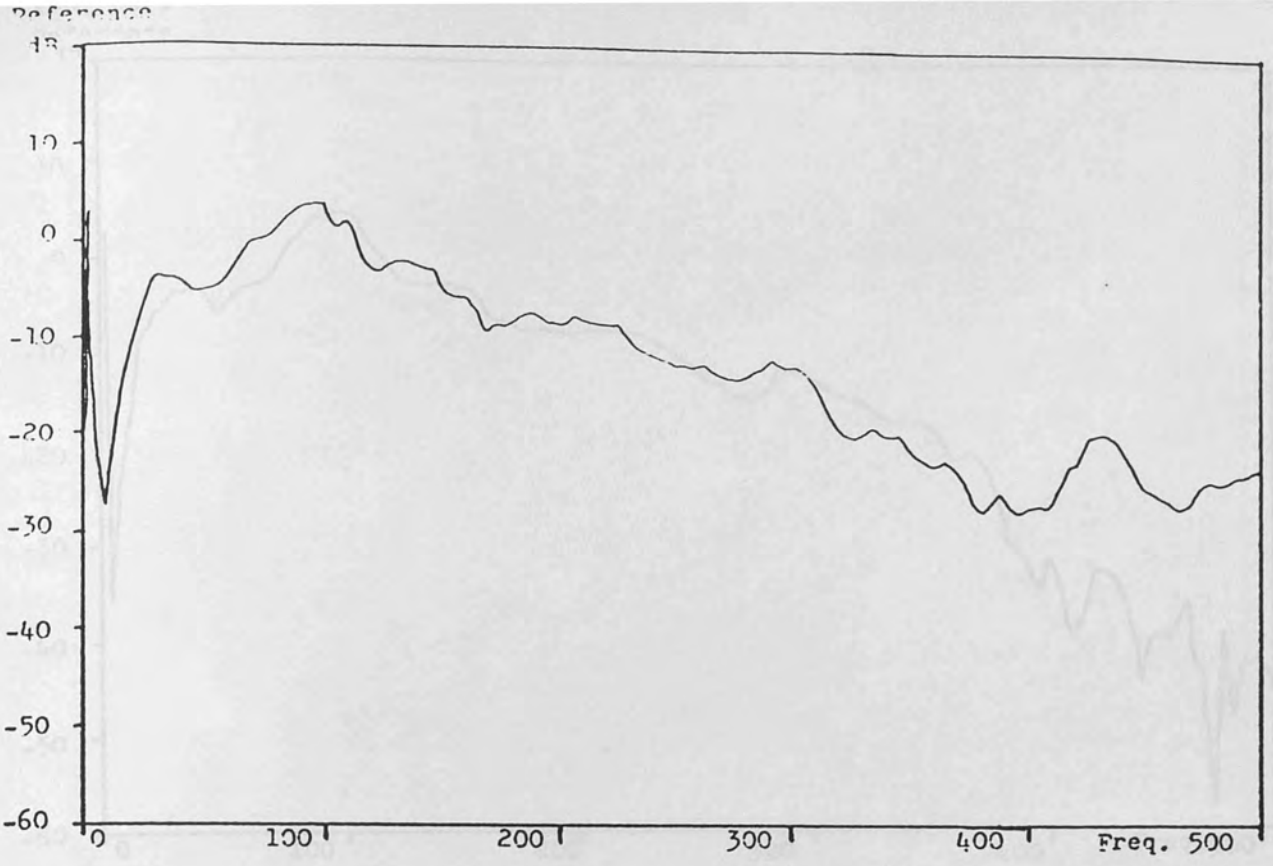

(a)

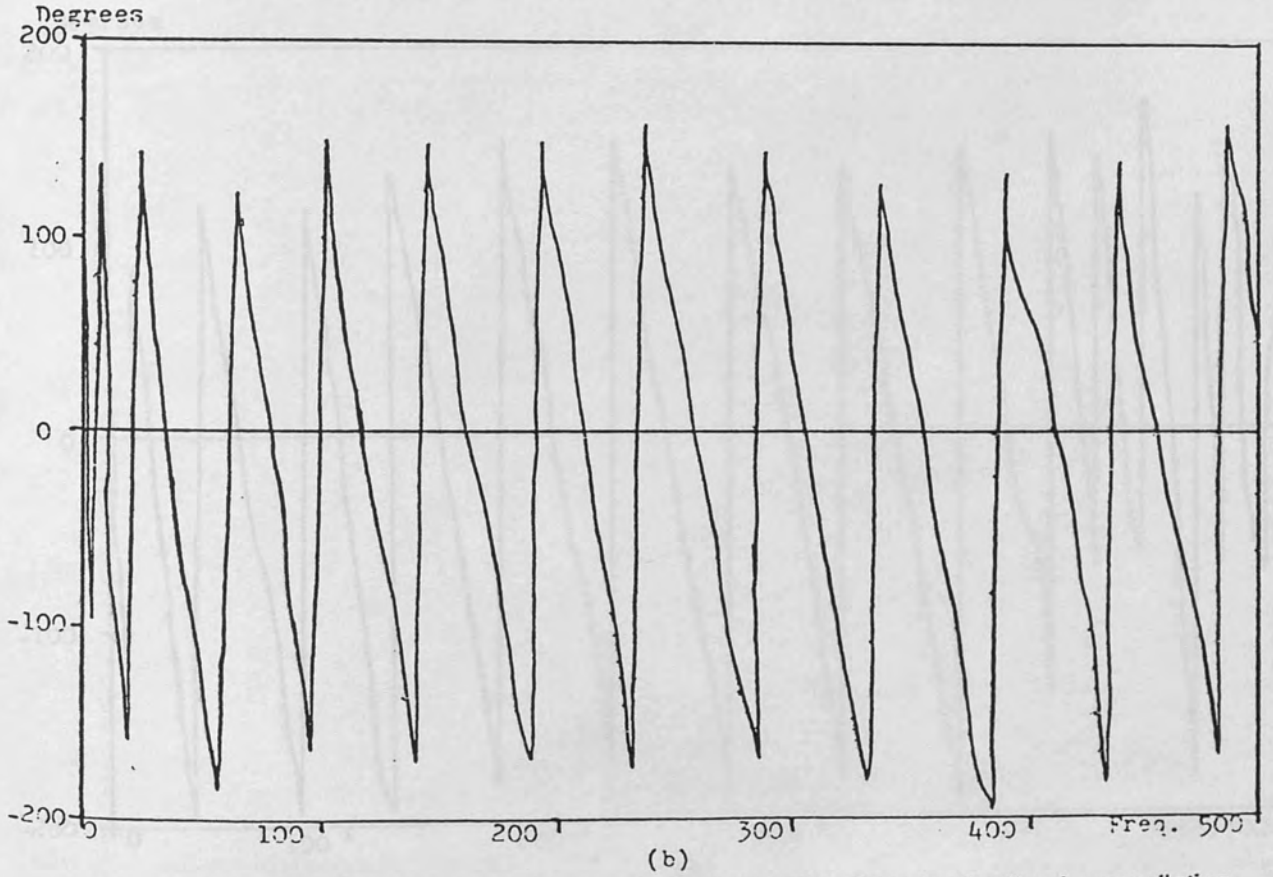

(b)

Figure 4.14 Hybrid system, anechoic/anechoic termination.Test for feedback cancellation
Measured transfer function for the electroacoustic feedback path
(a) amplitude response
(b) phase response

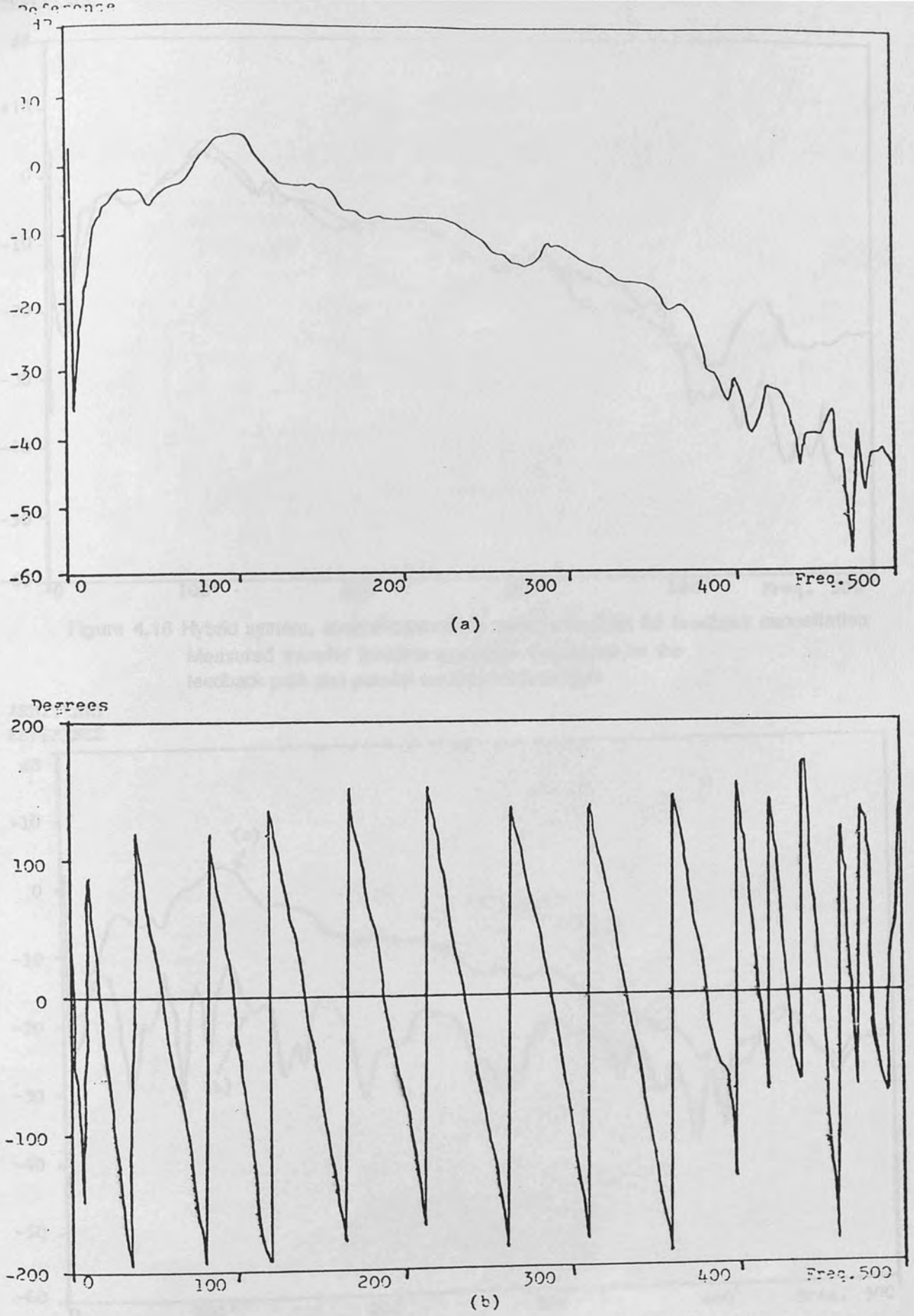

Figure 4.15 Hybrid system, anechoic/anechoic termination.Test for feedback cancellation
Measured transfer function for the sampled data system
(a) amplitude response
(b) phase response

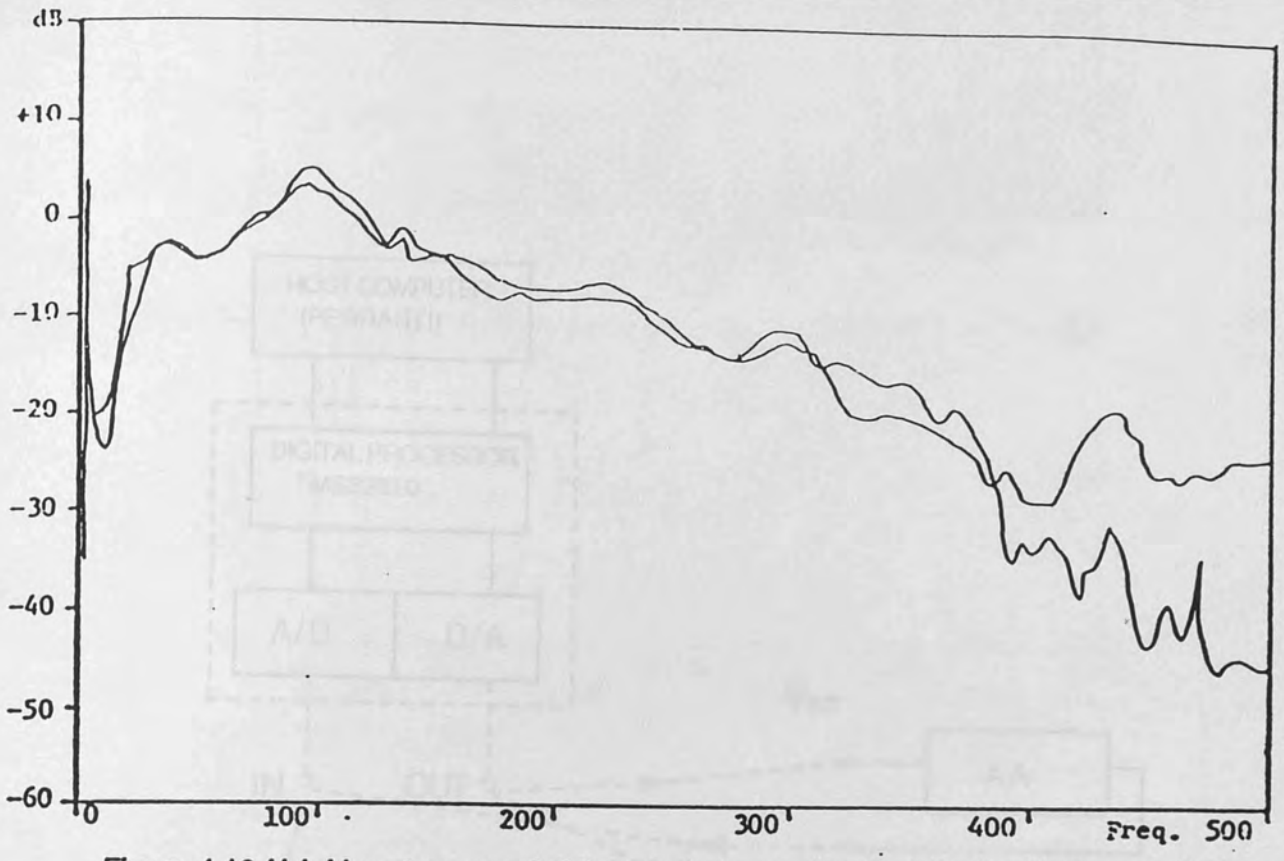

Figure 4.16 Hybrid system, anechoic/anechoic termination.Test for feedback cancellation
Measured transfer function amplitude responses for the
feedback path and parallel sampled data system

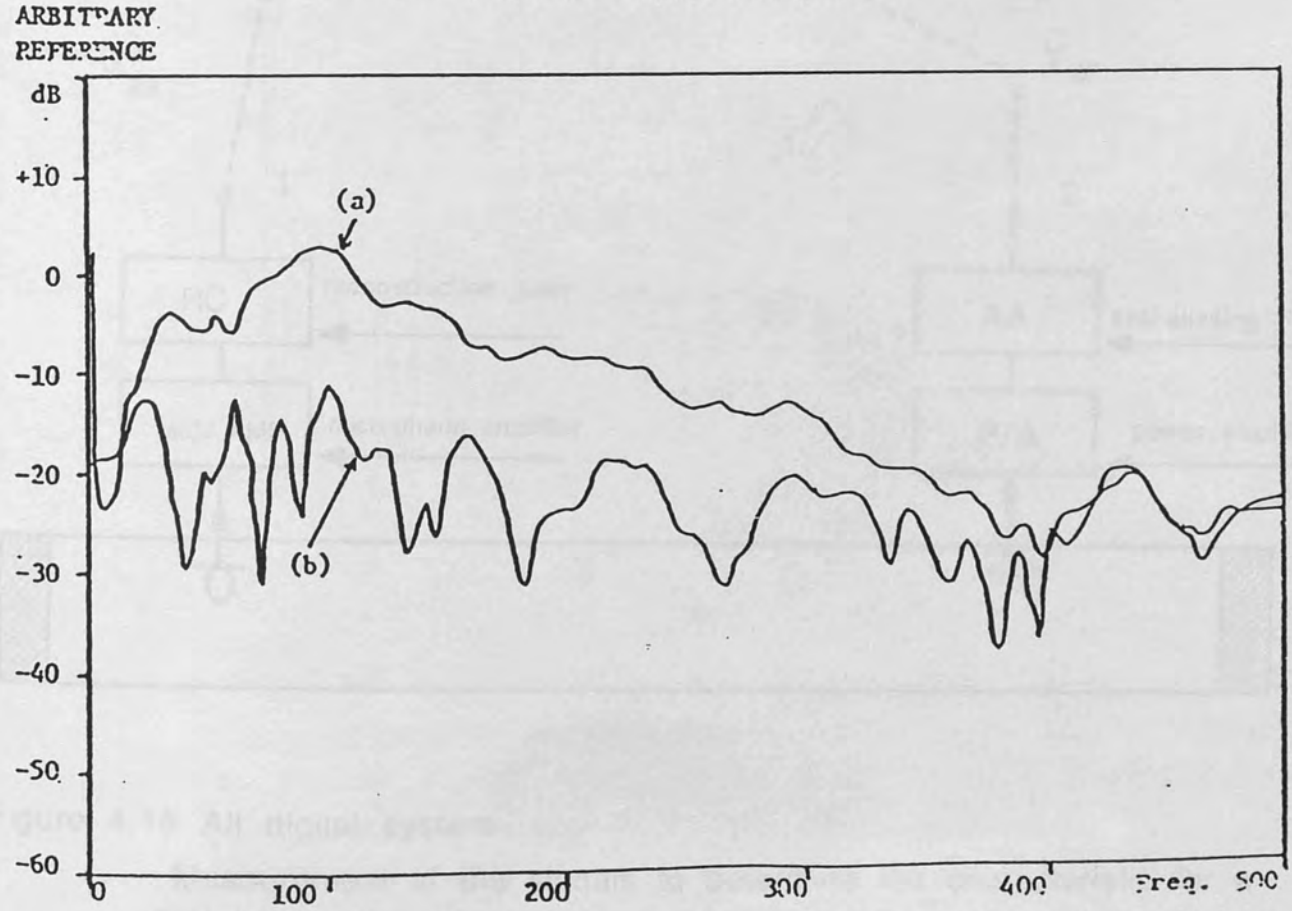

Figure 4.17 Hybrid system, anechoic/anechoic termination.Test for feedback cancellation
Measured cancellation (a)without,and (b) with the sampled data system
employing an 61 point FIR filter

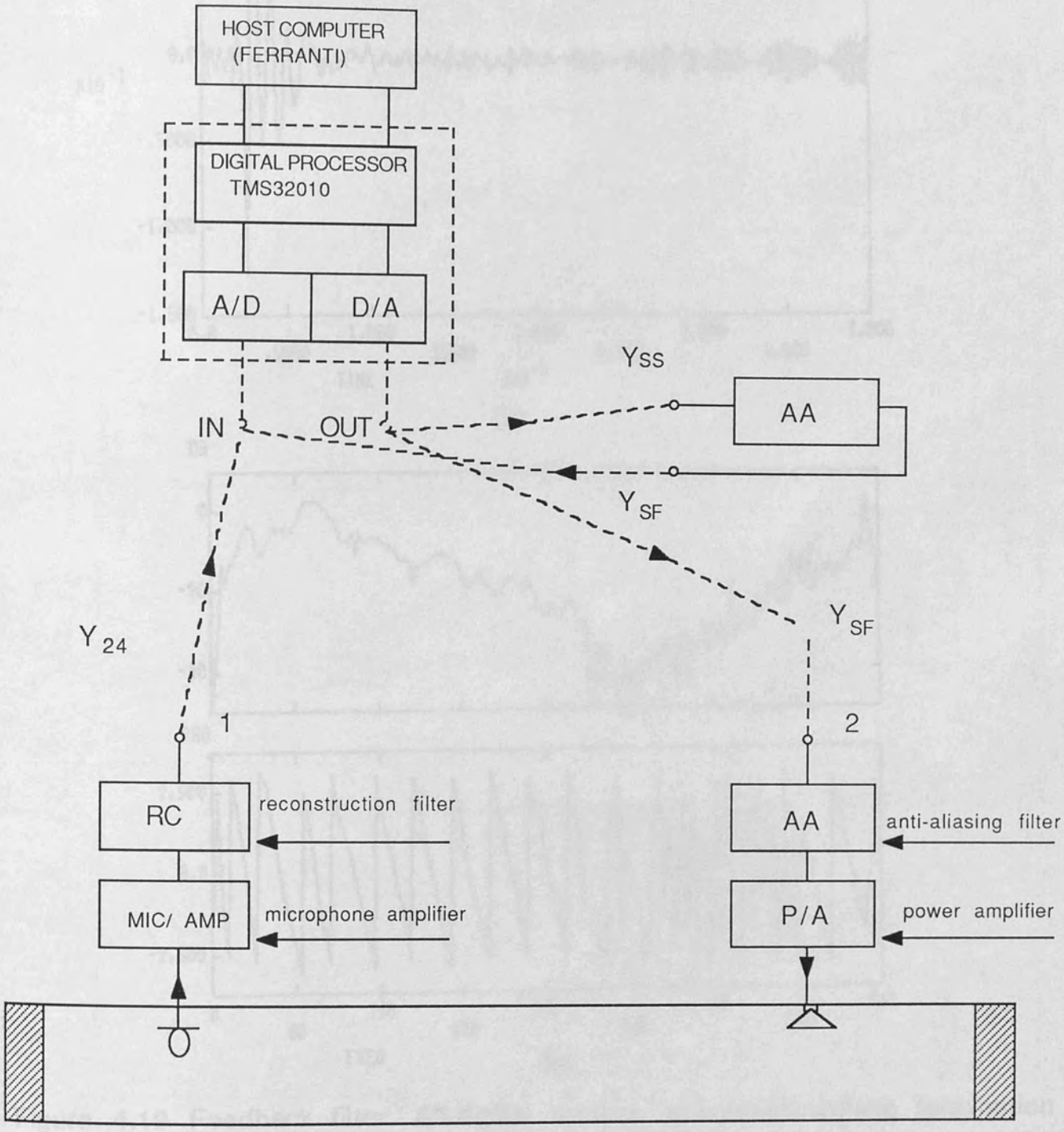

Figure 4.18 All digital system

Measurement of the signals to determine the characteristic for a digital filter for parallel feedback cancellation

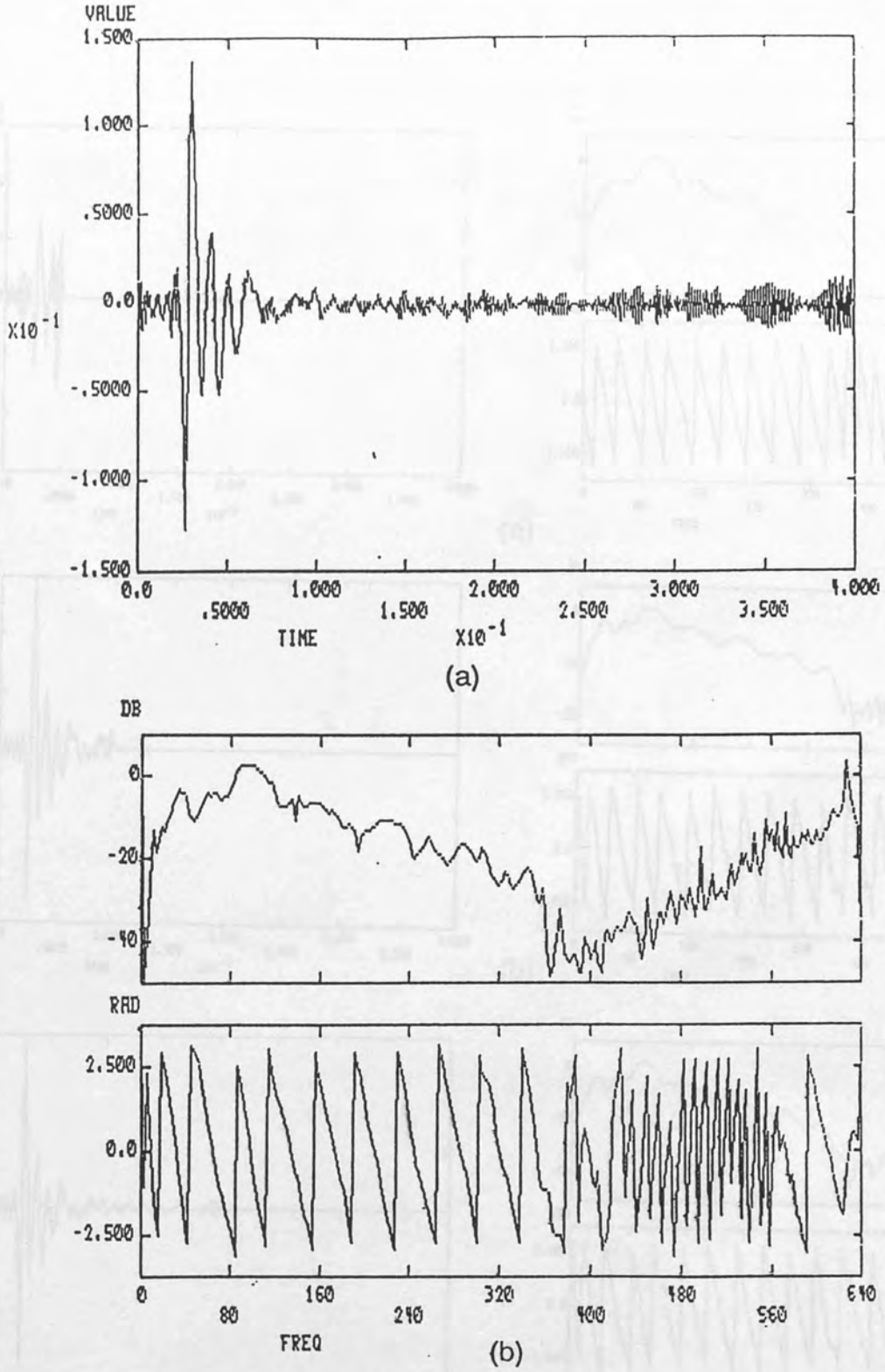

Figure 4.19 Feedback filter. All-digital system, anechoic/anechoic termination

Measured impulse and frequency response for the feedback filter required for all digital cancellation of the electroacoustic feedback path

(a) amplitude response

(b) phase response

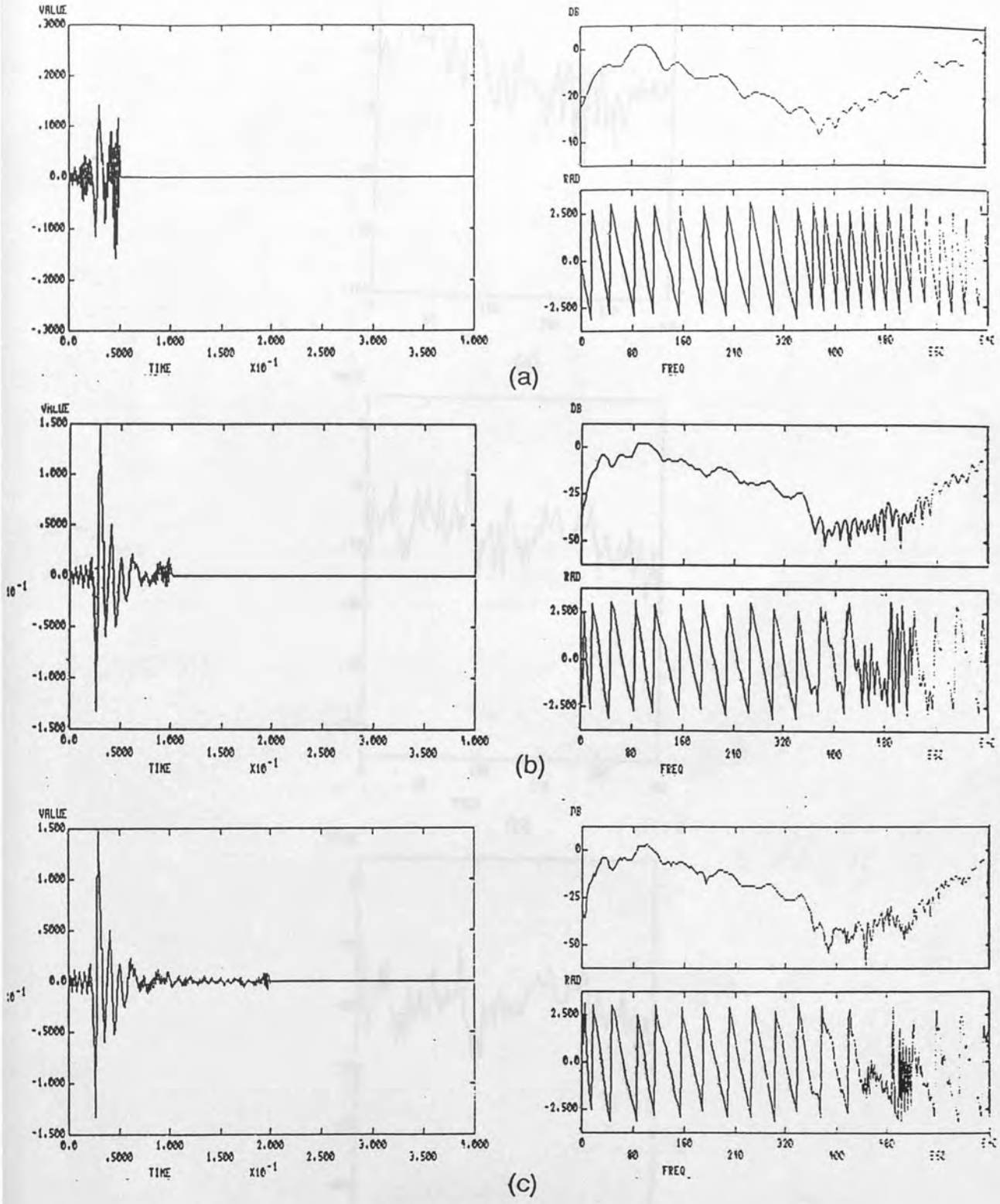

Figure 4.20 All-digital system, anechoic/anechoic termination
FIR filter approximations to figure 4.19, using the following number of coefficients (a) 64, (b) 128, and (c) 256

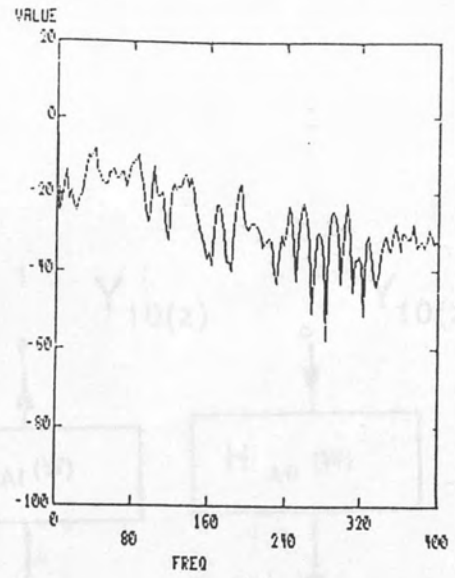

(a)

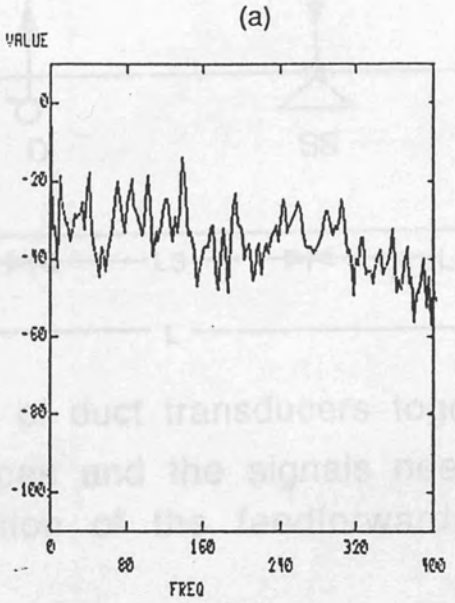

(b)

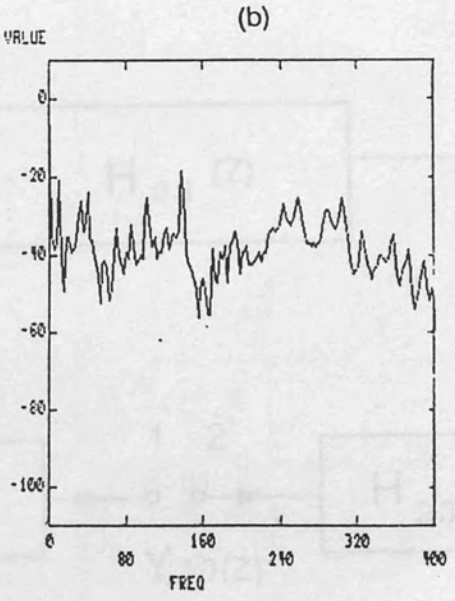

(c)

Figure 4.21 All-digital system, anechoic/anechoic termination
Feedback cancellation using the following number of FIR coefficients (a) 64, (b) 128, and (c) 256

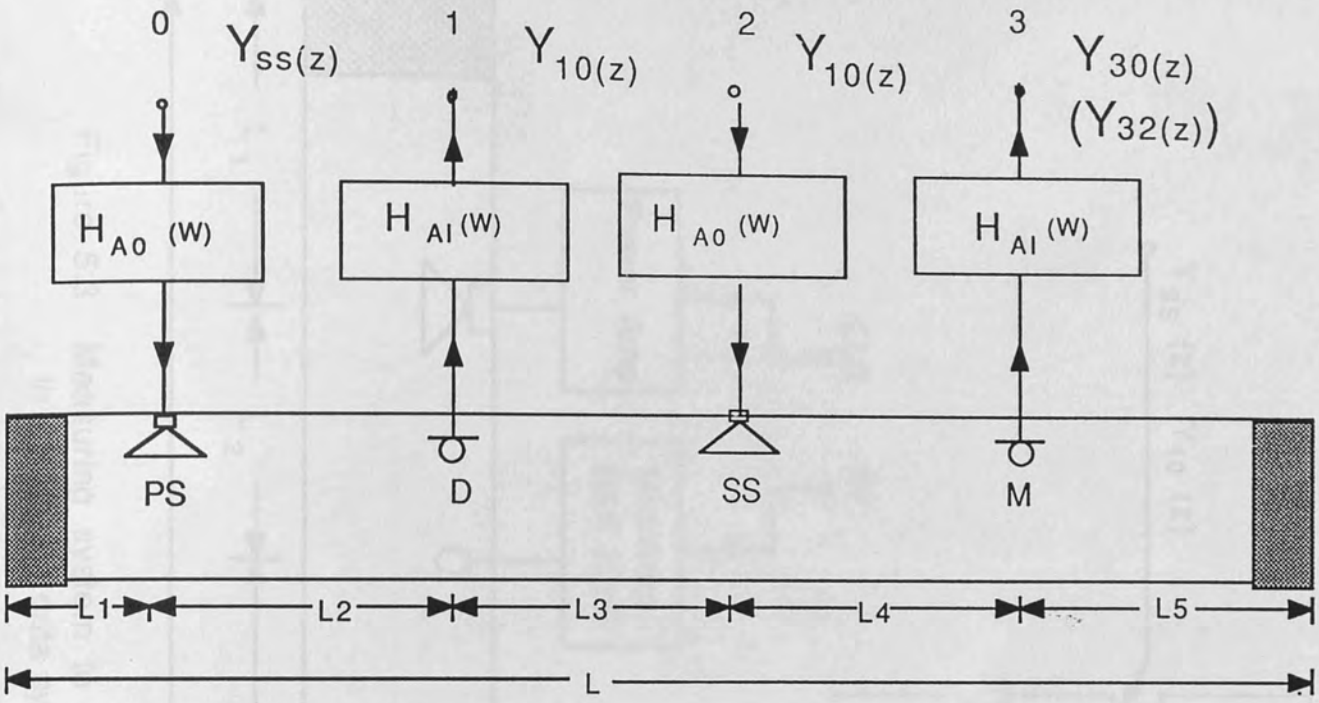

Figure 5.1 Layout of duct transducers together with the analog interfaces and the signals needed for digital implementation of the feedforward filter

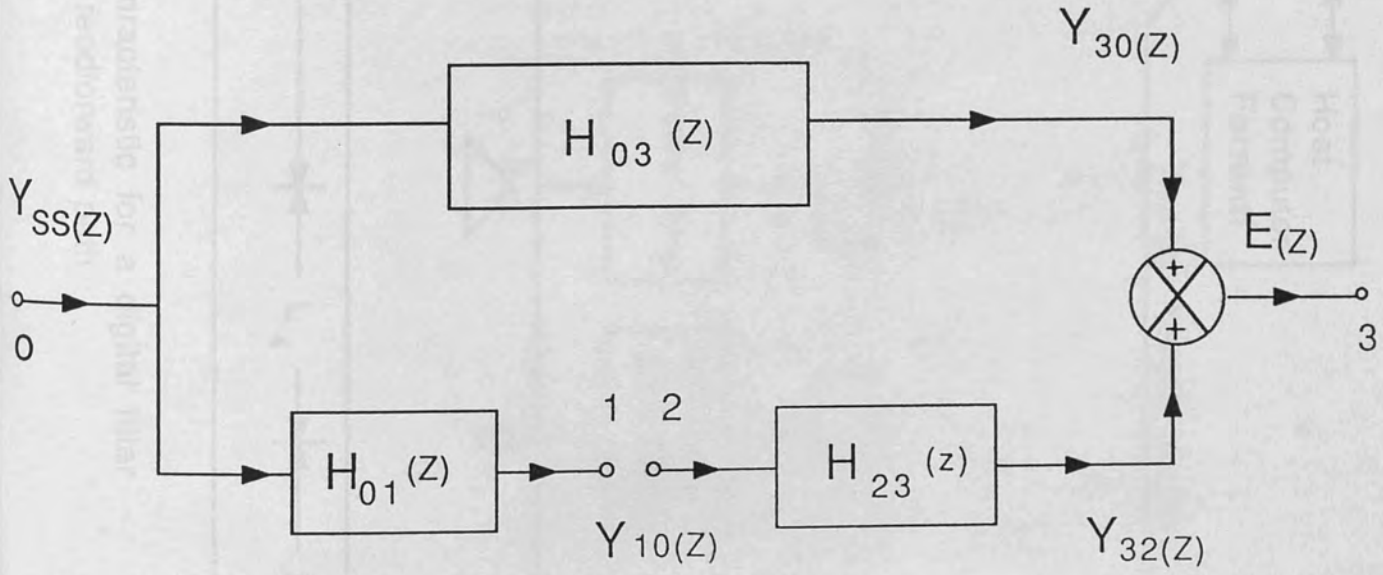

Figure 5.2 Block diagram representation for the system shown in figure 5.1

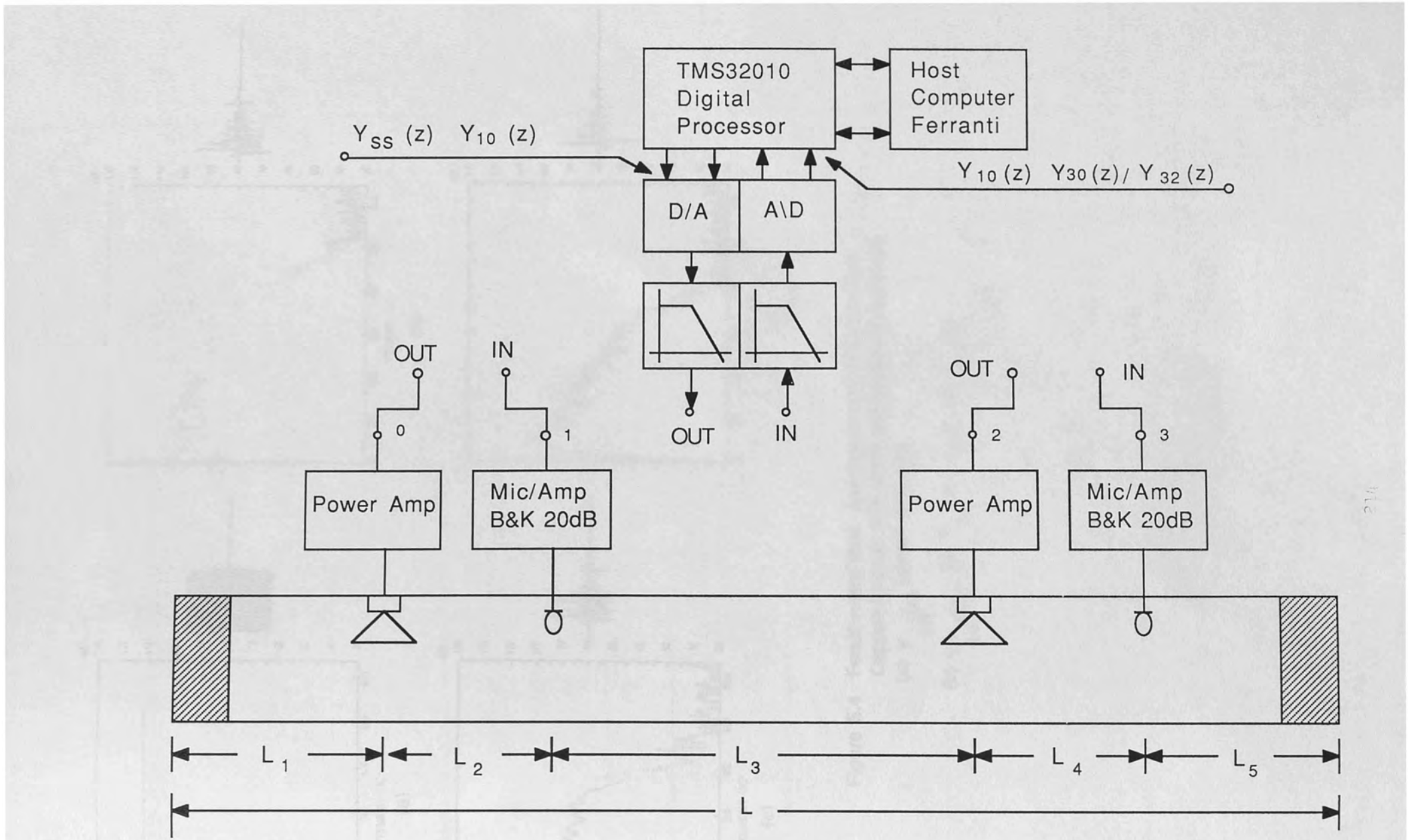

Figure 5.3 Measuring system to determine the characteristic for a digital filter in a sampled data system to model the feedforward path

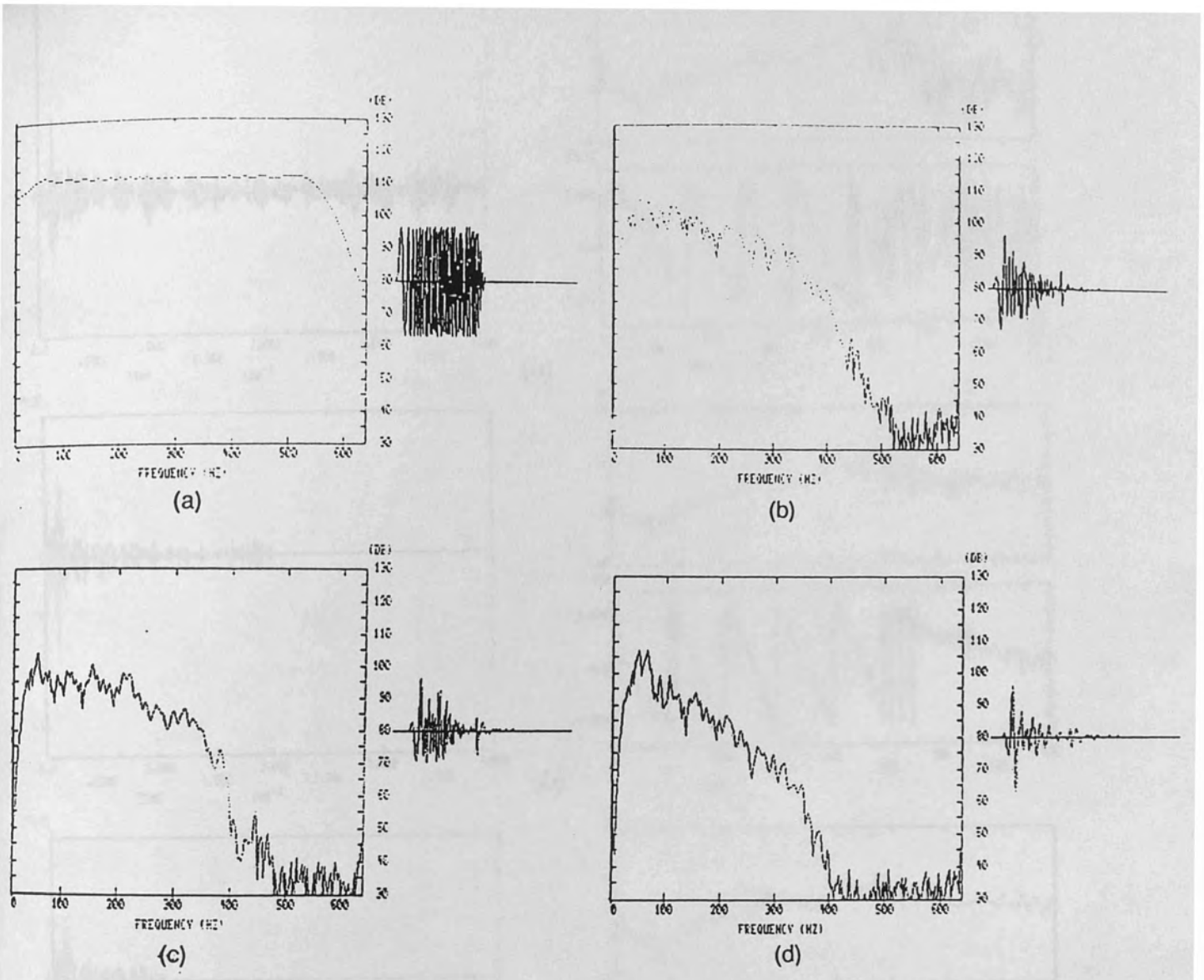

Figure 5.4 Feedforward filter. Anechoic/anechoic termination
Captured signals time series and frequency responses
(a) $Y_{SS}(z)$ (swept sinusoid)
(b) $Y_{10}(z)$, (c) $Y_{30}(z)$, and (d) $Y_{32}(z)$

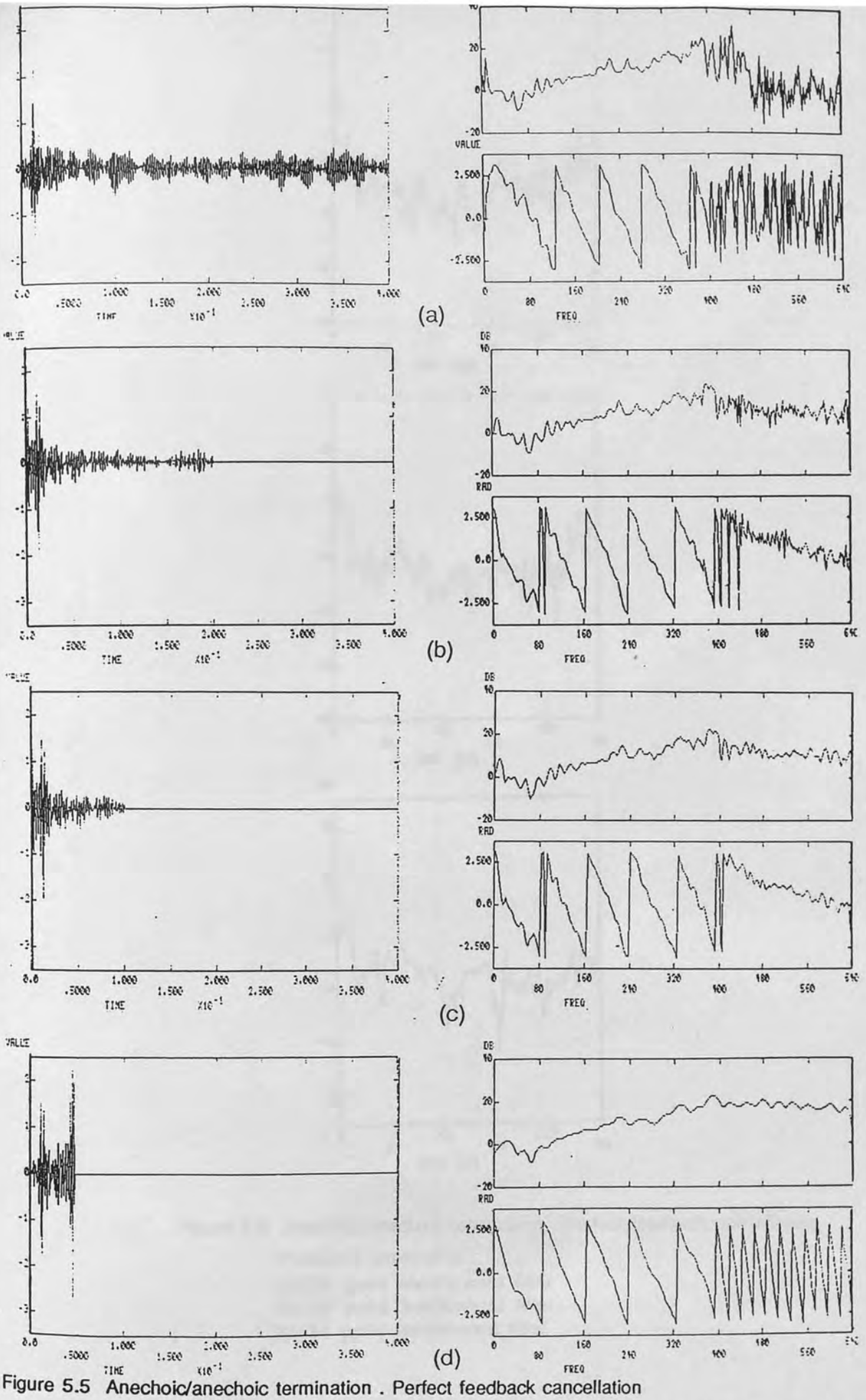

Figure 5.5 Anechoic/anechoic termination . Perfect feedback cancellation

Digital feedforward filter impulse and frequency response (a) computed directly from measured signals (b),(c), and (d) are FIR approximations to (a) using the following filter length 256,128,and 61 respectively

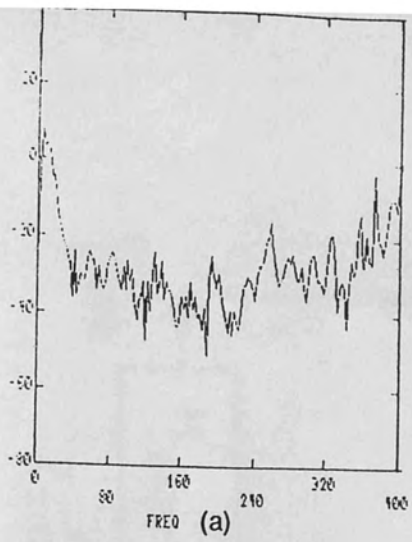

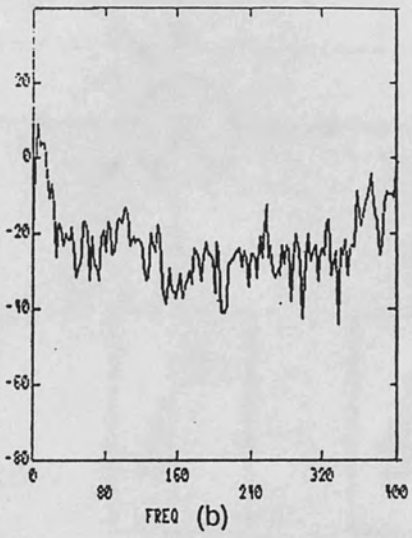

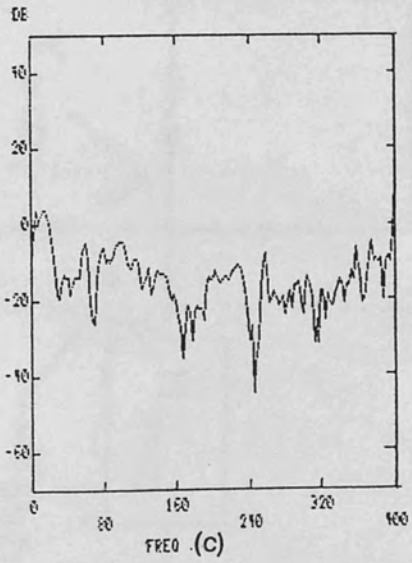

Figure 5.6 Anechoic/anechoic termination . Perfect feedback cancellation

Predicted attenuation
(a)256 point feedforward filter
(b)128 point feedforward filter
(c) 61 point feedforward filter

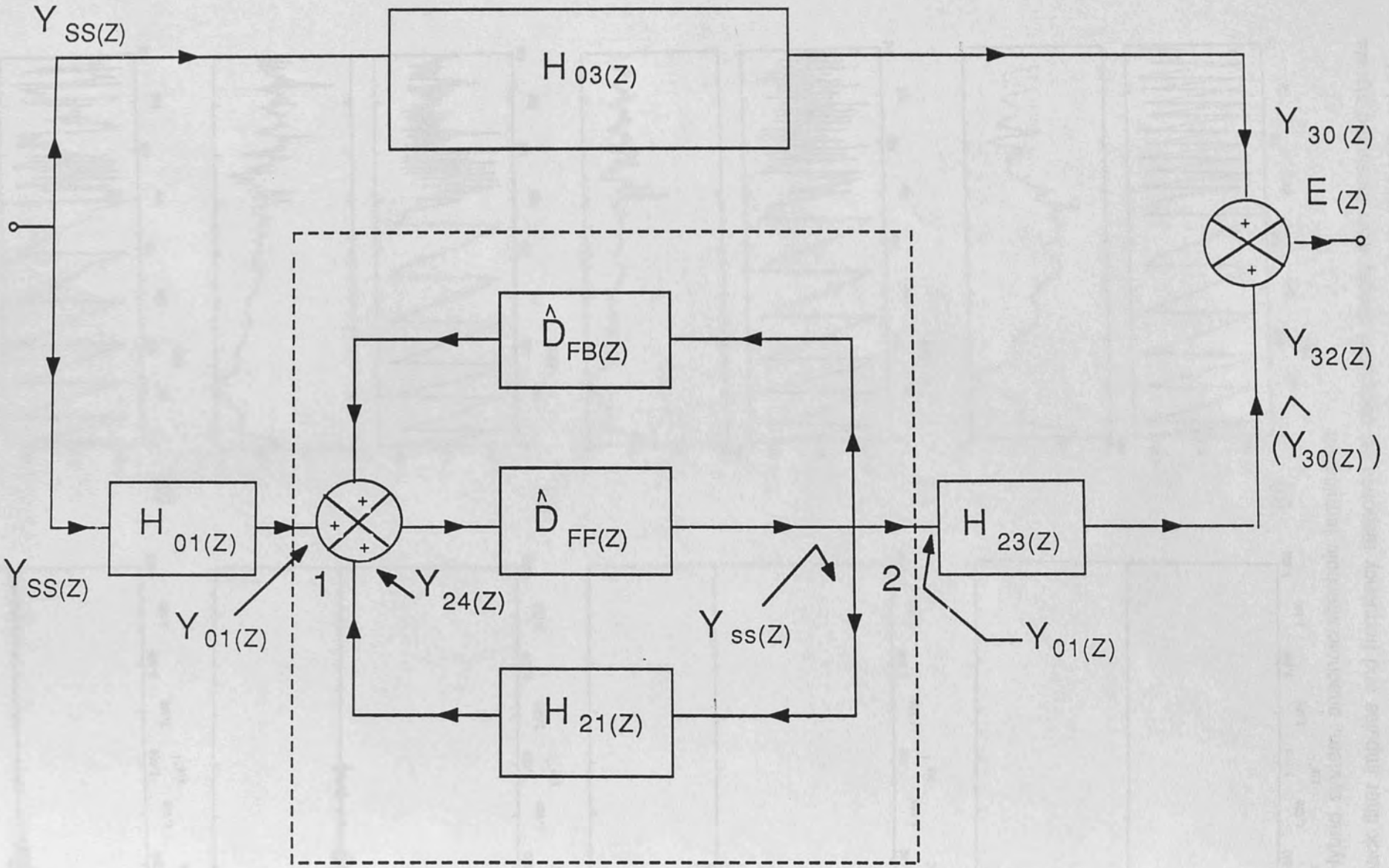

Figure 6.1 Shows the transfer functions and the signals involved in the realisation and evaluation of an ANC system

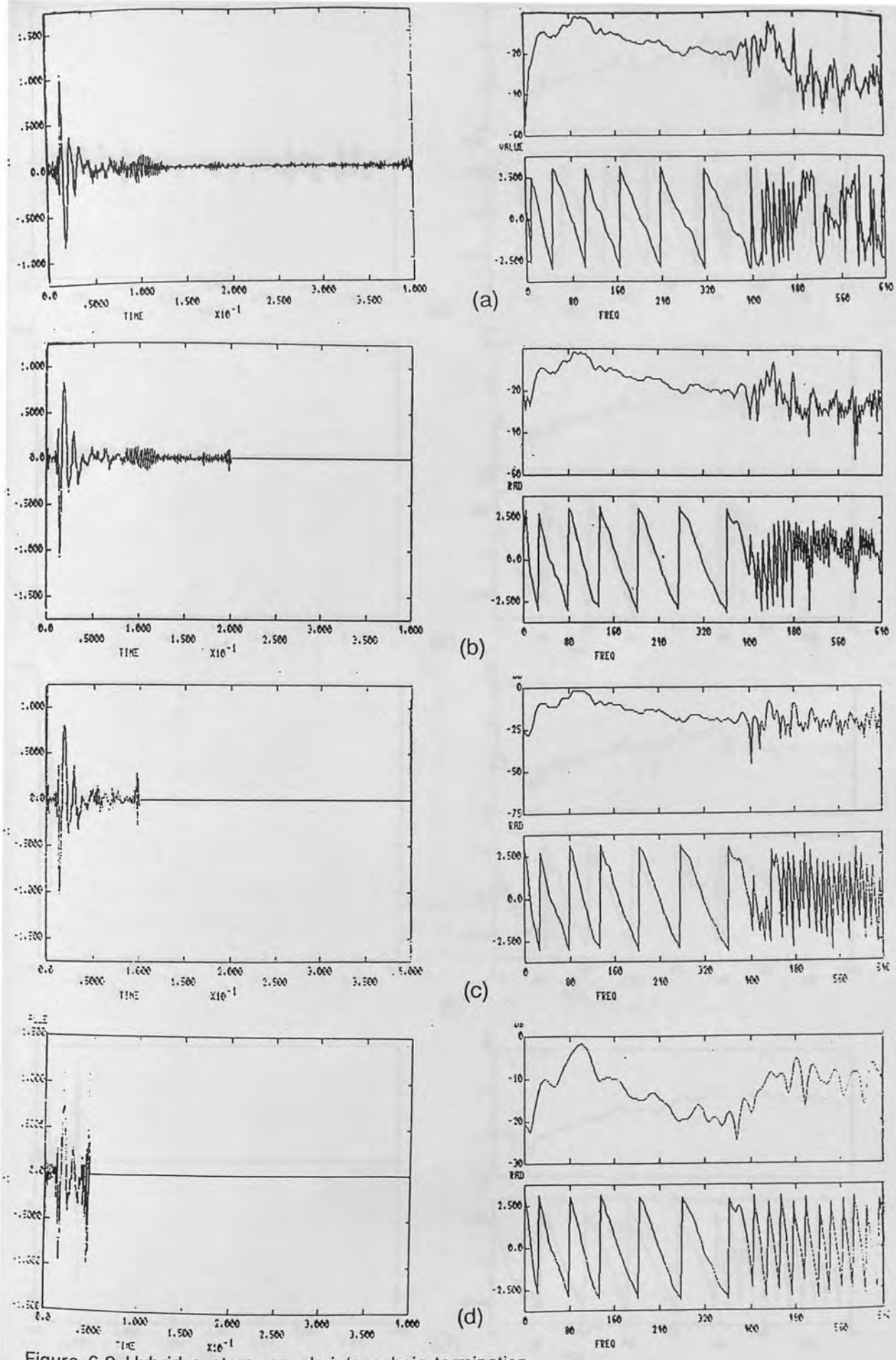

Figure 6.2 Hybrid system, anechoic/anechoic termination

Digital feedback filter impulse and frequency response (a) computed directly from measured signals (b),(c), and (d) are FIR approximations to (a) using the following filter length 256,128,and 61 respectively

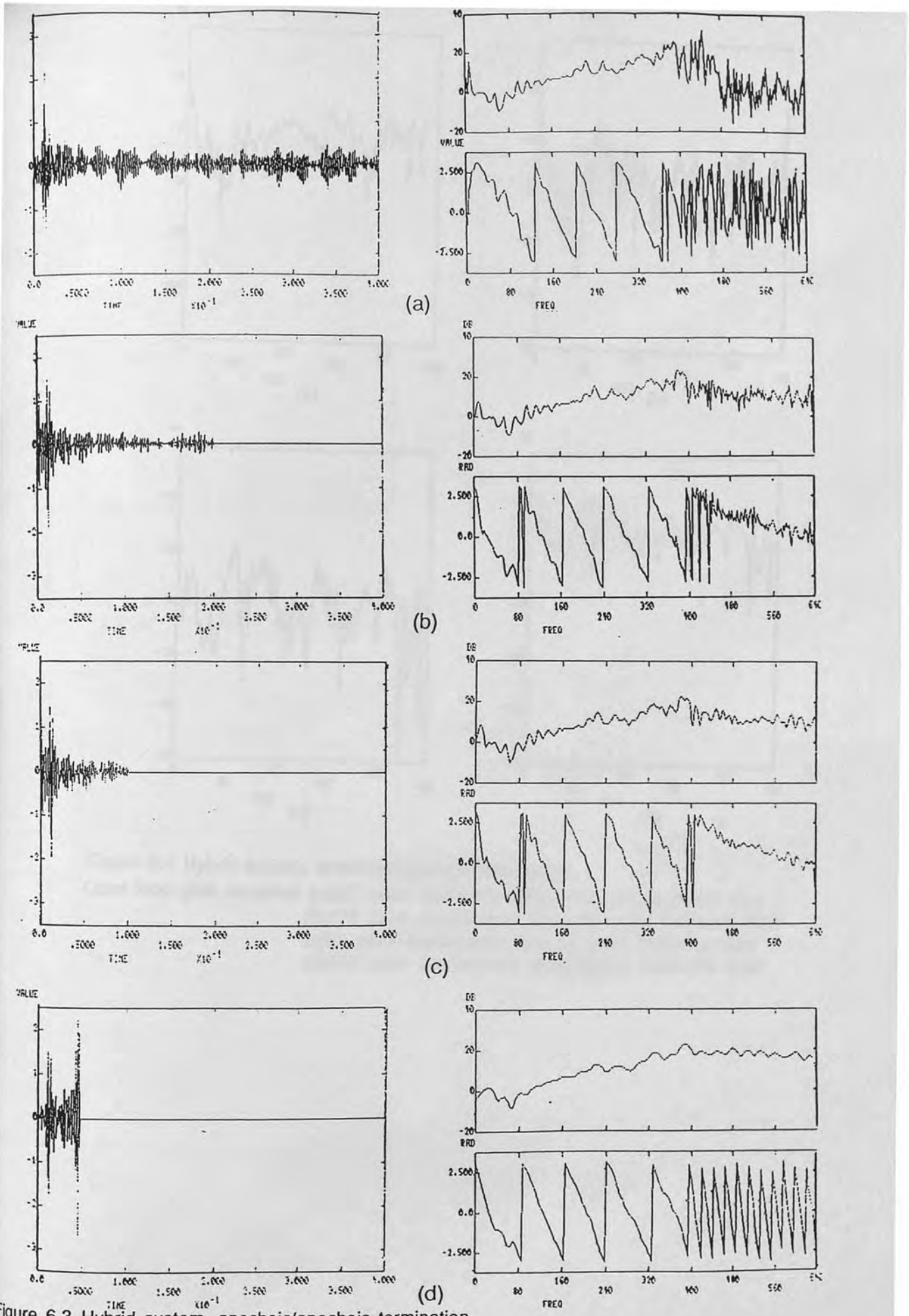

Figure 6.3 Hybrid system, anechoic/anechoic termination

Digital feedforward filter impulse and frequency response (a) computed directly from measured signals (b),(c), and (d) are FIR approximations to (a) using the following filter length 256,128,and 61 respectively

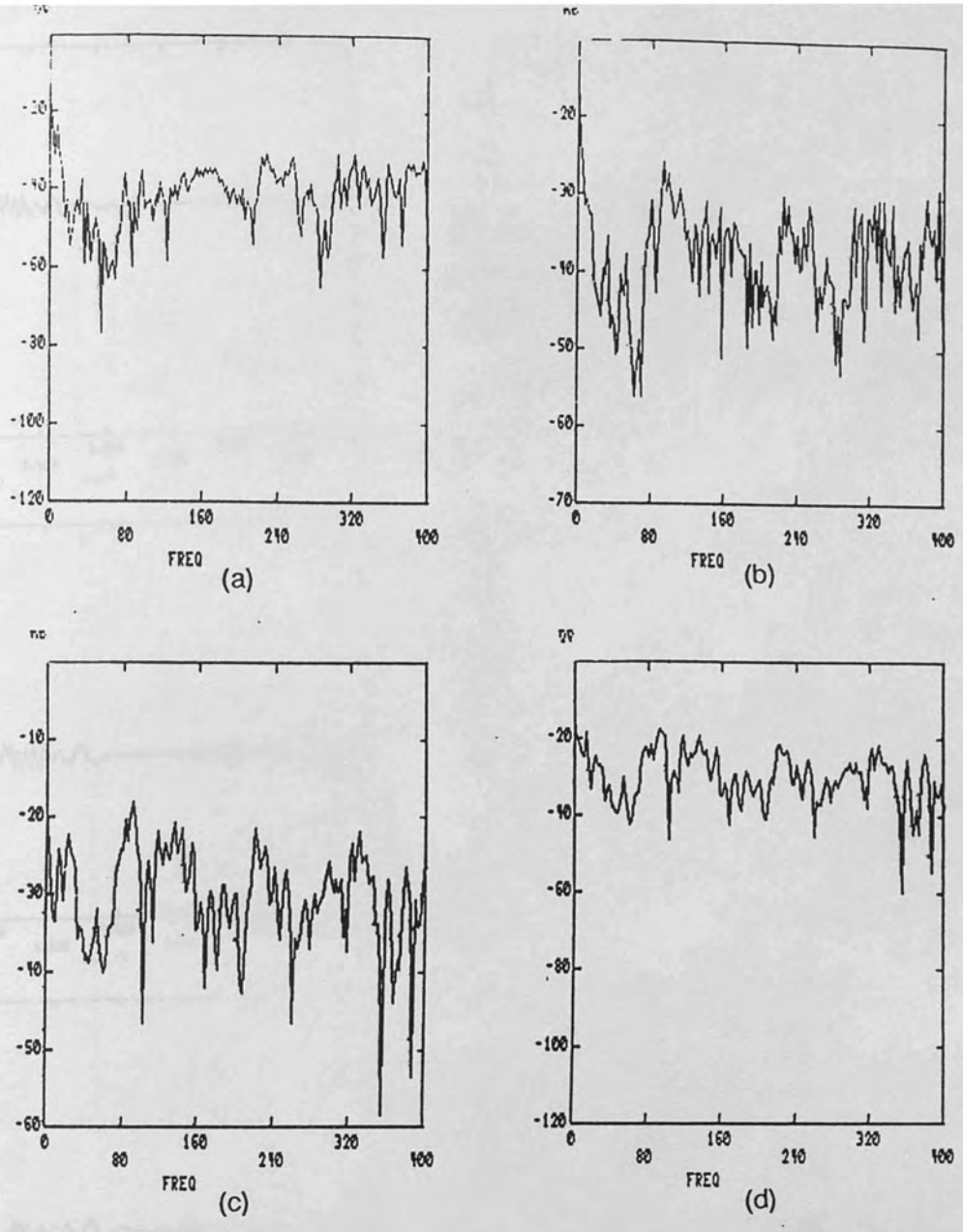

Figure 6.4 Hybrid system, anechoic/anechoic termination
Open loop gain response (a)256 point feedforward filter,256 point feedback filter
(b)128 point feedforward filter,128 point feedback filter
(c)61 point feedforward filter,61 point feedback filter
(d)256 point feedforward filter,61point feedback filter

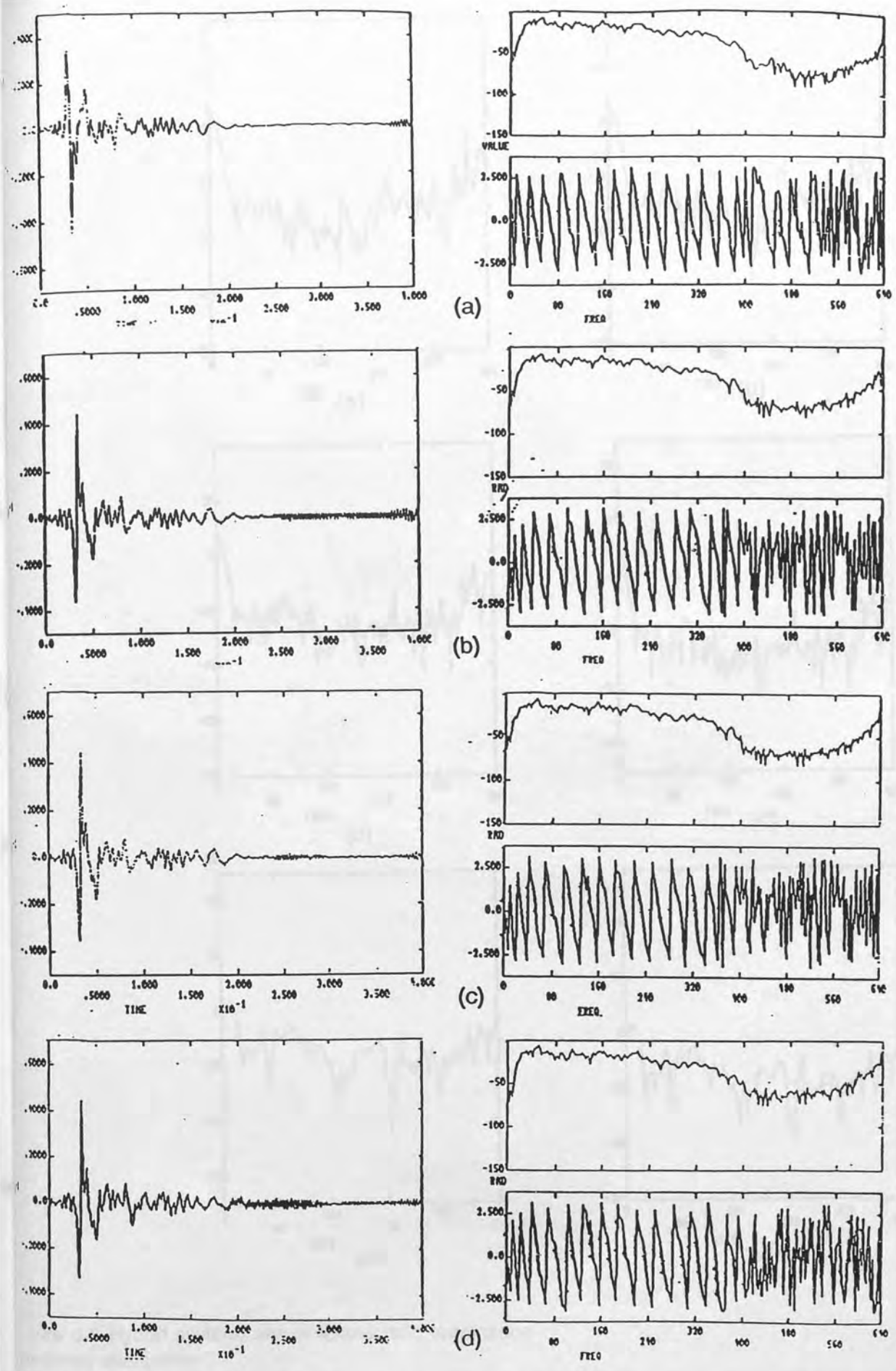

Figure 6.5 Hybrid system, anechoic/anechoic termination

Closed loop impulse and frequency response (a) computed directly from measured signals

(b) 256 point feedforward filter,256 point feedback filter(c)128 point feedforward filter, 128 point feedback filter and (d) 61 point feedforward filter ,61 point feedback filter

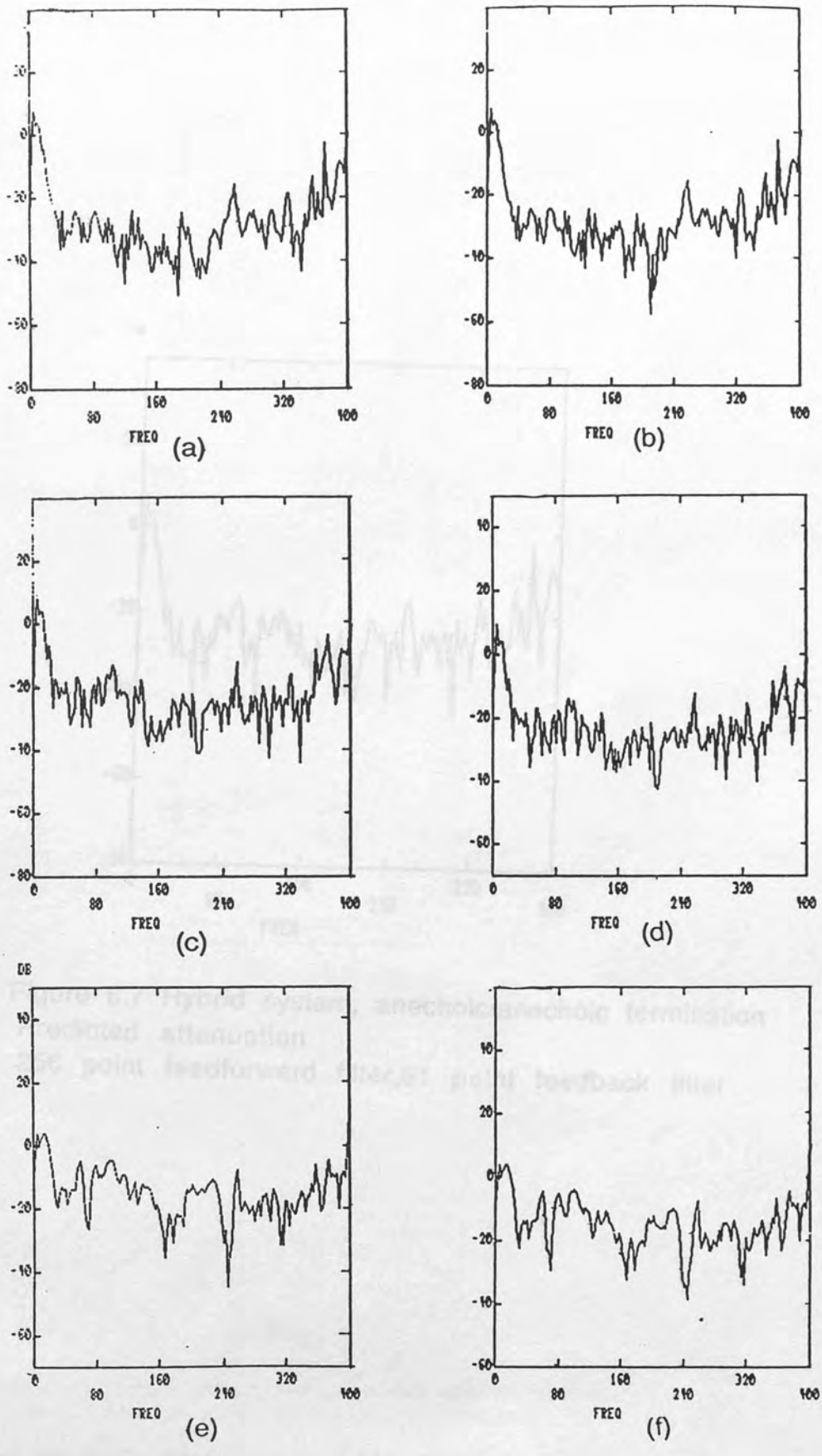

Figure 6.6 Hybrid system, anechoic/anechoic termination
Predicted attenuation
a)Perfect feedback cancellation,256 point feedforward filter,(b)256 point feedforward filter and 256 point feedback filter,(c)Perfect feedback cancellation,128 point feedforward filter,(d)128 point feedforward filter,128 point feedback filter,(e)Perfect feedback cancellation,61point feedforward filter,and(f)61 point feedforward filter,61 point feedback filter

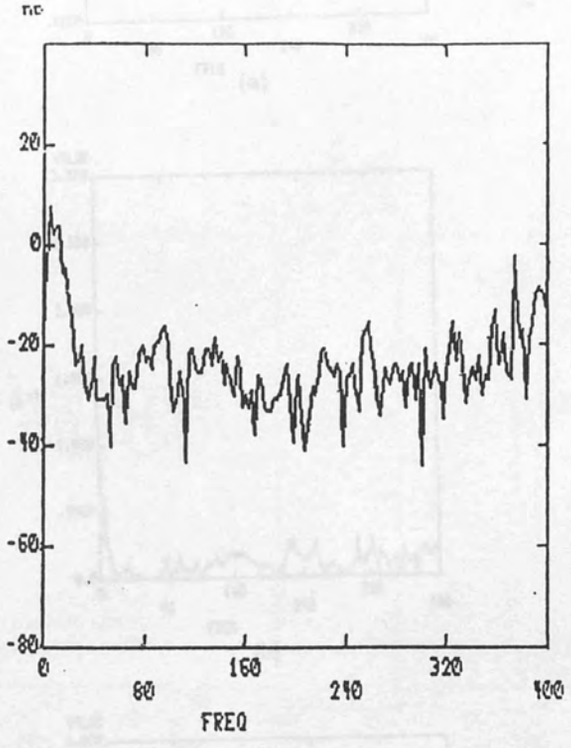

Figure 6.7 Hybrid system, anechoic/anechoic termination
Predicted attenuation
256 point feedforward filter,61 point feedback filter

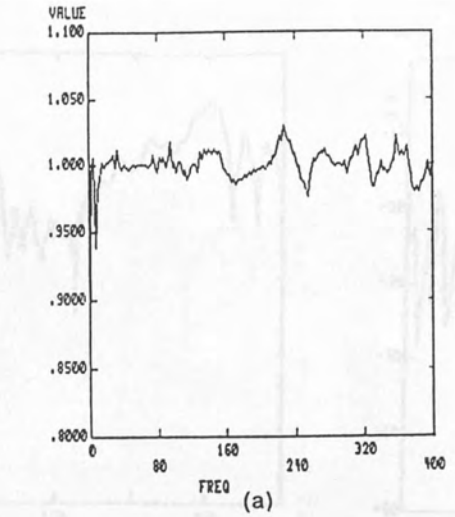

(a)

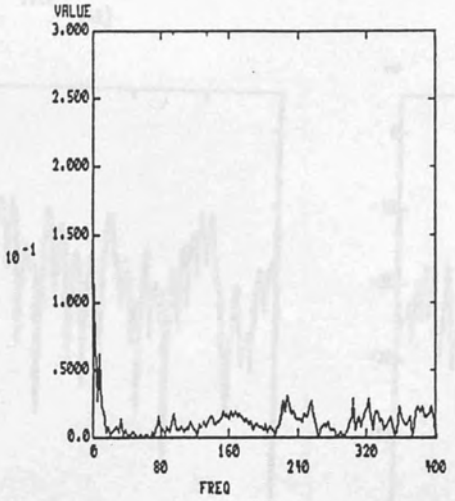

(b)

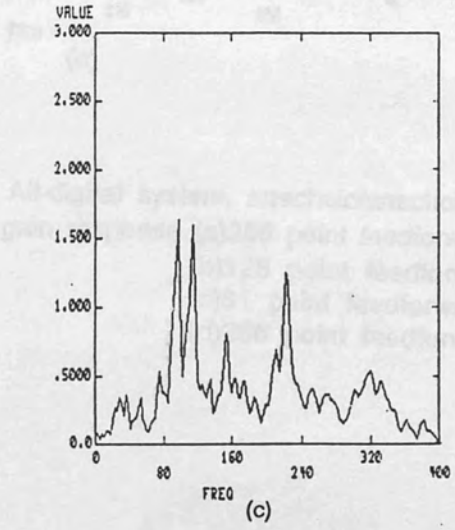

(c)

Figure 6.8 Sensitivity functions , hybrid system , anechoic / anechoic termination
Feedforward filter 256 points , and feedback filter 256 points

(a) Feedforward sensitivity function ($S_{HFF}(w)$) frequency response

(b) Residual feedback sensitivity function ($S_{T}(w)$) frequency response

(c) Acoustic feedback sensitivity function ($S_{H21}(w)$) frequency response

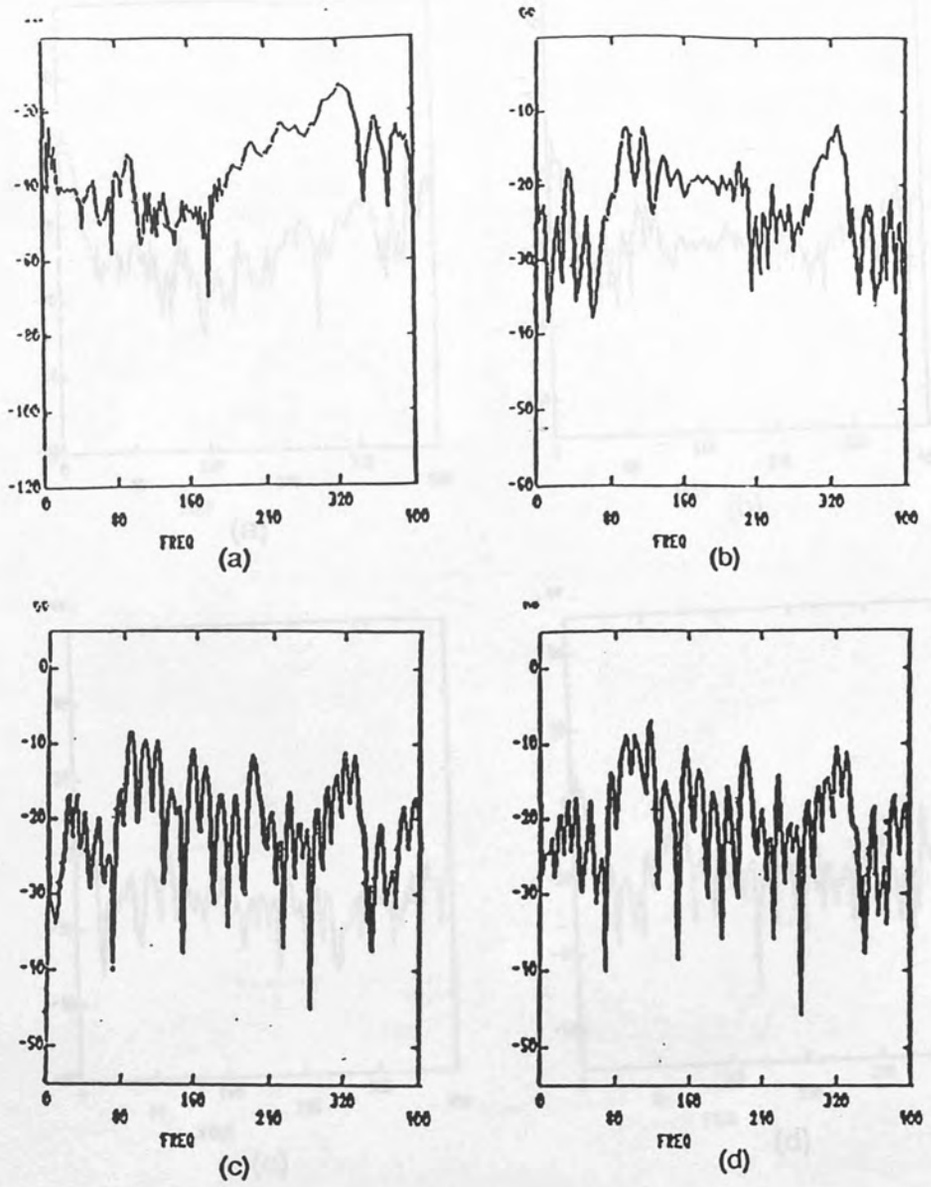

Figure 6.9 All-digital system, anechoic/anechoic termination
Open loop gain response (a)256 point feedforward filter,256 point feedback filter
(b)128 point feedforward filter,128 point feedback filter
(c)61 point feedforward filter,64 point feedback filter
(d)256 point feedforward filter,64 point feedback filter

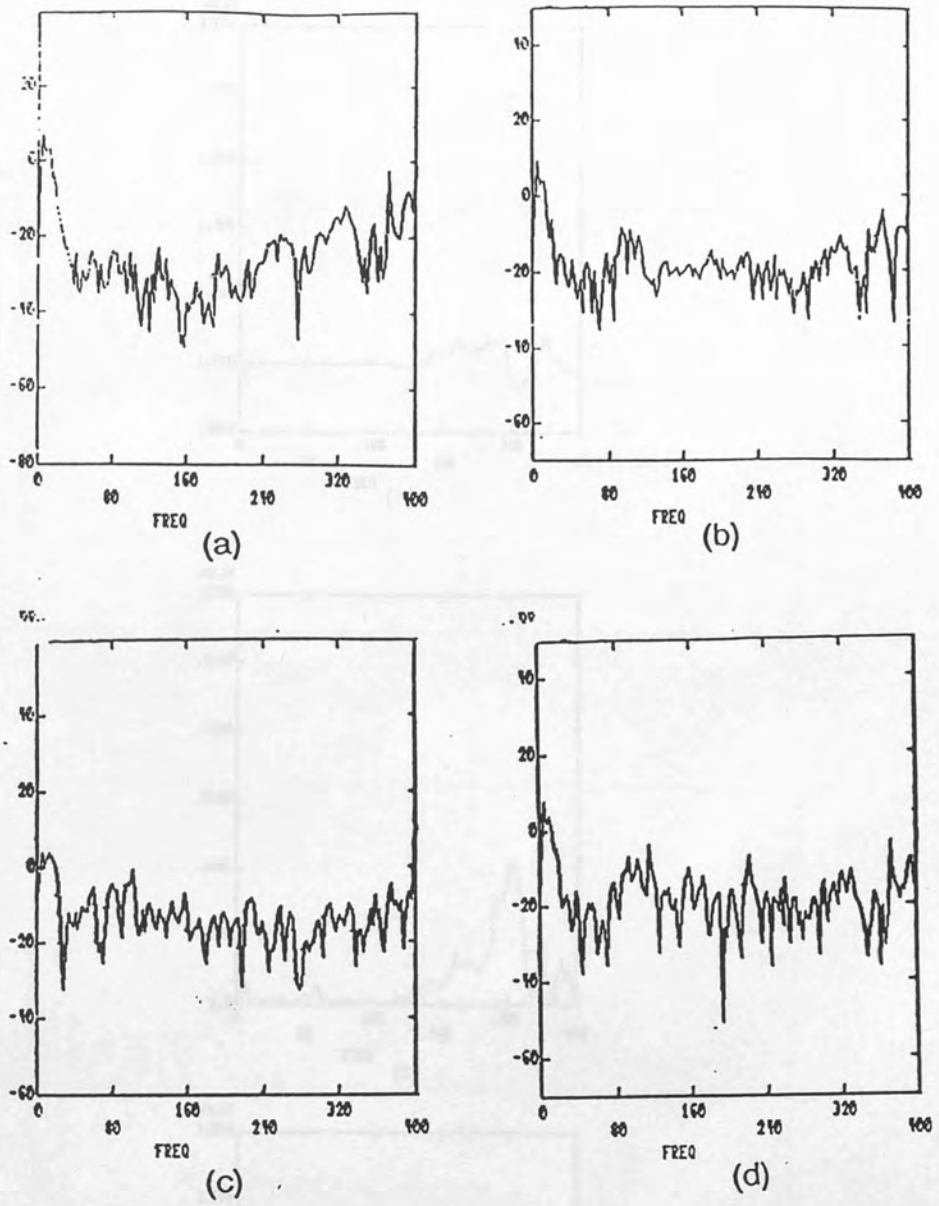

Figure 6.10 All-digital system, anechoic/anechoic termination

Predicted attenuation
(a)256 point feedforward filter,256 point feedback filter
(b)128 point feedforward filter,128 point feedback filter
(c)61 point feedforward filter,64 point feedback filter
(d)256 point feedforward filter,64 point feedback filter

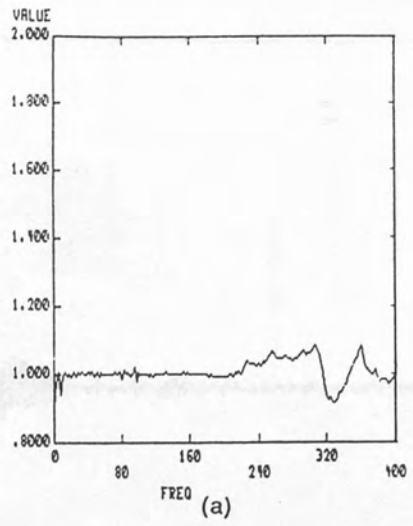

(a)

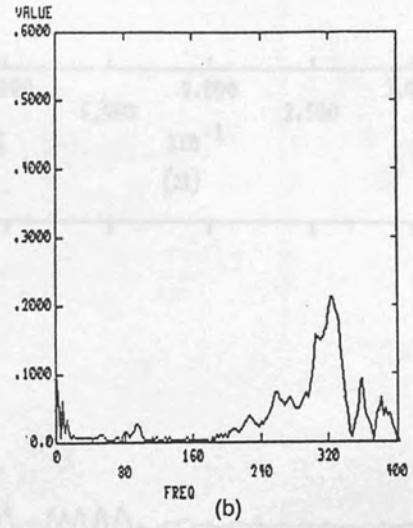

(b)

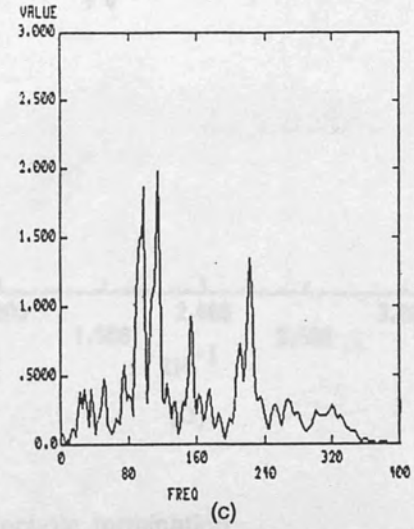

(c)

Figure 6.11 Sensitivity functions , all-digital system , anechoic / anechoic termination
Feedforward filter 256 points , and feedback filter 256 points

(a) Feedforward sensitivity function ($S_{HFF}(w)$) frequency response

(b) Residual feedback sensitivity function ($S_{T(w)}$) frequency response

(c) Acoustic feedback sensitivity function ($S_{H21}(w)$) frequency response

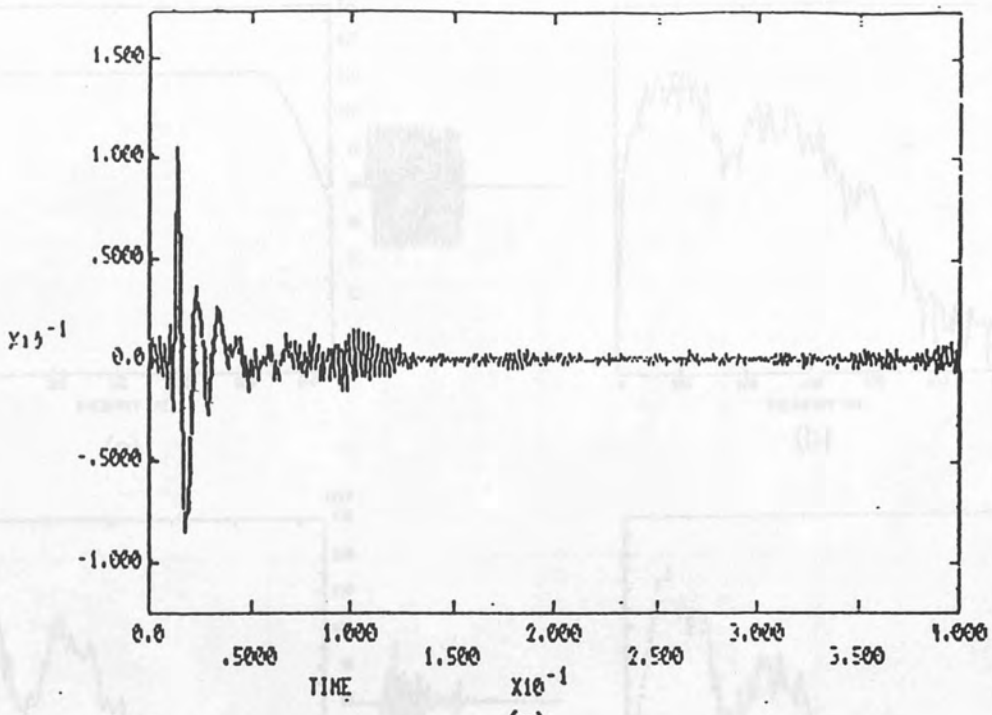

(a)

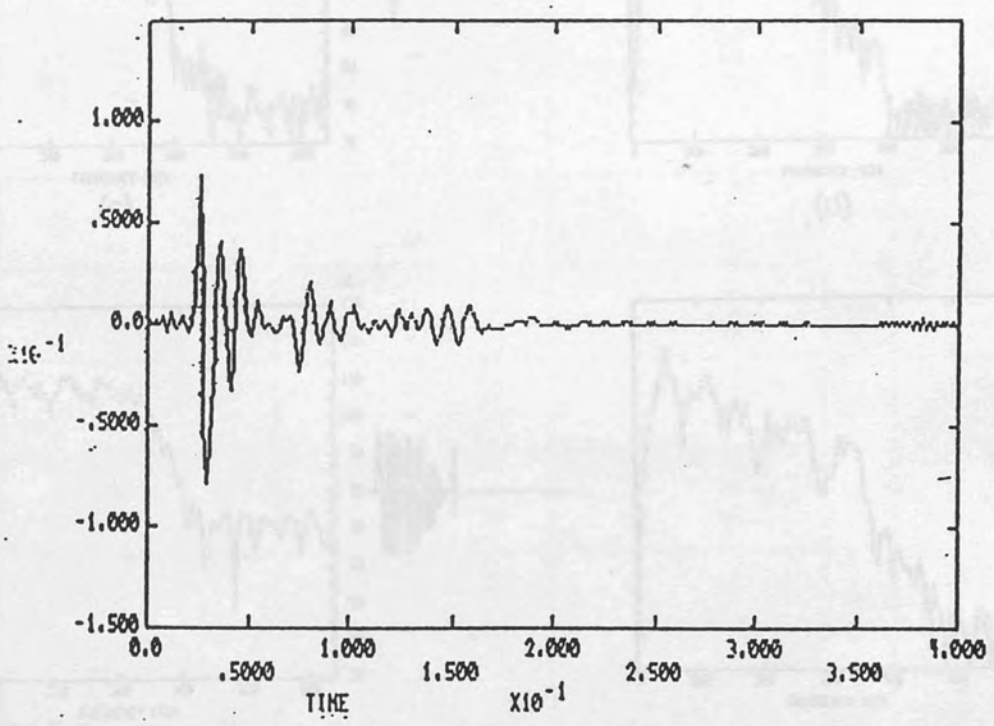

(b)

Figure 6.12 Anechoic/anechoic termination
Directly computed from measured signals ,the impulse responses of the two different feedback paths
(a)Desired impulse response for the feedback filter in a hybrid system
(b)Desired impulse response for the feedback filter in a all-digital system

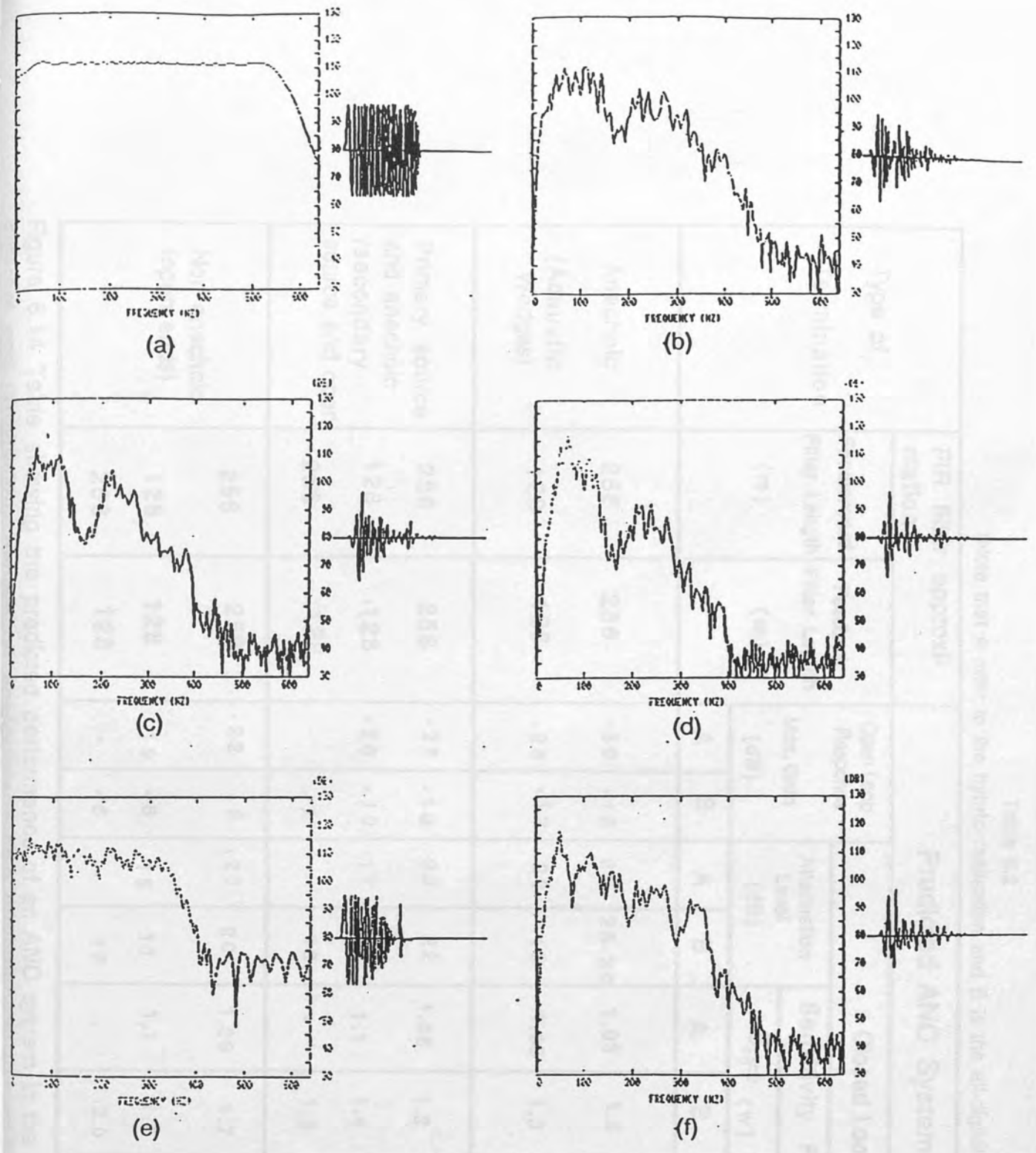

Figure 6.13 Hybrid and all-digital system, open/open termination
Captured signals time series and frequency responses

(a) $Y_{SS}(z)$ (swept sinusoid)

(b) $Y_{10}(z)$, (c) $Y_{30}(z)$, (d) $Y_{32}(z)$, (e) $Y_{AR}(z)$, and (f) $Y_{24}(z)$

Table 6.2

(Note that A refer to the hybrid realisation and B is the all-digital system)

Type of Termination	FIR filter approximation		Predicted ANC System Performance									
	Feedforward Filter Length (m)	Feedback Filter Length (m)	Open Loop Response Max. Gain (dB)		Closed Loop Response							
					Attenuation Level (dB)		Sensitivity Functions (maximum value)					
							$S_{HFF}(w)$		$S_{T}(w)$		$S_{H21}(w)$	
			A	B	A	B	A	B	A	B	A	B
Anechoic (Acoustic Wedges)	256	256	-30	-15	25	25-30	1.03	1.2	0.03	0.22	1.7	1.9
	128	128	-25	-12	20	18	1.06	1.3	0.06	0.34	1.5	1.9
Primary source end anechoic /secondary source end open	256	256	-25	-12	23	22	1.06	1.3	0.06	0.34	2.8	3.1
	128	128	-20	-10	17	12	1.1	1.4	0.11	0.46	2.0	2.3
	256	128	-	-7	-	18	-	1.8	-	0.81	-	3.1
Non anechoic (open ends)	256	256	-22	-8	20	20	1.09	1.7	0.07	0.66	1.6	1.6
	128	128	-19	-8	15	11	1.1	1.7	0.13	0.66	1.3	1.5
	256	128	-	-6	-	17	-	2.0	-	1.00	-	1.8

Figure 6.14 Table showing the predicted performance of an ANC system in the experimental duct using three different end terminations namely (a) anechoic/anechoic (b)primary source end anechoic/secondary source

FIGURES FOR THE APPENDIXES

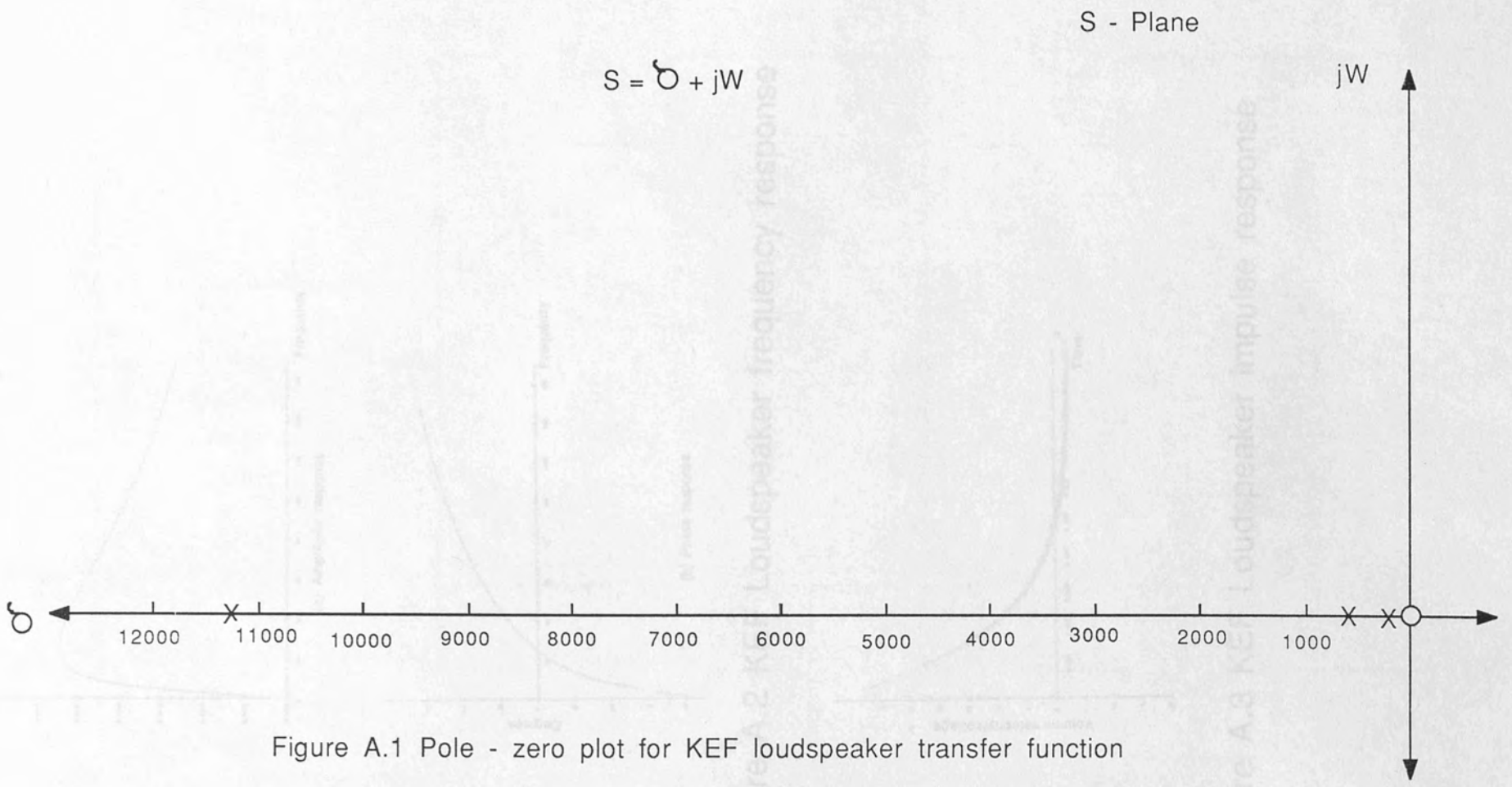

Figure A.1 Pole - zero plot for KEF loudspeaker transfer function

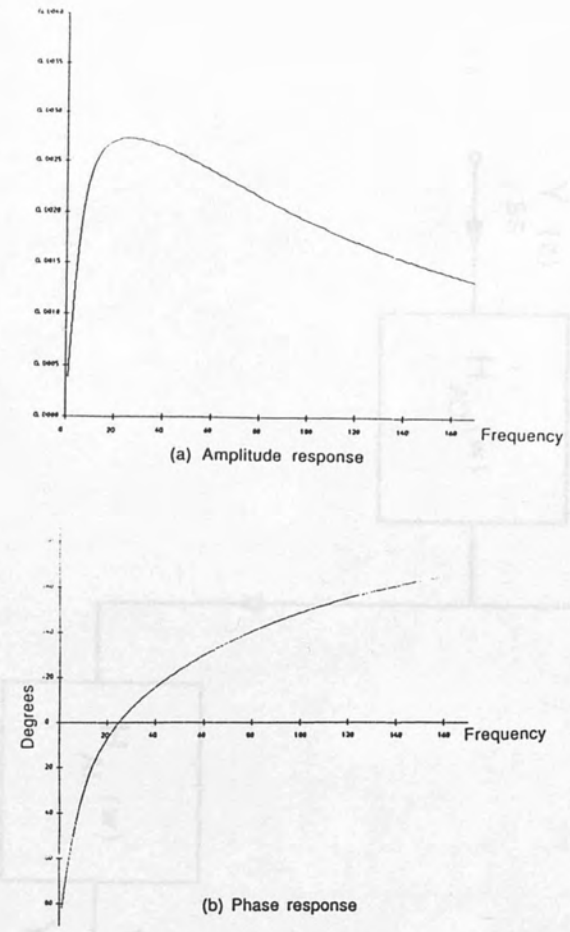

Figure A.2 KEF Loudspeaker frequency response

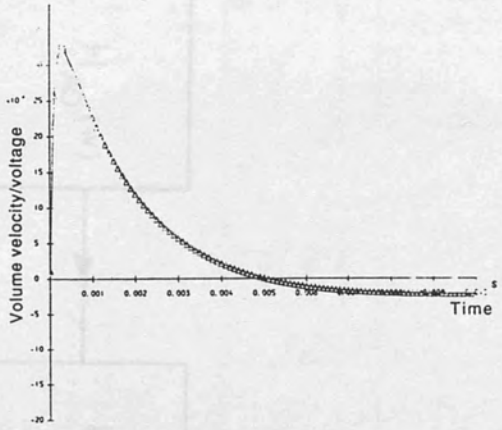

Figure A.3 KEF Loudspeaker impulse response

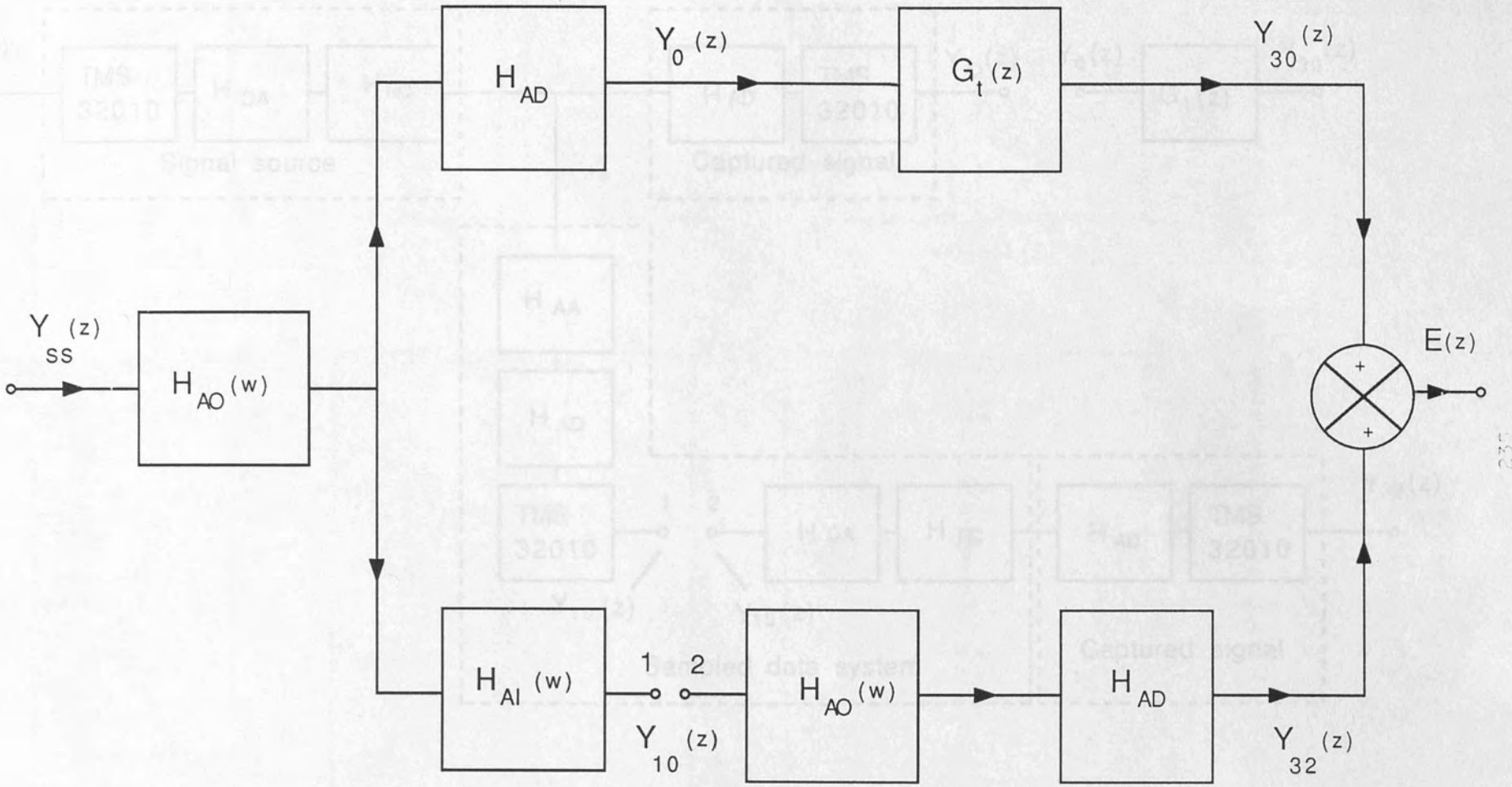

Figure C.1 Signals and transfer functions used in the modelling of a pure discrete time delay system

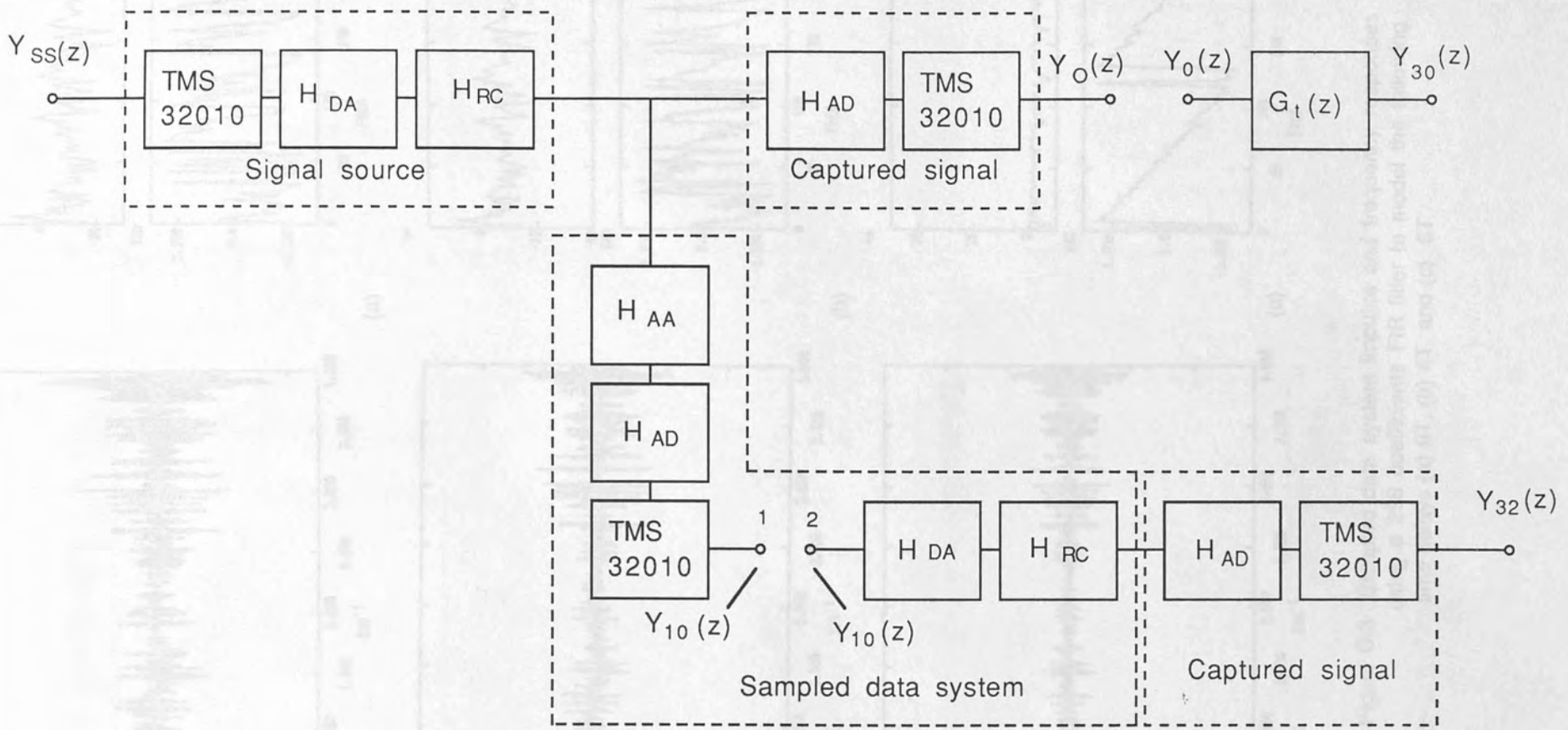

Figure C.2 Block diagram for the measuring sequence needed for a sampled data system to model a pure discrete time delay system

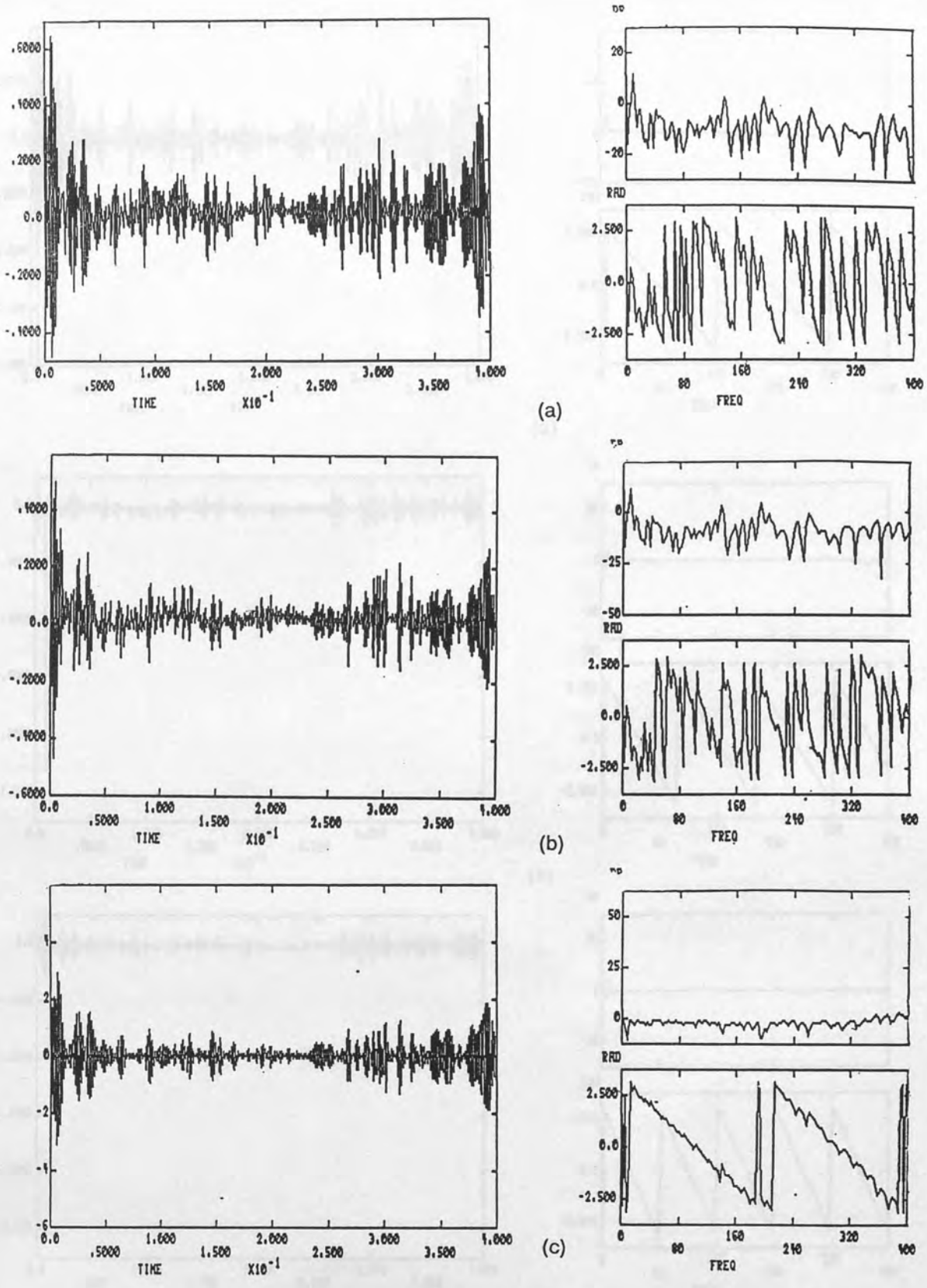

Figure C.3 Sampled data system impulse and frequency responses using a 256 coefficients FIR filter to model the following time delays (a) 0T, (b) 4T, and (c) 6T

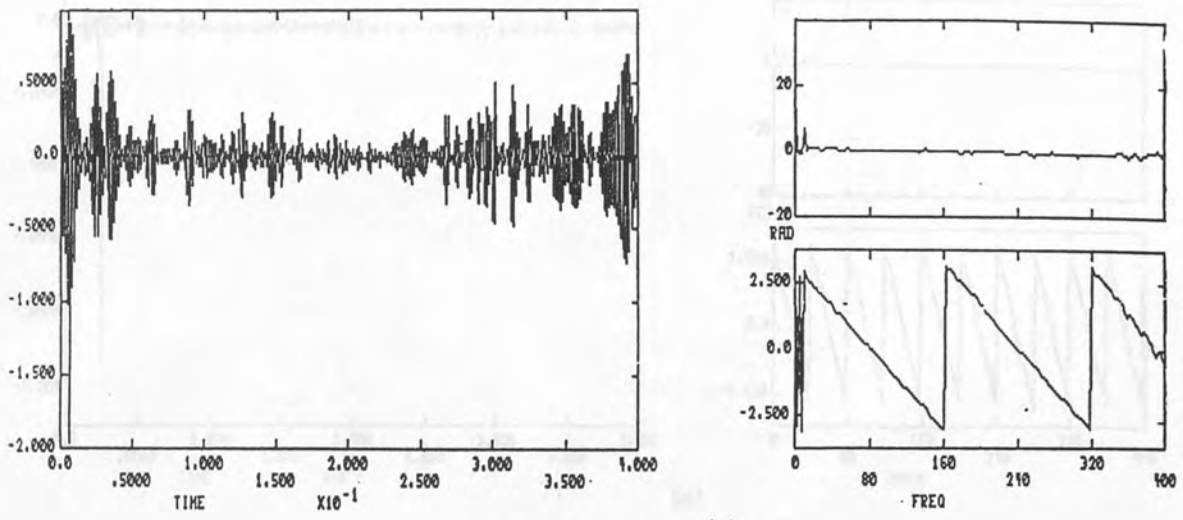

(a)

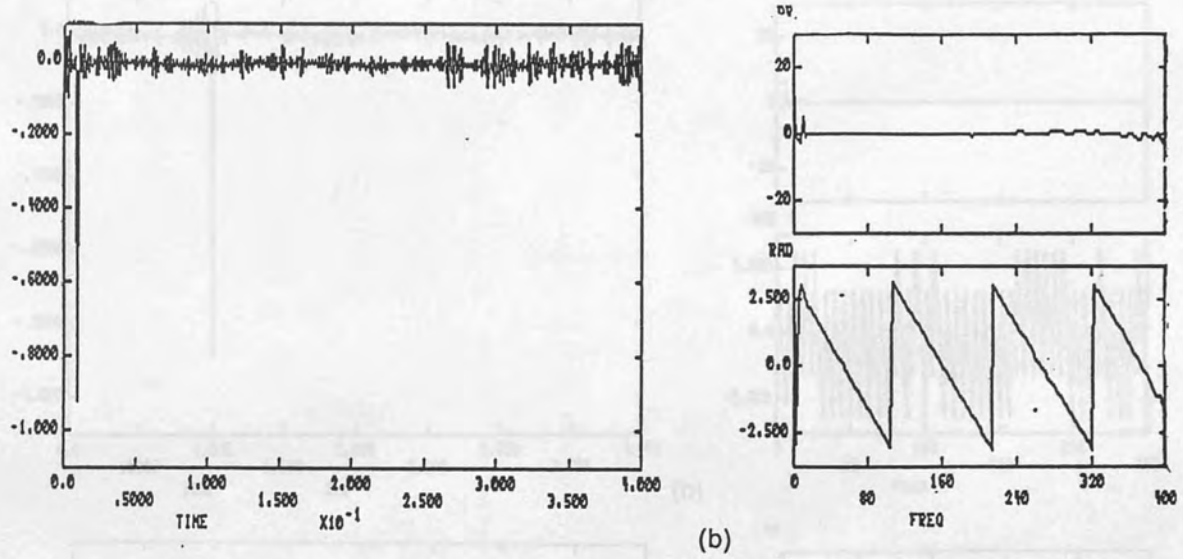

(b)

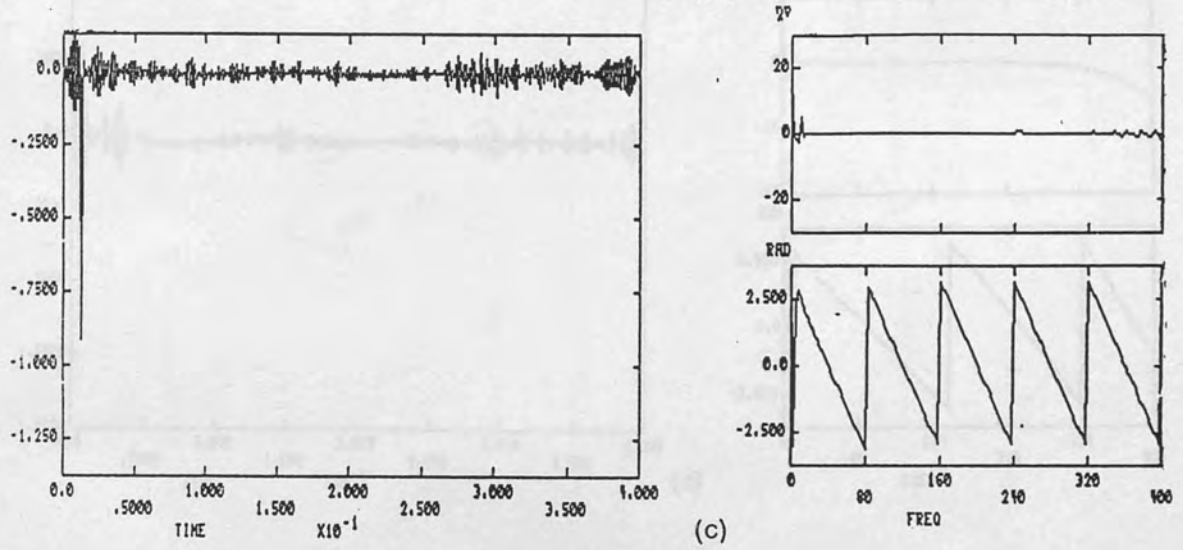

(c)

Figure C.4 The same as figure C.3 with the following time delays (a) 8T, (b) 12T, and (c) 16T

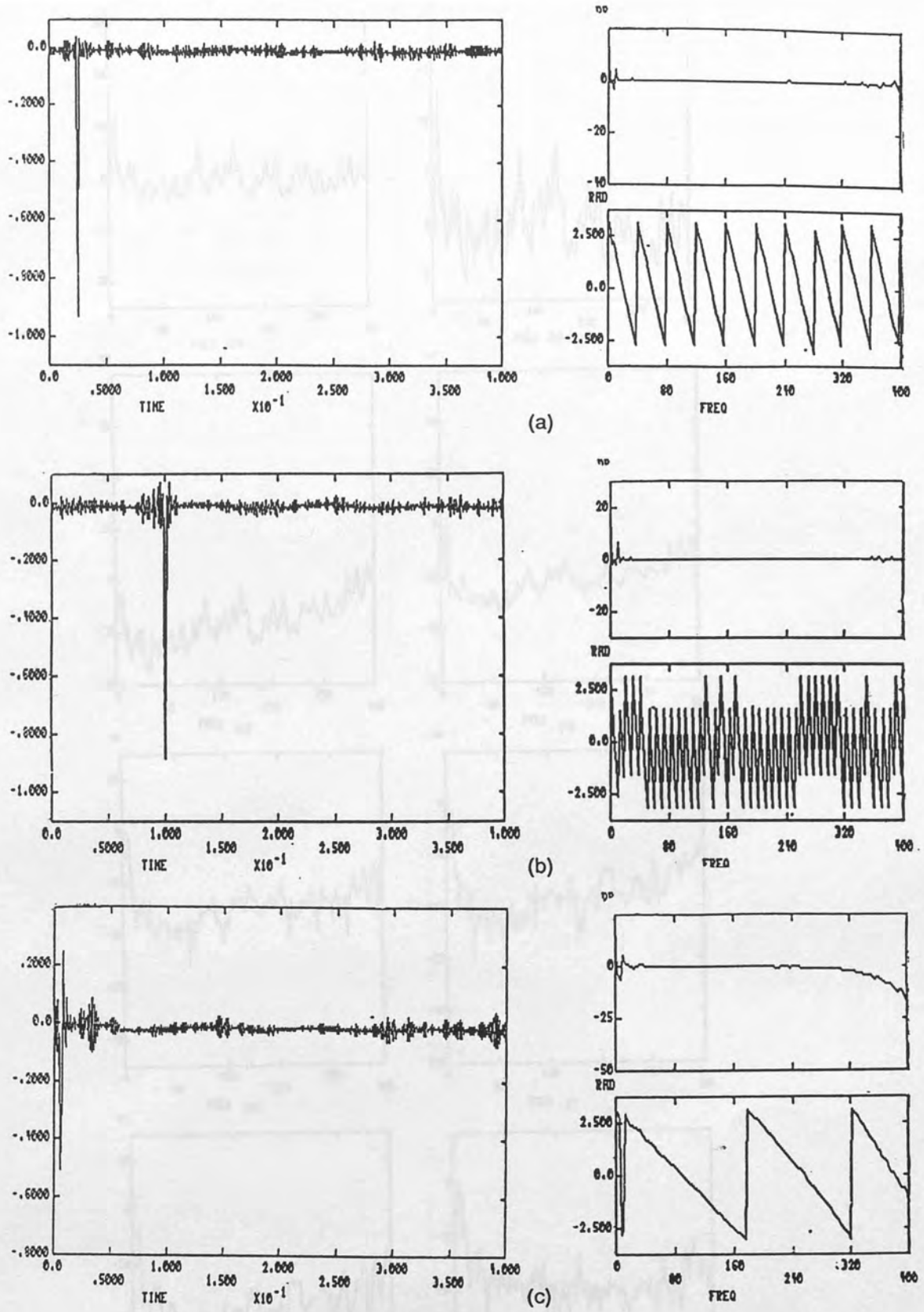

Figure C.5 The same as figure C.3 with the following time delays
(a) 32T, and (b) 128T
(c) impulse and frequency response for the input and output analog interfaces for the sampled data system

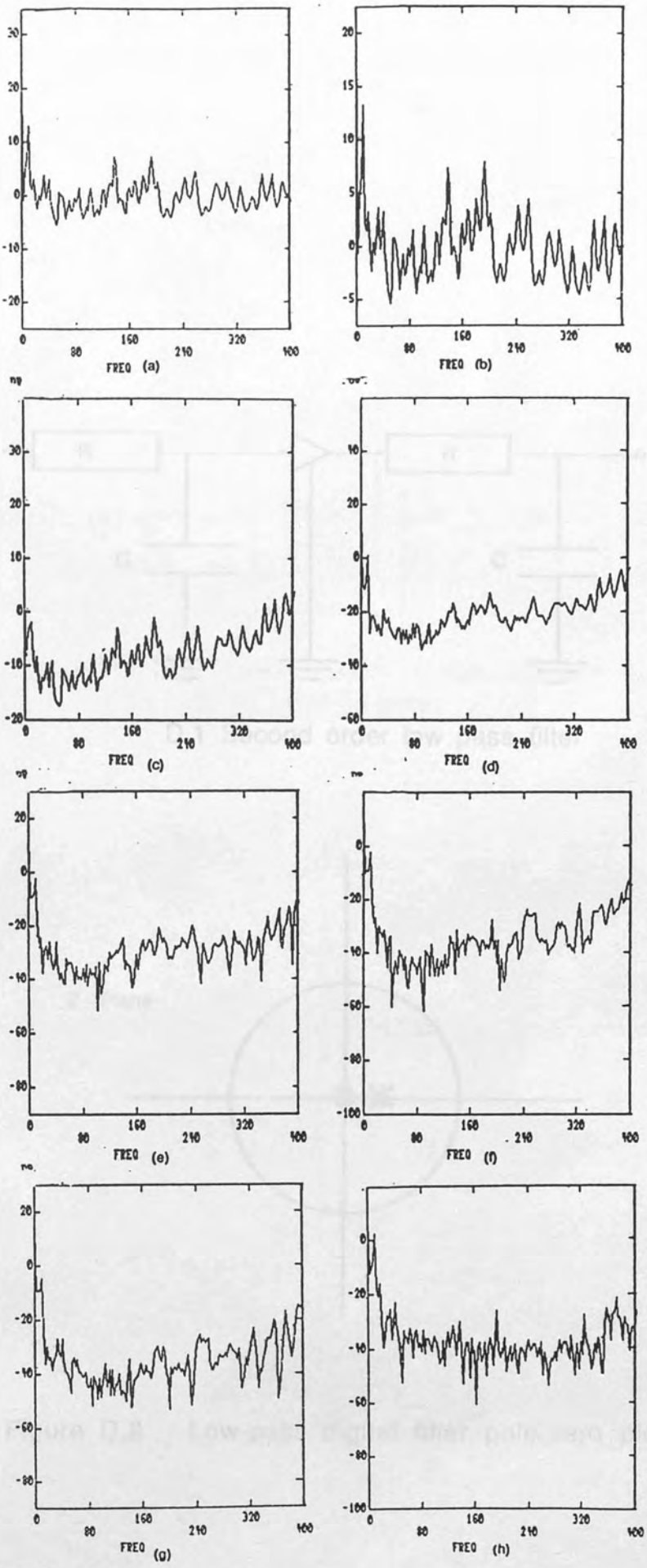

Figure C.6 Predicted attenuation

Sampled data system employing a FIR filter with 256 coefficients to model the following time delays :
(a) 0T,(b) 4T,(c) 6T,(d) 8T,(e) 12T,(f) 16T,(g) 32T and (h) 128T

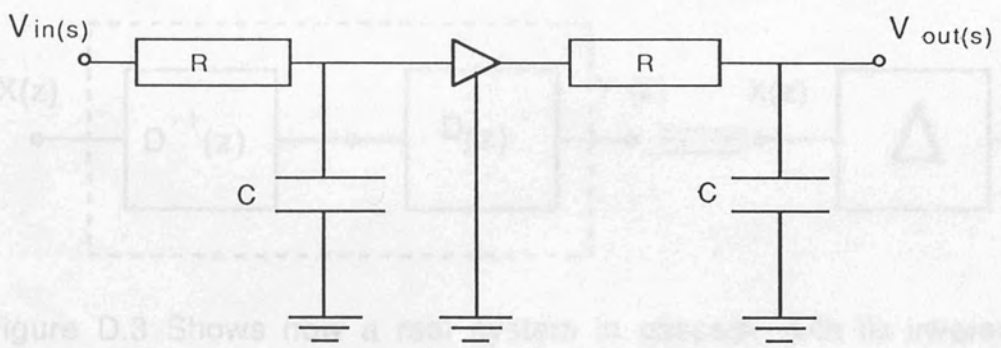

D.1 Second order low pass filter

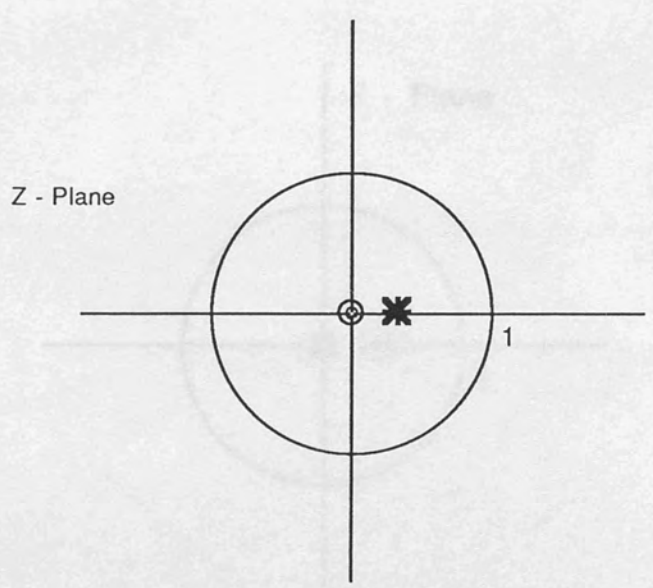

Figure D.2 Low-pass digital filter pole-zero plot

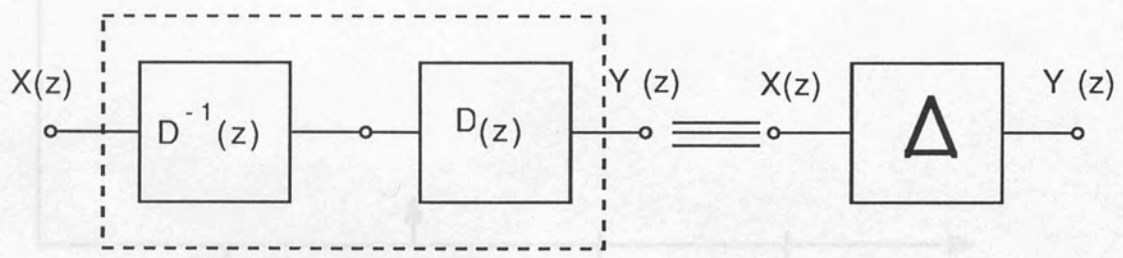

Figure D.3 Shows how a real system in cascade with its inverse can be used to model a delay

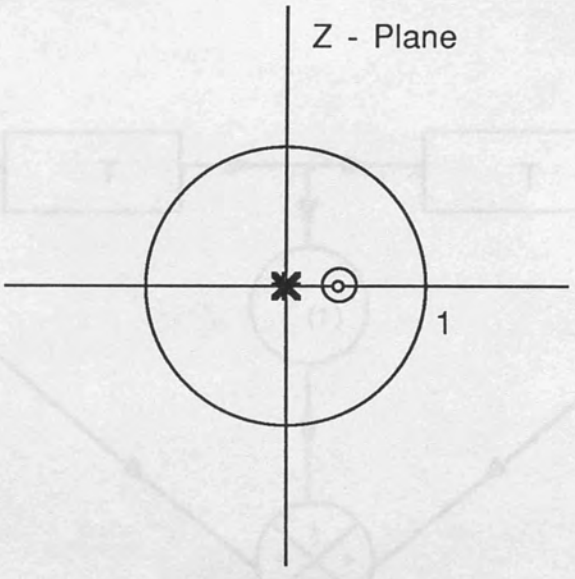

Figure D.4 Inverse lowpass digital filter Z-plane pole-zero plot

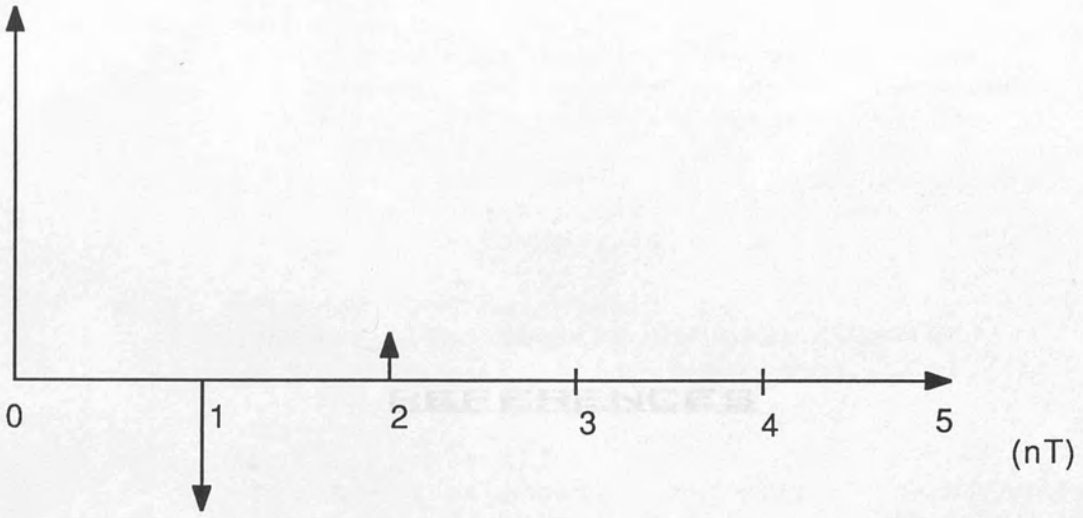

Figure D.5 Inverse lowpass digital filter impulse response

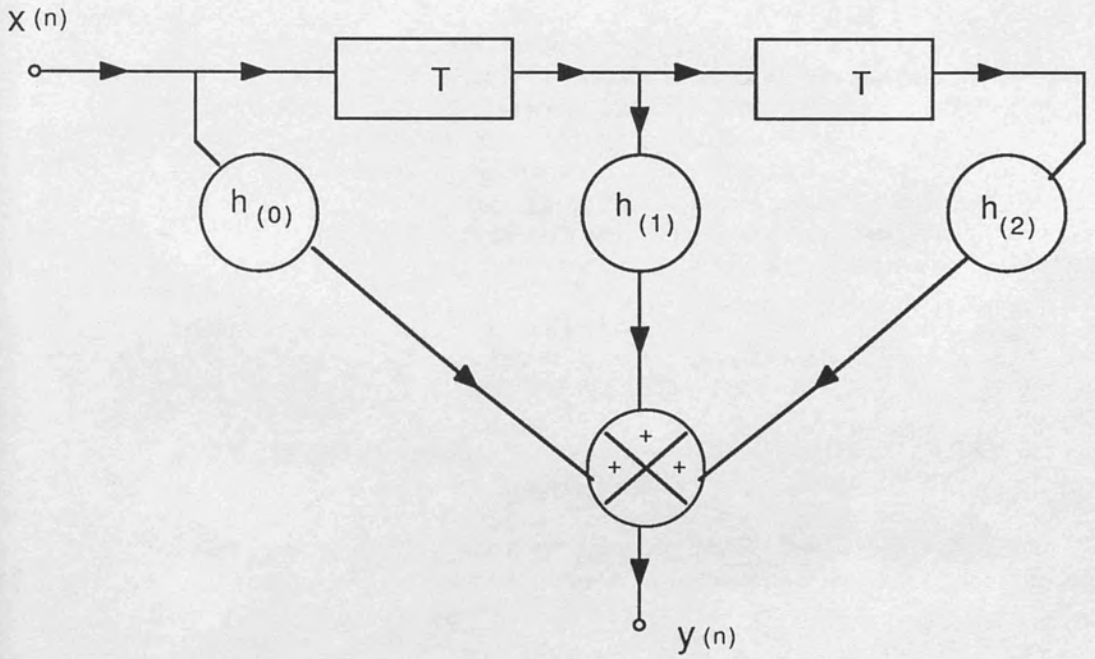

Figure D.6 Implementation of the inverse lowpass digital filter impulse response shown in figure D.5

REFERENCES

[1] Ross Experiments on the active control of transformer noise. JSV (1978) 61(4) 473-480.

[2] Kempton The ambiguity of acoustic sources - A possibility for active control. JSV (1976) 48(4), 475-483.

[3] Piraux and Nayroles
A theoretical model for active noise control attenuation in three-dimensional space. Proc. Inter-Noise 80, 703-706.

[4] Warnaka Active attenuation of noise. The state of the Art Noise Control Engineering, May-June (1982), 18.3, 100-110.

[5] Hong, Eghtesadi and Leventhall
The tight-coupled monopole (TCM) and tandem (TCT) attenuation in a duct. Proc. Inter-noise 83 439-442.

[6] Eghtesadi and Leventhall
Active attenuation of noise - The monopole system JASA 71(3) March 1982, 608-612.

[7] Tichy and Warnaka
Effects of evanescent waves on the active attenuation of sound in ducts. Proc. Inter-Noise 83, 435-438.

[8] Trinder and Nelson
Active noise control in finite length ducts. JSV (1983), 89(1), 95-105.

[9] Eghtesadi and Leventhall
Active attenuation of noise - The Chelsea Dipole. JSV (1981) 75(1), 127-134.

[10] Eghtesadi, Hong and Leventhall
The tight-coupled monopole active attenuator in a duct. Noise Control Engineering, January-February 1983, 16-20.

[11] Jessel and Mangiante
Active sound absorbers in an air duct. JSV (1972) 23(3), 383-390.

[12] Mangiante Active sound absorption. JASA, Vol. 61, no. 6, June 1977, 1516-1523.

[13] Canevet Active sound absorption in an air conditioning duct. JSV (1978) 58(3), 333-345

[14] Swinbanks
The active control of sound propagation in long duct. JSV (1973) 27(3), 411-436.

[15] Poole and Leventhall
An experimental study of a broadband active attenuator for cancellation of random noise in ducts. JSV (1983), 91(3), 1983, 351-362.

[16] Ross
An algorithm for designing a broadband active sound control system. JSV (1982) 80(3), 373-380.

[17] Ross
Application of digital filtering to active control of sound. Acustica (1982), 51 135-140.

[18] Ross
A demonstration of active control of broadband sound. JSV (1981) 74(3), 411-417.

[19] La Fontaine and Shepherd
An experimental study of a broadband active attenuator for cancellation of random noise in ducts. JSV (1983) 91(3), 351-362.

[20] Ross
An adaptive digital filter for broadband active sound control. JSV (1982), 80(3), 381-388.

[21] Poole and Warnaka
The implementation of digital filters using a modified Widrow-Hoff algorithm for the adaptive cancellation of acoustic noise. Paper 21.7.1, Proc. ICASSP (1984).

[22] Roure
Self-adaptive broadband active sound control system. JSV (1985) 101(3), 429-441.

[23] Burgess
Active adaptive sound control in a duct: a computer simulation. JASA (1981), 70(3), 715-726.

[24] Roebuck
The relationship between active noise control and adaptive signal processing. AUWE Publication no. 65837, June 1982.

[25] Flockton
Cancellation of acoustic noise in a pipe using adaptive filters, Proc. ICASSP 87 Dallas 5.8.1-5.8.4

[26] Eghtesadi and Leventhall
Comparison of active attenuators of noise in ducts. Acoustics Letters Vol.4, no. 10, 1981.

[27] Olson and May
Electronic Sound Absorber, JASA Vol.25 no.6, Nov.1953, 1130-1136.

[28] Olson Electronic Control of Noise, Vibration and Reverberation, JASA, Vol.28 no.5, Sept.1956, 966-972.

[29] Eriksson and Allie and Greiner
The selection and application of an IIR adaptive filter for use in active sound attenuation. IEEE Trans. ASSP Vol.35, no. 4, April 1987, 433-436.

[30] Elliott and Nelson
Error surfaces in active noise control. Proc. IOA Vol. 7 part 2 (1985) 65-72.

[31] Gabel and Roberts
Signals and Linear Systems. Wiley International Edition, Chapter 7, 373-374.

[32] Nagrath and Gopal
Control System Engineering, Wiley International Edition, Chapter 3, 62-63.

[33] Franklin and Powell
Digital Control of Dynamic Systems, Addison-Wesley. Chapter 8, 207-216.

[34] Brown Lecture Notes, Chelsea College, London.

[35] Bode and Shannon
A simplified Deviation of Linear Least Square Smoothing and Prediction Theory, Proc. I.R.E. 1950, Vol.38, 417-425.

[36] Nieman, Fisher and Seloog
A review of process identification and parameter estimation techniques. Int. J. Control, 1971, Vol. 13, no.2, 209-264.

[37] Mendel Some modelling problems in reflection seismology. IEEE ASSP Magazine April 1986, 4-17.

[38] Marple Efficient least squares FIR system identification. IEEE Transactions ASSP Vol. 29, no. 1, February 1981, 62-73.

[39] Farden Solution of a Toeplitz set of linear equations. IEEE Trans. antennas and propagat., (1976 Vol. AP24, 906-907.

[40] Fincham Refinements in the Impulse Testing of Lousdspeakers. J. Audio Eng. Soc. (1985) Vol. 33, no. 3, 133-140.

[41] Rabiner Techniques for designing finite duration impulse response digital filters IEEE Trans. on communication technology (1971), Vol. Com19, no.2, 188-195.

[42] Howes PhD thesis, Chelsea College, 1983.

[43] Wheeler PhD thesis, University of Southanpton, 1986.

[44] Capper MSc project report, Chelsea College, 1985.

[45] Downes and Elliott
The measurement of the free field impulse response of microphones in a laboratory environment, JSV(1985) 100(3), 423-442.

[46] Makhoul Linear Prediction, A Tutorial Review. Proc. IEEE, (1975) Vol.63 no.4, 561-580.